

International Atomic Energy Agency

**INDC**

**INTERNATIONAL NUCLEAR DATA COMMITTEE**

**NDS LIBRARY COPY**

CONSOLIDATED PROGRESS REPORT FOR 1974

ON NUCLEAR DATA ACTIVITIES

OUTSIDE THE NDS SERVICE AREA

Austria

Belgium

Greece

Italy

Netherlands

Switzerland

Turkey

**NDS LIBRARY COPY**

December 1974

**IAEA NUCLEAR DATA SECTION, KÄRNTNER RING 11, A-1010 VIENNA**

## FOREWORD

This consolidated progress report for 1973 has been prepared for the countries outside the NDS service area. A second report, INDC(SEC)-42/L, covers countries within the NDS service area.

The report is arranged alphabetically by country, and reproduces the content of each individual report as it was received by the INDC Secretariat. Also included in the Table of Contents is a list of each laboratory, institute and university referred to in the report, preceded by its internationally used EXFOR code.

As in all progress reports the information included here is partly preliminary and is to be considered as private communication. Consequently, the individual reports are not to be quoted without the permission of the authors.

# TABLE OF CONTENTS

	pages
<u>Austria</u> .....	1-16
(2AUSATI) Atominstitut der Oesterreichischen Hochschulen, Vienna	
(2AUSIRK) Institut fuer Radiumforschung und Kernphysik	
(2AUSSGA) Oesterreichische Studiengesellschaft fuer Atom- energie, Seibersdorf	
(2AUSGFK) Gesellschaft zur Foerderung der Kernenergie, Graz	
<u>Belgium</u> .....	17-30
(2BLGMOL) Nuclear Energy Center, Mol	
(2BLGLVN) University of Louvain, Louvain	
(2BLGCHT) University of Ghent, Ghent	
(2BLGANT) University of Antwerpen	
<u>Greece</u> .....	31-33
(2GRCATH) N.R.C. "Demokritos", Athens	
<u>Italy</u> .....	35-42
(2ITYPAD) University of Padua and Laboratori Nazionali di Leguaro	
(2ITYTRI) University of Trieste, Trieste	
(2ITYCAT) University of Catania, Catania	
(2ITYMIL) University of Milano, Milano	
(2ITYPAV) University of Pavia, Pavia	
(2ITYCAS) Centro di Studi Nucleari della Casaccia, Rome	
<u>Netherlands</u> .....	43-63
(2NEDRCN) Reactor Centrum Nederland, Petten	

	<u>pages</u>
<u>Switzerland</u> .....	69-113
(2SWTNEU) University of Neuchatel, Neuchatel	
(2SWTFRS) University of Fribourg, Fribourg	
(2SWTWUR) Institute for Reactor Research, Wuerenlingen	
(2SWTZUR) University of Zuerich, Zuerich	
(2SWTBAS) University of Basel, Basel	
(2SWTETH) Eidgenoessische Technische Hochschule, Zuerich	
(2SWTLAU) University of Lausanne, Lausanne	
 <u>Turkey</u> .....	 115-117
(2TUKCNA) Cekmece Nuclear Research Center, Istanbul	



PROGRESS REPORT TO NEANDC AND INDC  
FROM AUSTRIA

July 1974

O.J.Eder, Editor

This report contains abstracts about work performed at

Atominstitut der Österreichischen Hochschulen, Wien

Institut für Radiumforschung und Kernphysik der Österreichischen Akademie der Wissenschaften, Wien

Physikinstitut des Forschungszentrums Seibersdorf der Österreichischen Studiengesellschaft für Atomenergie

Reaktorinstitut des Vereins zur Förderung der Anwendung der Kernenergie, Technische Hochschule Graz

Österreichische  
Studiengesellschaft für  
Atomenergie Ges.m.b.H.  
A-2444 Seibersdorf  
Austria.

This report contains  
partly preliminary data.  
The information given  
is to be considered as  
private communication  
and is not to be quoted.

ATOMINSTITUT DER ÖSTERREICHISCHEN HOCHSCHULEN, WIEN

1. NEUTRON SOURCES AND NEUTRON DETECTION

1.1 The Emission Spectra of Na-D<sub>2</sub>O, In-Be and Na-Be Photoneutron Sources

K.Mueck, F.Bensch

The energy distribution of the photoneutrons of Na-D<sub>2</sub>O, In-Be, La-Be and Na-Be source systems were measured by means of a proton recoil proportional counting tube. Spherical lead-shields of various thicknesses (ranging from 1.5 to 13cm) were used to reduce the intense gamma field accompanying the neutron spectra to be measured. The spectra of spherical heterogeneous source arrangements for three different Be-target thicknesses (0.5, 1.1 and 2.0cm) were measured and compared with the theoretical distribution as obtained by Monte-Carlo calculations. The change in spectrum shape due to the lead shields was also calculated by a Monte-Carlo routine. Good agreement between theoretical predictions and experimental results shows values for the peak of the neutron distribution of  $264.1 \pm 0.5\text{keV}$  for the Na-D<sub>2</sub>O system,  $397.3 \pm 0.8\text{keV}$  for the In-Be system,  $761 \pm 0.7\text{keV}$  for the La-Be system and  $966.9 \pm 0.5\text{keV}$  for the Na-Be source system. With the La-Be system a second neutron group of much lower intensity (6.5 per cent of the main group) could be found with a peak energy of  $1097 \pm 1.0\text{keV}$  in good agreement to recent gamma-spectroscopic measurements.

1.2 Cadmium Correction Factors of Several Thermal Neutron Foil Detectors

K.Mueck, F.Bensch

If the epithermal activation  $C_{ep}$  of a foil detector is derived from its epicadmium activation  $C_{Cd}$ , the knowledge of the cadmium correction factor  $F_{Cd} = C_{ep}/C_{Cd}$  is usually required. The cadmium correction factors of V, B, <sup>10</sup>B, In, Au, Mn, Co and Dy foil detectors of thickness 0 - 0.25mm and cadmium cover thicknesses of 0.5, 0.8, 1.0 and 1.2mm have been numerically evaluated according to the most recent cross-section values and resonance parameters.  $F_{Cd}$  values are listed for both monodirectional and isotropic neutron incidence. While for most of these materials no results have been published so far, for gold and indium the results could be compared with previous calculations and measurements and a discussion of the results is given. Since the  $F_{Cd}$  values, particularly for Mn, Co and Dy exceed unity considerably, neglecting

this correction is not tolerable with precise measurements of the thermal neutron flux density. Comments on the use of  $F_{Cd}$  values in the Westcott convention are added.

## 2. NEUTRON SPECTROMETER

### 2.1 A neutron spin-flip chopper with Mezei-coils

G.Badurek, H.Rauch, G.P.Westphal, P.Ziegler

A neutron spin-flip chopper has been developed offering superior characteristics compared to the conventional r.f.-chopper. Flipping efficiencies of nearly 1.0 are achieved only by suitable DC-currents through the Mezei-coils. The chopping system consists of simple and reliable transistor switches operating in constant current mode. Fast on-off times (3 - 4  $\mu$ s) are obtained because of the extremely low coil inductivity (3.5  $\mu$ H) and delayed switching of the second coil according to the neutron time-of-flight through the first one resulting in an effective coil length of 1.5cm. The good symmetry of the neutron burst shape favours application of the correlation-as well as the Fourier method.

### 2.2 A high efficiency neutron spectrometer for elastic scattering

G.Badurek, H.Rauch, G.P.Westphal, P.Ziegler

The new concept for an elastic spectrometer giving good neutron economy is based on the combination of position sensitive detectors and a Fourier chopper. Investigations are in progress dealing with the gain factor for elastic scattering experiments compared to conventional methods.

## 3. NEUTRON DEPOLARIZATION MEASUREMENTS

### 3.1 Investigation of the magnetic domain structure in Dy with polarized neutrons

M.Waldauf, A.Zeilingner, H.Rauch, M.Th.Rekvelidt\*

Measurements of the depolarization action of a polycrystalline

---

\* Interuniversitair Reactor Instituut - Delft, Holland

sample with heavy internal stresses revealed the existence of a mixed state between ferromagnetic and antiferromagnetic domains. Experiments in Delft showed a marked anisotropy in the depolarization action of the samples, which can be explained by a correlation of the domain dimensions with the direction of their magnetic induction.

#### 4. NEUTRON INTERFEROMETRY

H.Rauch, U.Bonse\*, W.Treimer, P.Skalitzky\*\*, M.Suda

A perfect crystal interferometer has been operated successfully at the TRIGA-reactor (Phys.Lett. A47 (1974) 369). The separation of the coherent beams was about 4cm and up to 20 interference fringes could be observed. Now the whole facility will be installed at the high flux reactor at Grenoble to use the full capability of this new method. First measurements deal with a very accurate determination of scattering amplitudes to obtain new information about neutron-nucleus and neutron-electron interactions. New possibilities for the investigation of magnetic materials and for coherence properties of matter waves arise.

#### 5. NUCLEAR PHYSICS

##### 5.1 Fission of Highly Excited Heavy Nuclei

F.Bensch, G.Eder, H.Jasicek, H.Oberhummer, H.Rauch,  
P.Riehs

Investigations of the fission probability of heavy nuclei induced by light and heavy ions are planned at the "Schweizerisches Institut für Nuklearforschung" (SIN) in Villigen, Switzerland. The injector cyclotron of SIN will be used to get highly excited compound nuclei. By detecting the delayed neutrons certain fission products will be identified.

##### 5.2 Angular Correlation of $\gamma$ -Rays from Oriented Nuclei

H.W.Weber, R.Goblirsch, H.Rauch, P.Riehs

Covering some interests in nuclear and solid state physics a  $\text{He}^3$ - $\text{He}^4$  dilution refrigerator has been installed in order to obtain

---

\* Institut für Physik, Universität Dortmund

\*\* Institut für Angewandte Physik, TH Wien

oriented nuclei. First tests have been performed successfully and will be continued in making a transmission experiment with polarized thermal neutrons. Measurements of  $\gamma$ -rays following thermal neutrons capture and following radioactive decay are foreseen in future.

5.3 Measurements of low energy gamma rays following thermal neutron capture in  $^{235}\text{U}$

W.J.Schindler, C.M.Fleck

The low energy  $\gamma$ -rays were detected in a Ge(Li) detector using an enriched target of  $^{235}\text{U}$ . The evaluation of single and coincidence spectra leads to some new transitions. Spin and parity of the 1342keV level and a level at 1383keV are deduced.

6. REACTOR TECHNOLOGY

6.1 High sensitive detection of defect fuel elements in water cooled reactors by analysis of released fission gases

C.M.Fleck, H.Böck, P.Brunner, H.Erber, W.Fritsch  
(Work supported by the IAEA under contract no. 934)

The difference in the release mechanisms between intact and defect fuel elements indicate, that a change in the isotopic composition of the released rare gases could be more significant than a change in the absolute level of the fission gas activity for the detection of defect elements. The present studies were performed to measure release parameters for Uran-Zirconium-Hydride with which the release of the different fission gas isotopes in any operation state of the reactor at any power level could be calculated and compared with measured values for both intact and defect fuel elements.

6.2 Burnup measurements for reactor operation and safeguards

C.M.Fleck, H.Bauer\*, H.Moldaschl\*, E.Ruppert\*\*,  
H.Krinninger\*\*

Some new techniques for incore and out-of-core measurements on PWR's and BWR's are studied. Also theoretical and experimental.

---

\* KWU, Erlangen

\*\* INTERATOM, Bensberg

investigations are carried out for burnup measurements on the fuel of LMFBR's.

### 6.3 Transient response of self powered neutron detectors

H.Böck, F.Richter, P.Geburek\*, D.Stegemann\*

(Paper presented at the Reaktortagung 1974 in Berlin)

The transient response of self powered neutron detectors with Co, Er, Hf and Pt emitters were analyzed during reactor square wave and pulse operation. Characteristical deviations of the linearity were observed during high speed power level changes especially with Co and Er detectors compared to a standard ionization chamber.

## 7. MEASUREMENT AND DATA HANDLING

### 7.1 On line computer system for laboratory automation

G.P.Westphal

A laboratory computer system is just being completed, which is intended for automation of various beam hole experiments at the TRIGA reactor. The configuration consists of a PDP 11/45 with 64 kbyte of core (48 kbyte for program and 16 kbyte as DMA buffer), an RK05 disk drive, a dual DEC tape unit, a line printer, a storage scope, an X-Y plotter and three terminals. Three CAMAC crates are interfaced to the Unibus by means of Type U controllers (Borer 1533A), one of them being located at the computer, the other two at remote data stations at the reactor connected by means of differential Unibus extenders over a distance of appr. 100m. A fast multi-user Basic operating under the RT11/FB system includes all the CAMAC functions, which have been implemented via the CALL feature. Supported by a floating point processor, which significantly speeds up I/O operations and program execution, it allows for fast and efficient programming even by the unexperienced user.

### 7.2 On line computer control for polarized slow neutron experiments

G.P.Westphal, G.Badurek, H.W.Weber, A.Zeillinger

For the development of a remote data station at the polarized

---

\* TU Hannover

neutron beam hole of the TRIGA reactor a system analysis has been performed to find structural and procedural similarities between several typical experiments. This analysis has led to a modular hardware development and will be the basis for software modularity as well. The first experiment at this station, which is just in the setup phase, is the measurement of the transmission of polarized neutrons through an oriented target, performed by means of an  $\text{He}^3\text{-He}^4$  dilution refrigerator.

### 7.3 Position sensitive neutron detectors

G.P. Westphal, H. Rauch

Measurements with position sensitive  $^{10}\text{BF}_3$  proportional counters with a filling pressure of 2 atm. have shown an intrinsic resolution of 1.5 mm fwhm, which is degraded to appr. 3 mm for a counter of a length of 1 m by electronic noise and non-linearities of the analog pulse processing. Improvements of preamplifiers and the development of a digital position encoder very probably will reduce resolution to 2 mm fwhm.

## 8. RADIOCHEMISTRY

### 8.1 Activation analysis using short-lived nuclides or isomers

F. Grass

Activation analysis was developed using short-lived isotopes, e.g. the 20 ms nuclides or isomers  $^{12}\text{B}$  or  $^{24}\text{Na}^m$ . The advantages of using short-lived nuclides for activation analysis especially in combination with reactor impulse are outlined. The maximum increase of sensitivity in relation to the half-life is shown graphically. The practical application of AA with 20 ms nuclides is demonstrated on the simultaneous analysis of sodium and boron in Jenaer G 20 glass. In five determinations the mean errors of the average were 2.5 and 3.5% for sodium and boron respectively. As the two simultaneous measurements require only 400 ms, this method is very useful for serial analysis, particularly if a computer in on-line operation is available.

## 9. NEUTRON RADIOGRAPHY

E. Granzer, W. Pochman, H. Rauch, N. Skiadopoulos, A. Zeilinger

Experiments on the diffusion of hydrogen in various media are

continued. The resolution and image contrast of neutron radiographs of objects containing hydrogen are experimentally and theoretically investigated.

INSTITUT FÜR RADIUMFORSCHUNG UND KERNPHYSIK DER ÖSTERREICHISCHEN  
AKADEMIE DER WISSENSCHAFTEN, WIEN

1. Study of the short-lived activities of  $^{70}\text{Cu}$  and  $^{67}\text{Ni}$

W.Reiter, W.H.Breunlich, P.Hille

Work described in the last reports has been completed. Abstract of the thesis see below.

W.L.Reiter, Thesis, Univ. Wien:

After irradiation of  $^{70}\text{Zn}$  with 14 MeV neutrons three activities observed have been assigned to two isomers of  $^{70}\text{Cu}$  ( $^{70a}\text{Cu}$ ,  $T_{1/2} = 4 \pm 1$  s and  $^{70b}\text{Cu}$ ,  $T_{1/2} = 52 \pm 5$  s) and to  $^{67}\text{Ni}$  ( $T_{1/2} = 16 \pm 4$  s). Ge(Li) single gamma-ray spectra, plastic scintillation single beta-ray spectra and plastic-NaJ(Tl) beta-gamma coincidences were measured. A  $\beta$ -ground-state transition ( $6.20 \pm 0.20$  MeV) and a transition to the first excited  $2^+$ -level of  $^{70}\text{Zn}$  ( $5.45 \pm 0.12$  MeV) due to  $(1^+)$   $^{70a}\text{Cu}$  and three  $\beta$ -branches with  $4.57 \pm 0.12$  MeV,  $3.45 \pm 0.15$  MeV and  $2.30 \pm 0.17$  MeV to the levels at 1786.5 keV, 3038.2 keV and 4146.9 keV, respectively, due to  $(5^-)$   $^{70b}\text{Cu}$  were found. Five gamma-rays were placed in the decay schema. A  $\beta$ -transition of  $3.75 \pm 0.20$  MeV has been assigned to  $^{67}\text{Ni}$ . Branching ratios for the  $\beta$ -components have been estimated and the log ft-values deduced.

2. Measurement of energy spectra and angular distributions of charged particles emitted in nuclear reactions induced by 14 MeV neutrons

P.Hille, M.Uhl, K.Richter, W.Weisz

Work described in the last reports is continued. The final version of the cylindrical multiwire chamber has been built and tested.

3. A pulsed neutron generator

G.Stengl



The pulsed neutron generator is now working according to the design aims (1 nsec pulse duration > 10mA D<sup>+</sup>-peak current, = 250 keV D<sup>+</sup>-energy). The <sup>56</sup>Fe(n,n' $\gamma$ )-reaction is now under study with the new facility using time-of-flight technique.

4. Age-determination of bones by activation with 14 MeV neutrons

P.Eisenbart, P.Hille

The age of bones is determined by measuring the Nitrogen/Fluorine ratio using 14 MeV neutron-activation. The  $\beta^+$ -radiation of <sup>13</sup>N and <sup>18</sup>F from the reactions <sup>14</sup>N(n,2n) and <sup>19</sup>F(n,2n) is followed over several half-lives by counting the 511 keV-annihilation quanta with a Ge(Li)-spectrometer. For a number of bones of known age from the Roman military camp Carnuntum the N/F-ratio is measured in order to study the variation with soil composition.

5. Activation Analysis Applications in Archaeology

W.Czerny, G.Winkler

In cooperation with the "Österreichisches Archäologisches Institut" nondestructive activation analysis work with fast neutrons is in progress on ancient pottery. A straight-forward method was developed for determining the Si, Al, Mg and Fe contents which seem to allow to differentiate between samples of different origin.

In cooperation with the "Institut für Antike Numismatik" (Universität Wien) a bronze coin could be identified as a contemporary, that is ancient, forgery of cast white bronze using activation techniques described below (to be published in Sitzber. Österr. Adad. Wiss, mathem.naturw. Klasse).

6. Non-destructive Analysis of Ancient Bronze Coins by Activation with 14 MeV Neutrons

G.Winkler

For the purpose of numismatic studies ancient bronze coins have been analyzed by nondestructive fast neutron activation analysis using a comparison technique. Series of measurements were performed with different experimental set-up. After irradiation gamma ray spectra were measured by a highly resolving Ge(Li)-spectrometer. A relative error of one and two per cent was achieved for the absolute copper and tin contents respectively. Iron contents down to 0,1 per cent can be measured easily.

Results from activation analysis were also compared with X-ray fluorescence studies. Work is being published in the Internat. Journal of Applied Radiation and Isotopes.

7. Measurement of (n,p) cross sections on Isotopes of Cd, Sn and Te for 14 MeV Neutrons

W.Struwe, G.Winkler

Work described in the last reports has been completed and published in Nucl.Phys. A222 (1974) 605. The (n,p) cross sections measured on several isotopes of the elements mentioned have been discussed and compared to values predicted by semiempirical formulas and with calculated values based on the statistical model of nuclear reactions.

8. Measurement of Neutron Spectra from Inelastic Scattering of 14 MeV Neutrons

H.K.Vonach, W.Bertl, G.Winkler, G.Stengl, H.Kratschmar, W.Breunlich, S.Tagesen

A Program is started to measure the neutron spectra and (or) neutron- $\gamma$ -coincidences from (n,n' $\gamma$ )-reactions, respectively, on several isotopes of Mg, Al, Si, S, (Ca), Mn, Co, Ni, Zn, Ge, Se, (Sr), Nb, Y, Au, Pb, Bi.

PHYSIKINSTITUT DES FORSCHUNGSZENTRUMS SEIBERSDORF,  
ÖSTERREICHISCHE STUDIENGESellschaft FÜR ATOMENERGIE

1. NUCLEAR PHYSICS

1.1 Observation of Parity Violation by  $\beta$ - $\gamma$  directional correlation

F.Dydak, G.Serentschy, P.Weinzierl

Having obtained a positive result for the coefficient  $A_1$  in the directional correlation of the Tl 203 decay -  $A_1 = -(2,7 \pm 0,7) \cdot 10^{-4}$  - which is in disagreement with the measurements of other groups,

we are trying to do a zero-effect experiment with the same apparatus using a nucleus for which no measurable parity admixture is to be expected. The choices are Ru 103 and Sc 46. As the mass separation of a Ru-source of suitable quality turned out to be unfeasible a high temperature ion source was constructed for Sc-separations. Test runs with Sc-metal and Sc-compounds are under way.

1.2 Preliminary Results for the Electron-Neutrino Angular Correlation Coefficient  $a$  measured from Free-Neutron Decay

R.Dobrozemsky, E.Kerschbaum, G.Moraw, C.Stratowa,  
P.Weinzierl

Measurements of the electron-neutrino angular correlation coefficient  $a$  in the free-neutron decay are reported. The method is based on the measurement of the shape of the energy spectrum of recoil protons obtained from neutrons inside a highly evacuated cavity near a reactor core. Spectroscopy is done by means of an electrostatic condenser and an ion-electron converter detector of the coincidence type. By this arrangement counting rates of several counts/sec are obtained at the detector which promise considerable improvement in accuracy compared to previous experiments. 17 proton spectra were evaluated up to now and their shape yielded the preliminary result:

$$a = -0.096 \pm 0.013, \text{ giving } |G_A/G_V| = 1.242 \pm 0.041.$$

2. NEUTRON SCATTERING

2.1 Microscopic Grueneisen Parameters in Rubidium Iodide measured by Inelastic Neutron Scattering

O.Blaschko\*, G.Ernst\*, G.Quittner, R.Lechner\*\*, W.Kress\*\*

About 40 mode Grueneisen parameters in Rubidium Iodide have been evaluated from the measurements on the high-flux reactor in Grenoble. They have been compared to and interpreted in terms of an anharmonic breathing shell model of W.Kress.

2.2 Mode Grueneisen in Potassium Bromide by Inelastic Neutron Scattering

O.Blaschko\*, G.Ernst\*, G.Quittner

Eight acoustical mode Grueneisen parameters have been measured at the Seibersdorf reactor. The results are compared with several

\* I. Phys. Institut der Universität Wien

\*\* Institut Max von Laue - Paul Langevin, Grenoble

theoretical predictions. A paper has been submitted to the Journal of Physics and Chemistry of Solids.

2.3 Pressure induced changes in the mosaic structure of KBr and RbI crystals measured with 412 keV  $\gamma$ -rays

O.Blaschko, G.Ernst, J.Schneider\*

Changes in the mosaic distribution of KBr and RbI single crystals under pressure up to 3,4 kbar have been investigated with 412 keV  $\gamma$ -rays. In KBr only small distortions are observed. In RbI larger pressure effects occur both in the shape of the mosaic distribution function and in the integrated reflecting power of the measured rocking curves. These effects may have some connection with the pressure induced phase transition in alkali halides.

2.4 Improvement of the convolution approximation

O.J.Eder

An improvement of the convolution approximation for the coherent scattering law has been found which satisfies the known moment conditions by using an interpolation function.

REAKTORINSTITUT DES VEREINS ZUR FÖRDERUNG DER ANWENDUNG DER  
KERNENERGIE, TECHNISCHE HOCHSCHULE GRAZ

1. On the Theory of Coupled Core Configurations

E.Ledinegg, H.Rabitsch

A core consisting of more than one fuel zone can expediently be understood as coupled core configurations, if the individual multiplying regions differ in their properties as regards neutron physics, and if there is only little reaction. That makes it possible to calculate the flux distribution and the buckling for this multi-layer problem by applying the first order perturbation theory with optional arrangement and shape of the fuel zones. In the present work the core configuration is regarded as a multiple degenerated system (with n-zones the system is n-fold degenerated). The fuel zones are completely uncoupled in the initial state, and only after inserting intermediate layers they can come to an interaction. In this case the degeneration of the system is generally removed.

---

\* Institut Max von Laue - Paul Langevin, Grenoble

For a simple example we treat a three zones core in slab geometry and compare the results of the perturbation theory with the exact calculation.

2. Determination of the Activity in Combined Gas-Fluid Flows

Hj.Müller, H.Hubner, H.Lengger

The determination of the activity of small amounts of tiniest particles in flowing gas meets with considerable difficulties, if large quantities of gas occur, as the retention time of radioactive particles at the detector is very short.

The present investigation tries to determine the wear of piston rings in two stroke engines, which first appears in the exhaust gas. Two different methods are used: the enriching of radioactive particles in a filter which is continually measured out, or the chemical dissolution of the particles in a fluid. In this case the flow method helps to determine the radioactive component. Both ways demonstrate the abrasion depending on the operating conditions of the two-stroke engine.

3. Determination of the Resonance Self-Shielding in Materials of a Medium Atomic Weight

M.Heindler

To examine how far the up to now little regarded phenomena of resonance self-shielding in materials of medium atomic weight (Fe, Cr, Ni, Na...) are responsible for the discrepancy between theory and experiment with differential dates, respectively for the correspondence of integral dates - evidently caused by a compensation of errors - studies on s-, p- and d-resonances are carried out together with the reactor centers Saclay and Cadarache.

Improvements in regard to the comprehension of the Doppler-broadening in the calculation of the energy-dependent cross sections obtained from the resonance parameter are achieved, and the approximations concerning the computation of self-shielding factors are stated for the element Fe and compared with those used up to now.

4. Determination of the Leakage in Cell Calculation

M.Heindler

The theoretical determination of neutron physical parameters of a reactor assembly is preceded by the determination of the neutron flux  $\Phi(r, E)$ . The resonance structure of the cross sections and the heterogeneity of the individual reactor zones exclude ana-

lytical methods as well as multi-layer multi-group approximations. So one is left to cell calculations which disregard the spatial limitation of the examined region.

A method is presented which allows the determination of the neutron leakage from a heterogeneous domain without giving up the simple boundary condition of ideal reflexion. The energetic and spatial fine structure of the neutron flux in a cell with the boundary condition Albedo = 1 are determined in an iterative process. Then a reaction-equivalent homogeneous medium is defined and the buckling-dependent "leakage cross sections", introduced into the cell calculation as fictitious cross sections, are determined. This method can also be applied for the case of nonisotropic transfer cross sections.

5.     Project Study "Pebble Bed Reactor with Liquid Cooling"  
       M. Heindler

5.1    Design of Spherical Fuel Elements for a Power Pile with Liquid Cooling

According to the patent application of Prof. Dr. M. Ledinegg and Dr. F. Fraß on water-moderated pebble bed reactors a project study in three parts has been performed. Part 1 of this study concerns the thermal behaviour of the spherical fuel elements.

First of all the three types of spherical fuel elements are defined of which can be expected that they will meet the requirements of neutron physics and thermodynamics.

By regarding the technological and thermodynamic conditions the internal structure of the three types of fuel elements is determined. Then follows the calculation of the temperature distribution in the fuel elements. To introduce the effective temperatures of the individual zones of the fuel elements offers the advantage that the expenditure needed for an exact calculation can be considerably reduced. The formulas for the effective temperature of homogeneous spherical shell zones are deduced. Then the effective temperatures of all fuel element zones are computed, whereby assumptions on the heat transfer coefficient are to be made.

5.2    Neutron Physical Foundations

In the second part of the project study, devoted to neutron physical studies, the transport equation has been put down in a way that it is applicable to all geometries and heterogeneous structures which might be considered for reactor design. This approach is such that the numerical solution does not get prohibitively involved, even if anisotropic scattering processes and micro-inhomogeneities of the fuel (e.g. coated particles) are taken into account.

For that purpose the  $B_N$ -approximation of the Boltzmann equation in integral formulation is derived from the integro-differential transport equation. With the help of the first collision kernels relations between the scalar neutron flux and the neutron current are obtained. This leads to an integral equation for the space- and lethargy-dependent neutron flux. The energy variable is made accessible to numerical treatment with the help of the multi-group formalism, the space coordinates by means of the modified collision probabilities and a multizone mesh.

6. On the Theory of Gamma-Absorption in Scintillation Detectors of Cylindrical Geometry

H. Hubner

For concluding from the measured counting rate on the disintegration rate of a radioactive preparation the dependence of the impulse rate on the effects occurring in the counting arrangement must be known.

The dependence on the sensitivity, respectively on the "stopping power" in a cylindrical NaJ(Tl) scintillation counter is to be examined by using a rather rarely employed geometrical assembly. A point source, respectively line source, is on a straight line parallel to the cylinder axis; its distance from the axis of the cylinder is larger than its radius.

7. Measurement of Cross Sections with the Pile-Oscillator Method

W. NINAUS

A measurement system of high sensitivity for the determination of cross sections has been developed in form of a pneumatic pile-oscillator, which is to be installed in the central channel of the SAR Graz. With the help of this apparatus the calibration and sensitivity measurements with the  $1/v$  absorber boron have been accomplished.

In the medium S/M range deviations of the measured values from the calculated ones have been found for tungsten (thin slab-shaped samples) at examining the effective resonance integrals\*. By applying the pile oscillator method, a larger S/M interval is to be measured out in order to find out by comparison with theoretical-numerical results, if errors in the cross sections are responsible for the above mentioned deviations.

---

\* H. Heimel, M. Heindler, Effektive Resonanzintegrale von Molybdän, Wolfram und Tantal in ebener Geometrie; Atomkernenergie 20 (1972).

## 8. Transport-Theoretical Treatment of the Multisphere Problem

F. Schürer

In the determination of the system parameters of Wigner-Seitz cells in pebble beds the spatial anisotropy of the flux distribution is disregarded. It is assumed that on a spherical shell, concentric to the center of the unit cell, the net current vanishes or takes a constant value. To judge the error arising from that proceeding it is necessary to calculate the flux distribution with paying regard to the influence of neighbouring spheres.

First two, and the three spherical fuel elements are examined in an infinite, diffusing medium, and the flux distributions are approximately calculated with the help of the one group- and two group transport theory. A spatially constant, isotropic source distribution is used as a stimulation in the entire domain. The fluxes are represented by Neumann's series, the convergence and uniqueness of which is proved in  $L_\infty$ . This method can be extended to the case of  $n \geq 3$  neighbouring spheres.



**PROGRESS REPORT**  
**to INDC on**  
**NUCLEAR DATA RESEARCH**  
**performed at the**  
**Nuclear Energy Research Center**  
**C.E.N./S.C.K.**

**2400 - Mol, BELGIUM**

**July 1974**

## 1. NEUTRON SPECTROMETRY

(Joint SCK/CEN-CBNM(Euratom)-RUCA neutron cross-section programme. Contract Euratom-SCK/CEN N° 002/66/12 - PG PG B/Av. n° 2)

### Total cross-section of $^{226}\text{Ra}$ .

H. CEULEMANS

and long-lived  $^{226}\text{Ra}$  is probably the only naturally occurring nucleus on which no neutron resonance cross-section data are available above 40 eV. In the preceeding progress report a measurement of the total cross section between 0.02 eV and 1 eV with the BR2 crystal spectrometer has been reported. The measurements have now been extended up to about 700 eV neutron energy at the Linac CBNM using the same sample.

The transmission experiments with a thickness of  $5.9 \cdot 10^{-3}$  atoms/barn of  $^{226}\text{Ra}$  in the beam have shown resonances at the following energies (in eV) : 39.81 ; 55.66 ; 88.29 ; 237.38 ; 262.96 ; 291.42 ; 329.29 ; 347.58 ; 377.07 ; 385.10 (?) ; 397.93 ; 524.08 ; 628.01 ; 630.95 ; 676.97. Taking into account the resonance at 0.539 eV, this would give  $\bar{\Gamma} = 42.3$  eV and lead to an average reduced neutron width of  $0.004 \text{ eV}^{1/2}$ , if a strength function of  $10^{-4} \text{ eV}^{-1/2}$  is assumed. The data have been obtained using a flight path of 29.73m. The timing resolution varied from 40 ns to 320 ns in four zones

starting at 688 eV with zone limits at 306 eV, 110 eV, 34 eV and 9.5 eV. Our measuring conditions allow a minimum sensitivity at the highest measured energy of about 35 barn-eV cross-section integral which corresponds to a resonance with a reduced width of 0.05 times the average. The conclusion is that very few resonances have been missed.

The observed resonance spacing provides information in a mass region where few data are available. The nearest even nucleus is  $^{232}\text{Th}$  with an s-level spacing of 16.7 eV (F. Rahn et al. Phys. Rev. C 6, 1854 (1972)). The Q-value for the (n, $\gamma$ ) reaction is 4.787 MeV in  $^{232}\text{Th}$  (from the 1971 Atomic Mass Evaluation by N.B. Gove and A.H. Wapstra) and 4.565 MeV in  $^{226}\text{Ra}$ . This difference is too small to explain the large difference in the level density.

Cross-section measurements on  $^{237}\text{Np}$

F. POORTMANS, L. MEWISSEN, G. ROHR\*, J.P. THEOBALD\*,  
G. VANPRAET\*\*, H. WEIGMANN\*

Capture, scattering and total cross-section measurements have been performed between 7 eV and 250 eV on a 30 m flight path of the CBNM Linac. The partial cross-section measurements were done with a sample thickness of  $1.372 \cdot 10^{-3}$  at./barn. The total energy detector (two  $\text{C}_6\text{F}_6$  scintillators) was used as capture detector and a set of six  $^3\text{He}$  gaseous scintillators as scattering detectors. The analysis is in progress.

---

\* CBNM, Euratom, Geel

\*\* R.U.C. Antwerpen

The total cross-section was measured for three samples with thickness of respectively  $1.682 \cdot 10^{-3}$ ,  $5.231 \cdot 10^{-3}$  and  $2.316 \cdot 10^{-2}$  at./barn. The area analysis has been completed up to 50.5 eV for the three samples. The neutron widths were obtained for 62 resonances and the capture widths for 19 resonances. The shape analysis was completed only for the thinnest sample measurements. From this shape analysis, the capture width for 28 resonances could be deduced.

Although the analysis is not yet completed one can already deduce the following preliminary results :

- (1) From the thin sample shape analysis one obtains a mean capture width of 45.2 meV and from the area analysis a value of 46.1 meV. The error can be estimated as approximately 5 %. This result is in good agreement with the Saclay value of 44 meV,
- (2) Our previous results for 14 strong resonances from the 1970 run disagree with the present results. We could not find any error in the normalization or in the analysis of the first experiments. The most probable explanation, however, is that the sample was damaged during the measurements. Indeed, the previous sample ( $\varnothing = 83$  mm) was made of only 8 g of neptunium oxide powder canned between two aluminium plates of 0.25 mm thickness. This corresponded to a layer thickness of only 1 mm and it is very difficult to keep such thin layers homogeneous during long term experiments. The present experiments could be done with thicker samples due to the availability of 35 grams of neptunium oxide, and the canning plates are 2 times thicker.

Partial cross-section measurements on  $^{238}\text{U}$

H. WEIGMANN\*, L. MEWISSEN, F. POORTMANS, G. ROHR\*, G. VANPRAET\*\*

A new series of partial cross-section measurements on  $^{238}\text{U}$  has been started. As a first step, the capture cross-section has been measured up to 1.8 keV neutron energy with  $\text{C}_6\text{F}_6$  liquid scintillator detectors, which simultaneously yield information on the gross shape of the capture  $\gamma$ -ray spectrum. This information is of interest for the analysis of coupling conditions in the sub-barrier fission process, and hopefully may allow assignment of some stronger p-wave resonances.

The scattering cross-section was measured with a very thin sample ( $5.527 \cdot 10^{-5}$  atoms / barn) between 15 eV and 1 keV using  $^3\text{He}$  gaseous scintillator system as neutron detector. A contribution from resonant capture is not detected and the total background is very low ( $4 \cdot 10^{-3}$  of the intensity in the detector if all the neutrons were scattered.)

Additional measurements with samples of different thickness are planned.

---

\* CBNM, Euratom, Geel

\*\* R.U.C. Antwerpen

Resonance parameters and statistical properties of  $^{236}\text{U}$

L. MEWISSEN, F. POORTMANS, G. ROHR\*, J.P. THEOBALD\*,  
G. VANPRAET\*\*, H. WEIGMANN\*, R. WERZ\*

The scattering, capture and transmission measurements of  $^{236}\text{U}$  have been analyzed to obtain  $\Gamma_n$ -values for 97 resonances and  $\Gamma_\gamma$ -values for 57 among them, up to 1.8 keV. The energy  $E_0$  of 50 resonances up to 3.1 keV has been determined from the same experiments. The statistical properties of the resonance parameters have been deduced from the parameters of the individual levels. Below 1200 eV the mean level spacing  $D$  was found to be :

$$\bar{D} = (17.3 \pm 0.5) \text{ eV.}$$

The experimental distribution of  $D$  agrees with the calculated Wigner distribution.

The mean capture width  $\bar{\Gamma}_\gamma$ , an important value for the calculation of the  $^{238}\text{Pu}$  production in reactors, was obtained by weighting over 57 resonances :

$$\bar{\Gamma}_\gamma = \{23.0 \pm 0.5 \text{ (statistic.)} \pm 1.0 \text{ (systematic) meV.}\}$$

The average reduced neutron width  $\bar{\Gamma}_n^0$  up to 1200 eV is found to be :

$$\bar{\Gamma}_n^0 = (2.03 \pm 0.34) \text{ meV.}$$

Finally the neutron strength-function,  $S_0 = \bar{\Gamma}_n^0/D$ , deduced from the resonance parameters, has the value :

$$S_0 = (1.05 \pm 0.15) 10^{-4}.$$

---

\* CBNM, Euratom, Geel

\*\* R.U.C. Antwerpen

Only 5 % of the levels have a reasonable possibility of being enhanced by p-wave neutrons, as has been calculated according to the formalism of Bollinger and Thomas (Phys. Rev. 171, 1293, (1968)). The number of degrees of freedom  $\nu$ , for the  $\chi^2$ -distributions of the reduced neutron widths and of the radiation widths have been determined. For the neutron width distribution, it was found that  $\nu = 1.5 \pm 0.1$ . For the radiation width distribution,  $\nu = 83 \pm 12$ , which is a typical value in the actinide region.

According to a formalism of Fuketa and Harvey (Nucl. Instr. and Methods 33, 107 (1965)) the number of missed levels was calculated with a computer code. In the case of  $^{236}\text{U}$  nine small levels should be missed. Taking into account this value, the number of degrees of freedom for  $\Gamma_0$  agrees very well with  $\nu = 1$ . This means that the s-wave mean level spacing should be  $D = (15.2 \pm 0.5) \text{ eV}$ , instead of the value mentioned above.

Total cross-section of  $^{143}\text{Nd}$

H. CEULEMANS

The analysis of the data obtained previously at the Nevis Synchro-cyclotron of Columbia University N.Y. has been continued. Results were obtained on resonance parameters for up to  $\sim 4 \text{ keV}$  neutron energy.

The conclusion from the comparison between our data and the results obtained by other authors is that the strength function  $0.5 [S_0(3^-) + S_0(4^-)]$  is  $(3.42 \pm 0.7) 10^{-4} \text{ eV}^{-1/2}$  where  $S_0(3^-)$  and  $S_0(4^-)$  are the partial s-wave strength function for  $3^-$  and  $4^-$  compound nucleus spin states. The strength function shows no variation outside the normal fluctuations, from one energy interval to the other, or from one spin state to the other.

## 2. FISSION PHYSICS AND CHEMISTRY

### Search for $^{110}\text{Ru}$

P. del MARMOL and P. FETTWEIS

It was attempted to separate the still dubious  $^{110}\text{Ru}$  isotope from other fission products of  $^{235}\text{U}$  by a fast radiochemical separation using the BR1 "chemical rabbit" and to determine its half-life by measuring the 374 keV  $\gamma$ -ray decaying from its daughter  $^{110}\text{Rh}$  (5 s).

The separation procedure was based on the formation of the volatile  $\text{RuO}_4$  by passing  $\text{Cl}_2$  through a basic solution containing the fission products. A typical recovery yield for Ru was 10 % for a 5 s burst when Ru was recovered on polyethylene beads heated to  $90^\circ \text{C}$ . Although the decontamination factors from other fission products were high, up to the present time any 374 keV activity was still blurred by the activity of large fission yield iodine activities. This could also be due to the very low fission yield of  $^{110}\text{Ru}$  and possibly to a very short half-life.

Further tests are underway.



Fission barrier measurements at the Ottignies cyclotron

\*  
P. del MARMOL and F. HANAPPE)

About 15 fission cross-sections were measured for the  $^{185}\text{Re}$  compound nucleus obtained by bombarding  $^{181}\text{Ta}$  with  $\alpha$ -particles of energies from 28.5 to 90 MeV and measuring the fission products in glass detectors, etched in HF, and counted through a microscope.

Fission cross-sections varied from  $2.7 \times 10^{-33}$  to  $1.3 \times 10^{-27} \text{ cm}^2$  and showed the expected exponential rise.

The analysis of the results is underway.

JOINT SCK/CEN-CBNM (EURATOM) STUDIES IN FISSION PHYSICS  
AND STANDARDS.

(Contract EUR/C/4146/67 f)

Ratio of the ternary (LRA) to binary fission cross-section  
induced by resonance neutrons

C. WAGEMANS\*\*, A.J. DERUYTTER\*\*\*

$^{239}\text{Pu}$  : This work was presented at the Third Symposium on Physics and Chemistry of Fission, Rochester (USA) and published in detail.

$^{241}\text{Pu}$  : With the same basic apparatus as used for the  $^{239}\text{Pu}$  T/B experiment two sets of data were obtained with different sets of surface-barrier detectors.

---

\* I.I.S.N. bursar, U.L.Bruxelles

\*\* NFWO, aangesteld navorser, Rijksuniversiteit Gent and S.C.K./C.E.N.

\*\*\* now at "Instituut voor Nucleaire Wetenschappen",  
Rijksuniversiteit Gent

The measurements were performed at a 8 m flighthpath and covered the energy region from 0.1 eV to 55 eV ; the bias in the ternary  $\alpha$ -spectrum was 15 MeV (aluminium foil + electronic bias) and the corresponding pulse-height spectrum was checked continuously. A rough analysis of both sets of data indicated that they are consistent. It was found that the T/B ratio varies from resonance to resonance, although less marked than in the  $^{235}\text{U}$  and  $^{239}\text{Pu}$  case. The measurements are extended so as to obtain a better statistical accuracy on T/B for some smaller resonances.

Absolute determination of the ternary (LRA) to binary fission cross-section ratio for thermal neutron induced fission in some fissile isotopes.

C. WAGEMANS\*

In recent years the absolute determination of the Long Range Alpha particle yield for fission induced by thermal neutrons received little attention despite the rather strong discrepancies remaining between the different results.

The efforts were mainly concentrated on  $^{235}\text{U}$ .

Recently some new experiments were performed by Marshall and Vorobiev, resulting in a considerably lower LRA-yield than generally adopted until now, and by Kugler and Clarke who claimed to have detected also a short range  $\alpha$ -component which would result into a much higher ternary  $\alpha$ -yield.

---

\* NFWO, aangesteld navorser, Rijksuniversiteit Gent and S.C.K./C.E.N.

Due to the importance of this LRA-yield for our measurements reported previously, we started a systematic study of this phenomenon at the BR2 high flux reactor. LRA pulse-height spectra and the corresponding binary fission pulse-height spectra for  $^{233}\text{U}$  and  $^{235}\text{U}$  were measured with and without Cd into the thermal neutron beam. A rough analysis of the data indicates a lower LRA yield for both isotopes than previously adopted.

Moreover the results with and without Cd in the beam are the same within the statistical accuracy.

The measurements are extended further and a more precise analyzing program is being prepared.

Total kinetic energy of fission fragments in  $^{235}\text{U}$  resonances

C. WAGEMANS\*, A.J. DERUYTTER\*\*

The detection system has been improved and the measurements have been started at the CBNN Linac.

Scattering of fission fragments

A.J. DERUYTTER and Gerda WEGENER-PENNING

\*\*\*

An experiment was started to study the backscattering of fission fragments from solid surfaces.

The aim of the experiment is to study the correlation between the Z- and A-values of the scattering foils and the scattering angle, the intensity and the energy of the scattered fragments.

and

\* NFWO, aangesteld navorser, Rijksuniversiteit Gent / S.C.K./C/E/N/  
\*\* now at "Instituut voor Nucleaire Wetenschappen", Rijksuniversiteit Gent

\*\*\* IWONL, aangesteld navorser, Rijksuniversiteit Gent and S.C.K./C.E.:

Several scattering foils, covering a wide range of Z-values were chosen.

Preliminary measurements with a thin  $^{235}\text{U}$  source and 4 surface barrier detectors were done at the BR1 reactor. A computerprogramme for the data handling was written. The final measurements have been started at the BR2 reactor.

Normalization of fission cross-sections in the resonance region.

C. WAGEMANS\*, A.J. DERUYTTER\*\*

$^{233}\text{U}$  : A new measurement was done at a 8 m station of the Linac in the energy region 0.01 - 30 eV. These data were analyzed and compared with previous results. Based on these and on our previous measurements we propose a common normalization procedure via the fission integral

$$\int_{8.1 \text{ eV}}^{17.6 \text{ eV}} \sigma_f(E) dE = (968.7 \pm 10) \text{ barn.eV}$$

using as reference :  $\sigma_f^{\text{O}} = 533.7 \text{ barn.}$

The complete results are finalized in a report sent to Nuclear Science and Engineering for publication.

$^{241}\text{Pu}$  : Two series of measurements were performed at a 8 m flightpath. In the first series we went down to 0.01 eV allowing a direct normalization to the 2200 m/s fission cross-section :

\* NFWO, aangesteld navorser, Rijksuniversiteit and S/C.K./C.E.N.

\*\* now at "Instituut voor Nucleaire Wetenschappen",  
Rijksuniversiteit Gent

here Rh was used as a permanent neutron filter. The second series covered the energy region from 0.1 eV to 55 eV using Cd as a permanent filter. Background laws were determined with the black sample technique. These data are being analysed.

Fission cross-section of  $^{235}\text{U}$  in the range up to 100 keV

A.J. DERUYTTER<sup>\*\*</sup>, C. WAGEMANS<sup>\*</sup>

After substantial improvements in counting-rate and signal-to-background ratio, these measurements were continued at a 30 m flightpath station.

The energy region from 5 eV to about 100 keV was covered (useful region 5 eV - 30 keV), allowing a normalization to our previously determined fission integral

$$\int_{7.8 \text{ eV}}^{11 \text{ eV}} \sigma_f(E) dE = (240.2 \pm 2.1) \text{ barn.eV}$$

A first run is under analysis, but the data taking will continue in order to improve the statistical accuracy.

---

\* NFWO, aangesteld navorser, Rijksuniversiteit Gent and S.C.K./C.E.N.

\*\* now at "Instituut voor Nucleaire Wetenschappen",  
Rijksuniversiteit Gent

The mass distribution of neutron-induced fission for  
 $^{239}\text{Pu}$  at the 0.297 eV resonance.

P.H.M. VAN ASSCHE, G. VANDENPUT\*, L. JACOBS,\* J.M. VAN den  
CRUYCE\*, R. SILVERANS\*

The mass distribution of fission products for neutron-induced fission of  $^{239}\text{Pu}$  has been studied in an epi-Sm spectrum, with more than 90 % of the fissions being due to the 0.297 eV resonance. The experimental method consists in a detailed comparison of gamma spectra from  $^{239}\text{Pu}$  targets, irradiated in resp. thermal and epi-Sm spectra. Fission product identification is made without chemical separation ; only gamma energies and lifetimes are used for this purpose.

Significant variations of the mass distribution for epi-Sm induced fission are observed for more than 7 mass numbers.

The decrease in symmetric fission, as observed previously, is confirmed. In addition, evidence for a narrowing of the mass distribution is also found. This could be related to the increase of  $(0.73 \pm 0.04)$  MeV in the total kinetic energy of the fission products of the epi-Sm fission of  $^{239}\text{Pu}$ , as compared to thermal neutron fission (J. Toraskar and E. Melkonian, Phys. Rev. 4C, 267, (1971)).

---

\* Departement Natuurkunde, K.U. Leuven

**PROGRESS REPORT to I.N.D.C.**

**from GREECE**

**August, 1974**

**Edited by**

**S. Dritsa**

**N.R.C. "Demokritos"**

**Athens, Greece**

## 1. Gamma-Ray Spectroscopy

P.A. Assimakopoulos N.R.C. 'D',, G. Andritsopoulos and N.H. Gangas, University of Ioannina, A.Hartas and C.T. Papadopoulos, N.R.C.'D' and University of Ioannina.

Nuclei in the  $f\ 7/2$  shell were investigated through the inelastic scattering of protons and the  $(p,n)$  reaction. The protons were obtained from the Demokritos' T II/25 Tandem Van der Graaff accelerator. The information was extracted from singles gamma-ray spectra taken at a series of angles with respect to the incident proton beam.

From these spectra exact energies of transitions, branching ratios and in favourable circumstances, spins and mixing ratios were extracted. In addition half-lives of excited states were determined by performing Monte Carlo simulations of Doppler shifted peaks.\*

A systematic study of the odd Copper and odd Zinc isotopes is currently under completion.

---

\* "  $0^+ \rightarrow 1^+$  inelastic transition in  $^{12}\text{C}$  induced by complex particles ", P.A. Assimakopoulos, G. Andritsopoulos, N.H. Gangas, Bull. Am. Phys. Soc., Vol. 19, 1974 (431).

## 2. Spin-iso-spin flip reactions.\*

P.A. Assimakopoulos, N.R.C.'D', N.H. Gangas and G. Andritsopoulos University of Ioannina, A. Hartas and C.T. Papadopoulos N.R.C.'D' and University of Ioannina.

The inelastic scattering of nuclei of the form  $d + n\alpha$ , ( $n = 0, 1, 2, \dots$ ), is being carried out. The  $d$  above, denotes a proton-neutron system in the triplet state and  $\alpha$  the nucleus of  $^4\text{He}$ . Examples of such nuclei are  $^2\text{H}$ ,  $^6\text{Li}$ ,  $^{10}\text{B}$  etc. These nuclei exhibit a  $J=0$ ,  $T=1$  state in the vicinity of 2.5 MeV and the population of these states requires a  $\Delta J = \Delta T = 1$  transition, so that in a microscopic picture only the Majorana term  $(\sigma_1 \cdot \sigma_2)(\tau_1 \cdot \tau_2)$  of the two-nucleon potential is expected to contribute.



The aim of this research is to investigate systematically, the Majorana term of the two-nucleon potential in a nuclear environment of spectator  $\alpha$ -particles as in the cases described above.

\* Activity financed in part by NATO contract SA;5-2-05B(694)823(74)MDL.

3. Excited States in  $^{107}\text{Ag}$  from the decay of  $^{107}\text{Cd}$ .

T. Paradellis and C.A. Kalfas.

The decay of  $^{107}\text{Cd}$  has been studied with Ge(Li) and Si(Li) detectors. Thirty three gamma rays were observed in this decay. Gamma-gamma directional correlation experiments were used to determine spins. Excited states have been located at 93.1(7/2<sup>+</sup>), 125.4(9/2<sup>+</sup>), 324.8(3/2<sup>-</sup>), 423.0(5/2<sup>-</sup>), 786.7(3/2<sup>-</sup>), 922.1(5/2<sup>+</sup>), 949.7(5/2<sup>-</sup>), 972.9(7/2<sup>-</sup>, 5/2<sup>-</sup>), 1143.0(5/2<sup>-</sup>), 1223.0(5/2<sup>-</sup>), 1258.8(5/2<sup>-</sup>), 1325.7 (5/2<sup>-</sup>) keV. A tentative level has been introduced also at 1389.8(7/2<sup>+</sup>) keV.

4.  $\gamma$ - $\gamma$  correlations in  $^{150}\text{Sm}$

C.A. Kalfas, T. Paradellis, A. Xenoulis.

Using a proton beam from the Tandem Van der Graaff accelerator, a natural Nd target was bombarded to get  $^{150}\text{Pm}$  by the Nd(p,n)Pm reaction. The gamma spectra from the decay of the  $^{150}\text{Pm}$  to  $^{150}\text{Sm}$  have been measured. Studies of mixing ratios using ( $\gamma$ ,  $\gamma^*$ ) correlation techniques, are in progress.



PROGRESS REPORT FROM ITALY SUBMITTED TO 7<sup>th</sup> INDC MEETING

I. EXPERIMENTAL WORK

A. Neutron Reactions

A.1 Padua Group

A.1.1. Forward scattering of 2 MeV neutrons from oriented  $^{165}\text{Ho}$

The scattering in the forward hemisphere of 2 MeV neutrons from a  $^{165}\text{Ho}$  sample oriented normally to the scattering plane, with a nuclear orientation degree of 0.25 was measured. A deformation effect given by  $\{[G(\theta) \text{ oriented} / G(\theta) \text{ unoriented}] - 1\}$ , reaching its maximum value of  $0.13 \pm 0.02$  at  $70^\circ$  is observed.

A.1.2. Fast neutron transmission through a polarized Holmium target

The transmission of fast neutrons through a polarized holmium sample is measured. A "deformation effect" is observed in good agreement with a theoretical prediction.

A.1.3. Polarization of neutrons elastically scattered from Oxygen

A systematic measurement of the polarization of neutrons elastically scattered from  $^{16}\text{O}$  was carried out at seven angles from  $25^\circ$  to  $155^\circ$  at the energies of 2.25, 2.56, 2.76, 3.00, 3.35, 3.56 and 3.90 MeV using the PAROL polarimeter.

In the experiment the polarized neutrons were produced from the  $^7\text{Li}(p,n)$ ,  $^{12}\text{C}(d,n)$  and  $\text{O}(d,n)$  reactions, and the target was liquid oxygen.

The data correction and analysis are in progress.

A.2 Trieste Group

A.2.1. The  $^{12}\text{C}(n,n)^{12}\text{C}$  reaction

The elastic scattering of neutrons from carbon was studied in the incident neutron energy range 1.98 to 4.64 MeV. Angular distributions were obtained by means of a neutron time-of-flight spectrometer. Data were taken for eight energies and for thirteen scattering angles. A phase-shift analysis was carried out and a set of phase angles capable of reproducing the elastic data was obtained.

### A.2.2. Elastic scattering of fast neutrons by ${}^6\text{Li}$

The angular distributions of the neutrons scattered by  ${}^6\text{Li}$  have been measured by means of a neutron time of flight spectrometer, for eight values of the incident neutron energy in the interval from 1.98 MeV to 4.64 MeV. The angular distributions have been determined at thirteen angles in the interval from  $30^\circ$  to  $140^\circ$ , in the laboratory frame of reference. The differential and the total elastic cross-sections have been then deduced from the angular distributions.

## B. Charged Particle Reactions

### B.1 Padua Group

#### B.1.1. Analogue resonances in ${}^{48}{}^{50}\text{Ti}+p$ reactions

The analogue states of the 1.72 MeV  $J^\pi = 1/2^-$  level in  ${}^{49}\text{Ti}$  and of the  $J^\pi = 3/2^-$   ${}^{51}\text{Ti}$  ground state are studied via the (p,p) and (p, $\gamma$ ) reactions on  ${}^{48}\text{Ti}$  and  ${}^{50}\text{Ti}$ , respectively. Partial and total widths are given and spectroscopic factors are calculated. The elastic proton widths  $\Gamma_p$  correspond well with the results obtained from (d,p) reactions on the same target nuclei. The strengths and  $\gamma$ -ray branching ratios of the above mentioned resonances, together with the doublet at  $E_p = 1007$  and 1013 keV split analogue of the 1384 keV level in  ${}^{49}\text{Ti}$  ( $J^\pi = 3/2^-$ ) have been studied. Excitation energies and branching ratios of  ${}^{49}\text{V}$  and  ${}^{51}\text{V}$  bound states are also given. The results are compared with the ones obtained from other similar investigations.

#### B.1.2. Lifetimes of the first $7/2^-$ levels in ${}^{35}\text{Cl}$ and ${}^{37}\text{Cl}$

The lifetimes of the first  $7/2^-$  levels in  ${}^{35}\text{Cl}$  and  ${}^{37}\text{Cl}$  were determined to be  $42 \pm 3$  ps and  $27 \pm 4$  ps respectively by means of the plunger technique in the reactions  ${}^{32}\text{S}(\alpha, p)$  and  ${}^{34}\text{S}(\alpha, p)$ . Gamma-rays were detected at  $0^\circ$  in coincidence with backward protons. The experimental M2 transition strengths are in agreement with the prediction of phenomenological shell-wave function.

#### B.1.3. Spin-parity determination from neutron threshold measurements and the second excited state of ${}^{44}\text{Sc}$

The "counter ratio method", i.e. the ratio between slow- and fast-neutron yields has been used in the  ${}^{44}\text{Ca}(p, n){}^{44}\text{Sc}$  reaction to assign spin and parities to some  ${}^{44}\text{Sc}$  levels. The  ${}^{44}\text{Ca}(p, n){}^{44}\text{Sc}$  reaction has been

investigated by using the proton beam of the Van de Graaff accelerator of the Laboratori Nazionali di Legnaro. The results are consistent with the following spin-parity assignments to  $^{44}\text{Sc}$  levels: ground state ( $2^+$ ), 68 keV state ( $1^-$ ), 146 keV ( $0^-$ ), 667 keV ( $1^+$ ). Of special interest is the  $0^-$  assignment to the second excited state at 146 keV.

#### B.1.4. Study of $^{52}\text{Mn}$ by heavy-and light-ion reaction

The  $^{52}\text{Mn}$  nucleus has been studied by means of the following reactions:  $^{51}\text{V}(\tau, 2n)^{52}\text{Mn}$  (at the Van de Graaff of the Laboratori Nazionali di Legnaro, Padova) and  $^{24}\text{Mg}(^{32}\text{S}, 3pn)^{52}\text{Mn}$  (at Munich Tandem).

From the study of  $\gamma$ - $\gamma$  coincidences,  $\gamma$ -ray angular distributions and excitation functions (these last in the  $\tau$ -induced reaction), high-spin states are proposed at  $E_x=1492$ , 2908 and 3837 keV with  $J^\pi=(8^+)$ ,  $(9^+)$ ,  $(11^+)$ .

#### B.1.5. $^{51}\text{V}(^3\text{He}, d)^{52}\text{Cr}$ Reactions and Shell-Model Calculations for $^{52}\text{Cr}$

Angular distributions of the  $(^3\text{He}, d)$  reaction on  $^{51}\text{V}$  have been measured at 10.48 MeV with a counter telescope. Spectroscopic factors and values of  $^{52}\text{Cr}$  levels up to 7 MeV excitation energy were obtained by comparing the data with distorted wave Born approximation theory. Some unreported levels excited by  $\ell=1$  proton transfer have been observed. Shell-model calculations predict well the  $1f_{7/2}$  spectroscopic strength, but fail in reproducing the observed  $2p_{3/2}$  strength.

### B.2. Trieste Group

#### B.2.1. Study of the $T=3/2$ states in $^{33}\text{Cl}$ through the $^{32}\text{S}(p, n)^{32}\text{S}$ reaction

The study of the three lowest  $T=3/2$  states in  $^{33}\text{Cl}$  has been completed, allowing to propose the isospin  $T=3/2$  for the states at  $E_x=(5556\pm 12)$ ,  $(6998\pm 12)$ ,  $(7414\pm 12)$  keV ( $J^\pi=1/2^+$ ,  $3/2^+$ ,  $5/2^+$  respectively). The excitation energies of the three levels correspond to an incident proton energy of  $(3370\pm 1)$ ,  $(4855\pm 3)$ ,  $(5284\pm 3)$  keV respectively. The experiments have been performed by using the facilities of the 5.5 MeV accelerator of the "Laboratori Nazionali di Legnaro" (LNL). The elastic excitation function has been analyzed as a superposition of a background scattering (described by a spherical optical model) and of a resonant term (described by a simplified multilevel Breit-Wigner expression).

### B.2.2. Gamma decay of the lowest $T=3/2$ state of $^{33}\text{Cl}$

A study of the gamma decay of the  $T=3/2$  states of  $^{33}\text{Cl}$  has been performed by measuring first the gamma decay of the lowest  $T=3/2$  state ( $J=1/2^+$ ,  $E_x=(5556\pm 12)$  keV). The level has been reached by means of the  $^{32}\text{S}(p, \gamma)^{33}\text{Cl}$  reaction, at an energy of the incident proton of 3374 keV. By using large Ge(Li) detectors, the decay has been studied deriving that the  $T=3/2$  level decays with a branching ratio of 92% to the  $J=1/2^+$ ,  $E_x=809$  keV first excited state of  $^{33}\text{Cl}$ , and of 8% to the  $J=3/2^+$  ground state. The radiative width has been also determined.

### B.2.3. $(^3\text{He}, n)$ Reactions

The  $^{24}\text{Mg}(^3\text{He}, n)^{26}\text{Si}$  and  $^{28}\text{Si}(^3\text{He}, n)^{30}\text{S}$  two nucleon stripping reactions were studied at incident energies of  $E_{^3\text{He}} = 4.7$  and 5.5 MeV, using the pulsed-beam time-of-flight technique with the singled charged  $^3\text{He}$  beam provided by the 5.5 MeV Van de Graaff accelerator of the "Laboratori Nazionali di Legnaro". The angular distributions were obtained, in an angular range from  $\vartheta=0^\circ$  to  $\vartheta=150^\circ$  (in the laboratory system), for neutrons from: the ground state ( $J^\pi=0^+$ ), the first-excited state ( $J^\pi=2^+$ ,  $E_x=1.79$  MeV) and the second-excited state ( $J^\pi=2^+$ ,  $E_x=2.78$  MeV) of  $^{26}\text{Si}$ ; and for neutrons from: the ground state ( $J^\pi=0^+$ ) and the first-excited state ( $J^\pi=2^+$ ,  $E_x=2.21$  MeV) of  $^{30}\text{S}$ . The analysis of the data has been made by using the DWBA programme DWUCK.

## B.3. Catania Group

### B.3.1. $(^3\text{He}, \alpha)$ reactions on $^{24}\text{Mg}$ , $^{25}\text{Mg}$ and $^{26}\text{Mg}$

The angular distributions of the  $\alpha$  groups emitted in the  $^{24}\text{Mg}(^3\text{He}, \alpha)^{23}\text{Mg}$  reaction, have been measured in the ~~measured in the~~ angular range  $25^\circ - 160^\circ$  at  $\Delta=5^\circ$  steps and from 9 to 12 MeV of incident energy at 100 keV steps.

The energy averaged angular distributions are interpreted in terms of D.W.B.A. theory.

### B.3.2. Spectroscopic information from subcoulomb stripping reactions

It is known that the spectroscopic factors  $S_{dp}$  extracted by means of the  $(d, p)$  reactions for deuteron and proton energy below the Coulomb barrier, are practically independent on the optical parameters of the incident and outgoing particles.

Nevertheless, also in these conditions, the absolute values of the spectrospin factors are dependent on the geometrical ( $r_{on}$ ,  $Q_n$ ) parameters of the captured neutron potential well.

In order to reduce the ambiguity on the absolute of  $S_{dp}$  we determined the parameters  $r_{on}, Q_n$  in an independent way; <sup>the</sup> ~~they~~ has been made through a comparison of the calculated and the experimental values of the Coulomb displacement energy between an analog state and the parent one.

In particular we analyzed the  $^{40}\text{Ar}(d,p)^{41}\text{Ar}$  reaction data; the measurement of the  $^{22}\text{Ne}(d,p)^{23}\text{Ne}$  reaction is in progress.

### B.3.3. Three bodies reactions in the final state

We studied  $^7\text{Li}+d \rightarrow 2\alpha + n$  at  $E_d \geq 2.5$  MeV. We measured the bidimensional spectra and angular correlation of the  $\alpha$  particles.

The reaction proceeds by the formation of an  $\alpha$ -n complex in the final state, selected by the  $\alpha$ - $\alpha$  coincidences.

The complexes are produced polarized and the polarization degree is deduced from measurements at various azimuthal angles.

The Angular correlation of two  $\alpha$  particles produced by  $^{11}\text{B}+p \rightarrow 3\alpha$  reaction has been measured at  $E_p = 0.9 \div 1.95$  MeV.

We found that the correlation curves are symmetric with respect to the direction of the recoiling  $^8\text{Be}$  in the centre of mass system.

These results indicate that a double sequential decay with  $^{12}\text{C}$  compound nucleus formation is involved.

## B.4. Milano Group

### B.4.1. Preformation probability of $\alpha$ clusters in nuclei measured by means of (p, $\alpha$ ) reaction

Carrying on a previous research, (p, $\alpha$ ) reactions on many elements, in the rare earth region at  $E_p = 18-20$  MeV have been studied. The experiments were performed at the Munich MP tandem Van de Graaff Generator and at the AVF Cyclotron of the University of Milano.

The analysis of the spectrum shape angular distribution and cross-section absolute values shows that the dominant acting mechanism is the pre-compound one, only in some cases a contribution from statistical evaporation is present.

## B.5. Pavia Group

B.5.1. An experimental research on the asymmetry at small angles ( $\theta_{\text{LAB}} < 10^\circ$ ) in the elastic scattering of 40 MeV polarized protons on  $^{40}\text{A}$  nuclei is being done on the Milan AVF cyclotron using a diffusion cloud chamber.

## C. Fission Studies

### C.1. Catania Group

#### C.1.1. Nuclear Fission

We have in progress measurements of fission induced by photons of  $E_{\gamma \text{ max}} = 1000$  MeV with the aim to obtain information on the photofission yields also for elements with low  $Z$ .

At present we have measured the yield of photofission for 28 elements in the range  $Z=83$  to  $Z=29$ . The photon beam was obtained from 1 GeV electrosynchrotron of Frascati and the fission fragments were detected by means of glass plate sandwiches, as previously described.

The analysis of the results are in progress.

### C.2. Milano Group

#### C.2.1. Proton Induced Fission of $\text{Pb}^{207}$

Angular distribution of fission fragments have been measured at incident proton energies  $E_p = 36.4, 39.6, 43.4$  MeV for the reaction  $\text{Pb}^{207}(p,f)$ .

The experiment has been done with the external proton beam of the AVF cyclotron of the Milan University.

The experimental apparatus consists of a scattering chamber with two moving detectors at  $30^\circ$  each other, and one detectors, set at  $90^\circ$  with respect to the incident beam, as reference monitor.

The fission fragments are detected with solid state counters Ortec 7901 of 60  $\mu\text{m}$  depth and 100  $\text{mm}^2$  sensitive area.

The L.S. cross sections and angles are converted to the C.M. system assuming fragments mass corresponding to symmetric fission.

The Q-value is given by  $Q = \langle E_k \rangle - (E_p)_{\text{cm}}$  where the average fragment kinetic energy is evaluated according to the formula  $\langle E_k \rangle = (0.1071 Z^2/A^{1/3} + 22.2)$  MeV where  $Z$  and  $A$  refer to the fissioning nucleus.

A first analysis of experimental anisotropies with the Griffin formula gives an estimation of the anisotropy parameter  $K_0^2$  of the order of 40 for the fissioning nucleus  $\text{Bi}^{208}$ .

### C.3. Pavia Group

#### C.3.1. Angular distribution and angle-energy correlations of $^4\text{He}$ , $^6\text{He}$ and $^3\text{H}$ particles from $^{239}\text{Pu}$ thermal fission

The angular distributions of  $^6\text{He}$  and  $^3\text{H}$  particles have been measured. The characteristics of the results obtained show that the emission of  $^3\text{H}$ ,  $^4\text{He}$  and  $^6\text{He}$  derive from only one mechanism. In addition the angle-energy correlation makes clear that the long-range particles emitted during the



ternary fission assume less or more energy according to the emission distance from either fragment. The energy interval observed in the case of tritons is limited from 3.5 to 7 MeV.

#### D. Integral Measurements

##### D.1. Casaccia Group

##### D.1.1. The $^{23}\text{Na}(n,2n)$ cross-section in a fast spectrum

Previously reported inconsistencies between integral and differential measurements for  $^{23}\text{Na}(n,2n)$  reaction suggested a new measurement in the centre of the TAPIRO fast source reactor. For the present work a high purity sodium sample was irradiated in a fast spectrum with an integrated neutron flux of about  $5 \cdot 10^8$  nvt.  $^{58}\text{Ni}(n,p)$  and  $^{63}\text{Cu}(n,\alpha)$  reactions were used as integral flux monitors.

Relative to the  $^{58}\text{Ni}(n,p)$  monitor, the  $^{23}\text{Na}(n,2n)$  cross section averaged in a fission spectrum has a value of  $.0043 \pm .0008$  mb and the effective cross section in the energy group above 6.5 MeV is  $.260 \pm .05$  mb.

If the results are expressed in terms of the  $^{63}\text{Cu}(n,\alpha)$  reaction, consistency is found if the Fabry integral data are used, while a 40% discrepancy is observed with the differential data by Simons and McElroy.

## II. EVALUATION

- 1) All the evaluation work is carried out at the Centro di Calcolo of CNEN, Bologna, and reported in the Neutron Nuclear Data Evaluation Newsletter.
- 2) The NDF of Cu, Cu-63 and Cu-65 has been completely debugged and the data will be sent to the CCDN in UKNDL format before the end of October 1974 for free distribution.
- 3) The other activities underway have been temporarily stopped, and all the efforts at present are devoted to produce a complete evaluation from thermal up to 15 MeV of the following 24 F.P.:  
Mo-(95,97,98,100); Tc-99; Ru-(101,102,103,104); Rh-103; Pd-(105,107); Ag-109; Cs-(133,135); Pr-141; Nd-(143,145,146,148); Pm-147; Sm-(149,151); Eu-153.

### III. NEW FACILITIES

The fast-thermal RB-2/TV reactor went critical at the beginning of September 1974 in Bologna.

In the framework of a joint CNEN-AGIP/N-CCR/ISPRA-CEA agreement, integral measurements based on the null-reactivity method will be carried out during the 1975 in order to have experimental values of capture integrals of Fe, Ni, Cr in neutron fluxes having energy spectra similar to those of large fast reactors.

ANNUAL REPORT FOR THE YEAR 1973

REACTOR CENTRUM NEDERLAND, PETTEN, THE NETHERLANDS

1. FOM-RCN Nuclear Structure Group

(K. Abrahams)

1.1. Neutron Resonance Spins of  $^{235}\text{U}$  (E.R. Reddingius<sup>\*)</sup>, H. Postma<sup>\*\*</sup>,  
C. Olson<sup>\*\*\*</sup>, D.C. Rorer<sup>\*\*\*\*</sup>) and V.L. Sailor<sup>\*\*\*\*</sup>).

During a stay as guest scientist at the Brookhaven National Laboratory from January 1972 to October 1972, one of the authors (E.R.R.) took part in the experiment reported hereunder. In the first half of 1973 the final evaluation was made and a publication prepared.

Neutron resonance spins of  $^{235}\text{U}$  were determined by measuring the transmission of polarized neutrons through a target with polarized  $^{235}\text{U}$  nuclei. The experiment was performed at the High Flux Beam Reactor of Brookhaven National Laboratory. A beam of polarized neutrons was obtained by Bragg reflection from a magnetized Co-Fe single crystal. The best spectrometer resolution obtained was 0.4 eV at 10 eV neutron energy. The direction of the neutron spin polarization could be reversed. The intensities of the transmitted beam (for parallel as well as antiparallel polarizations of neutrons and nuclei) were measured.

The sample was prepared by pressing 7.8 g uranium monosulfide and an approximately equal amount of lead powder in a die. Uranium enriched to 99.99% in  $^{235}\text{U}$  was used in order to reduce the heat production from  $\alpha$ -decay of  $^{234}\text{U}$  as much as possible. The sample was cooled by adiabatic demagnetization of iron alum grown in a bundle of copper wires for good heat contact. After adiabatic demagnetization data were taken during about eight hours. During this time the sample warmed up from 0.04 K to slightly above 0.1 K. During the experiments the sample was in an external magnetic field of 28.7 kOe.

- 
- <sup>\*)</sup> FOM-RCN Nuclear Structure Group, Petten (N.H.), The Netherlands;  
until 1 July 1973.  
<sup>\*\*</sup>) State University of Groningen, The Netherlands.  
<sup>\*\*\*</sup>) Los Alamos Scientific Laboratory, U.S.A.  
<sup>\*\*\*\*</sup>) Brookhaven National Laboratory, U.S.A.

Experimentally the transmission effect,  $\epsilon$  was determined.

$$\epsilon = \frac{N_{\uparrow\uparrow} - N_{\uparrow\downarrow}}{N_{\uparrow\uparrow} + N_{\uparrow\downarrow}}, \quad (1)$$

where  $N_{\uparrow\uparrow}$  and  $N_{\uparrow\downarrow}$  are the numbers of counts with parallel and anti-parallel polarizations neutron and nuclei. For low values of the nuclear polarization  $f_N$  and neglecting the influences of spectrometer resolution and neutron depolarization in the sample, the transmission effect can be expressed as

$$\epsilon = -f_n f_N N \sigma t \rho. \quad (2)$$

Here  $f_n$  and  $f_N$  are the degrees of neutron and nuclear polarization,  $N$  is the number of nuclei per  $\text{cm}^3$ ,  $\sigma$  is the neutron capture cross section and  $t$  is the target thickness. The parameter  $\rho$  is  $1/(1+1)$  for a resonance with spin  $J = I + \frac{1}{2}$  and  $\rho$  is  $-1$  for a  $J = I - \frac{1}{2}$  resonance. In practice several resonances contribute to the capture cross section and the spectrometer resolution has to be taken into account. In that case the analysis is more complicated and a computer programme has to be used to analyse the data.

The degree of neutron polarization at the sample position was determined by measuring the transmission effect of an indium sample which was also attached to the sample holder. For  $^{115}\text{In}$  nuclei the degree of nuclear polarization in the external magnetic can be calculated (brute force polarization). The value of  $N\sigma t$  was measured and the  $\sigma$  values are known. Hence  $f_n$  can be estimated using Eq. 2.

The degree of nuclear polarization of the  $^{235}\text{U}$  nuclei can in principle be calculated from the known internal magnetic hyperfine field in US. It can also be estimated from the transmission effects of the most prominent resonances of  $^{235}\text{U}$  using Eq. 2.

In our experiment we obtained  $f_n \approx 0.50$  and  $f_N \approx 0.055$ .

The thickness of the sample was such that  $N\sigma t$  was 1-2 for the most prominent resonances. Inserting these numerical values in Eq. 2 shows that transmission effects of few percent can be expected which are positive or negative depending on the spin of the compound nucleus.

The final results are listed in table I and compared to results from a) an earlier experiment with polarized neutrons and polarized nuclei [1];

- b) resonance scattering experiments [2,3];
- c) intensity of primary gamma transition experiment [4];
- d) intensity ratio of secondary gamma transition experiment [5].

It is clear that several new spin assignments have been obtained and that the results presented here, compare reasonably well with the results of the experiments mentioned above.

### 1.2. A study of the $\text{Cu}(n,\gamma)$ reaction

(J. Kopecký)

During the last few years the low lying excited states of the odd-odd nucleus  $^{64}\text{Cu}$  have been the subject of several experimental investigations. In spite of all these efforts, the knowledge of the decay scheme and in particular of the spins is scarce.

In order to extend the spin assignments, the circular polarization of  $\gamma$ -rays from the capture of polarized thermal neutrons has been measured for primary transitions with  $E_\gamma > 5$  MeV and  $I_\gamma > 0.01$ . The results are given in table II for the  $^{63}\text{Cu}(n,\gamma)$  lines and a few strong  $^{65}\text{Cu}(n,\gamma)$  lines. The analysis of 12 primary transitions in  $^{64}\text{Cu}$  yielded 2 unique spin assignments and 8 probable spin values. No correlation between the (d,p) strength and the (n, $\gamma$ ) reduced transition strengths has been found, and a simple explanation in terms of Porter-Thomas fluctuations cannot be excluded for the strong spectra anomaly in the thermal capture. This work has been published in [16].

### 1.3. The $^{50}\text{Cr}(n,\gamma)^{51}\text{Cr}$ reaction

(J. Kopecký)

The analysis of the (n, $\gamma$ ) spectrum from a target enriched to 96.8% in  $^{50}\text{Cr}$  has been completed. The sample was on loan from the Oak Ridge National Laboratory. From 72 transitions ascribed to the  $^{50}\text{Cr}(n,\gamma)^{51}\text{Cr}$  reaction 62 transitions have been placed into a newly constructed decay scheme.

Transition energies, absolute  $\gamma$  intensities, 25 excitation energies, the reaction Q-value ( $9261.7 \pm 0.7$  keV) and branching ratios have been determined with a higher accuracy than in earlier work. For the 8 strongest primary transitions the measured intensities have been compared with those, calculated in the frame of the valency neutron approach. Shortly the data will be ready for publication.

Table I. Neutron Resonance Spins of  $^{235}\text{U}$

$E_n$	$\epsilon$	$J$	
		present	previous
0.275	$-0.515 \pm 0.025$	3	$3^a$
1.14	$+0.618 \pm 0.019$	4	$4^a$
2.04	$-0.88 \pm 0.13$	3	$3^{c,d,(a)}$
3.15	$-0.72 \pm 0.14$	3	
3.61	$+1.61 \pm 0.16$	4	
4.85	$+1.09 \pm 0.06$	4	$4^d,(c)$
6.15	$-0.18 \pm 0.05$	3	
6.39	$+1.39 \pm 0.23$	4	$4^d, 3^c$
7.08	$+0.79 \pm 0.10$	4	
8.79	$+1.30 \pm 0.13$	4 (+30% 3)	$3^b$
9.28	$+0.94 \pm 0.14$	4	
10.16	$+0.51 \pm 0.10$	4	
11.67	$+0.34 \pm 0.07$	4	$4^{b,d}$
12.39	$-1.09 \pm 0.10$	3	$3^{b,d}$
14.0	$-1.18 \pm 0.22$	3	

a) Polarized neutrons, polarized nuclei.

b) Resonance scattering.

c) Intensity of primary gamma transitions.

d) Intensity ratio of secondary gamma transitions.

Table II. Spin determination of  $^{64}\text{Cu}$ ,  $^{66}\text{Cu}$  levels.

f	E <sub>x</sub> (keV)	E <sub>γ</sub> (keV)	λ <sub>n</sub>	c)	d)	e)	f)	g)	h)	i)	j)	α	k)	R	This work J <sup>π</sup> l)	J <sup>π</sup> m)
<sup>64</sup> Cu																
1	0	7916	1+3	1 <sup>+</sup>	1 <sup>+</sup>	0 <sup>+</sup> -3 <sup>+</sup>	1 <sup>+</sup>	1 <sup>+</sup>	1 <sup>+</sup>	1 <sup>+</sup>	0	0	±0.02	-0.10±0.02	1 <sup>+</sup> 2 <sup>+</sup>	1 <sup>+</sup>
2	158.8	7756	1+3	1 <sup>+</sup>	2 <sup>+</sup> (1 <sup>+</sup> )	1 <sup>+</sup> -4 <sup>+</sup>	2 <sup>+</sup> (1 <sup>+</sup> )	2 <sup>+</sup>	2 <sup>+</sup>	2 <sup>+</sup> (0 <sup>+</sup> 1 <sup>+</sup> )	0.17	0.36±0.09	+0.2 ±0.2	+0.2 ±0.2	1 <sup>+</sup> 2 <sup>+</sup>	2 <sup>+</sup>
3	277.8	7637	1+3	1 <sup>+</sup> 2 <sup>+</sup>	2 <sup>+</sup> (1 <sup>+</sup> 3 <sup>+</sup> )	1 <sup>+</sup> -3 <sup>+</sup>	2 <sup>+</sup> (1 <sup>+</sup> 3 <sup>+</sup> )	1 <sup>+</sup> 2 <sup>+</sup>	2 <sup>+</sup>	2 <sup>+</sup> (0 <sup>+</sup> 1 <sup>+</sup> )	0.01	0.02±0.02	0 ±0.05	0 ±0.05	1 <sup>+</sup> 2 <sup>+</sup>	2 <sup>+</sup>
4	344.1	7571	1	1 <sup>+</sup>	(2 <sup>+</sup> 0 <sup>+</sup> )	1 <sup>+</sup> -3 <sup>+</sup>	(2 <sup>+</sup> 0 <sup>+</sup> )	1 <sup>+</sup>	(1 <sup>+</sup> )	2 <sup>+</sup> (0 <sup>+</sup> )	0	0.01±0.04	+0.6 ±0.3	+0.6 ±0.3	0 <sup>+</sup> 1 <sup>+</sup>	1 <sup>+</sup>
5	608.6	7307	1	1 <sup>+</sup> 2 <sup>+</sup>	2 <sup>+</sup> (1 <sup>+</sup> 3 <sup>+</sup> )	1 <sup>+</sup> -4 <sup>+</sup>	2 <sup>+</sup> (1 <sup>+</sup> 3 <sup>+</sup> )	1 <sup>+</sup>	2 <sup>+</sup>	0 <sup>+</sup> (2 <sup>+</sup> )	0	0.05±0.02	+0.06±0.05	+0.06±0.05	1 <sup>+</sup> 2 <sup>+</sup>	2 <sup>+</sup>
6	662.0	7252	1	1	3 <sup>+</sup>	2 <sup>+</sup> -3 <sup>+</sup>	1 <sup>+</sup> 2 <sup>+</sup> 3 <sup>+</sup>	1 <sup>+</sup>	(1 <sup>+</sup> )	1 <sup>+</sup> (2 <sup>+</sup> )	0.08	0.08±0.02	-0.8 ±0.2	-0.8 ±0.2	1 <sup>+</sup>	1 <sup>+</sup>
7	738.5	7176	1	1	1 <sup>+</sup> 2 <sup>+</sup> 3 <sup>+</sup>	1 <sup>+</sup> -3 <sup>+</sup>	1 <sup>+</sup> 2 <sup>+</sup> 3 <sup>+</sup>	(2 <sup>+</sup> 3 <sup>+</sup> )	(2 <sup>+</sup> 3 <sup>+</sup> )	2 <sup>+</sup> 3 <sup>+</sup>	0.08	0.08±0.02	+0.07±0.13	+0.07±0.13	1 <sup>+</sup> 2 <sup>+</sup>	(1 <sup>+</sup> )2 <sup>+</sup>
8	926.6	6988	1+3	1	1 <sup>+</sup>	1 <sup>+</sup> -3 <sup>+</sup>	1 <sup>+</sup>	(1 <sup>+</sup> )	(1 <sup>+</sup> )	2 <sup>+</sup> (0 <sup>+</sup> 1 <sup>+</sup> )	0	0.02±0.05	+0.07±0.13	+0.07±0.13	1 <sup>+</sup> 2 <sup>+</sup>	1 <sup>+</sup> 2 <sup>+</sup>
9	1298.3	6617	1	1	0 <sup>+</sup> -3 <sup>+</sup>	0 <sup>+</sup> -3 <sup>+</sup>	1 <sup>+</sup>	1 <sup>+</sup>	1 <sup>+</sup>	1 <sup>+</sup>	0	0.04±0.03	+0.5 ±0.4	+0.5 ±0.4	(0 <sup>+</sup> )1 <sup>+</sup> 2 <sup>+</sup>	1 <sup>+</sup>
10	1522.0	6394	1	1	0 <sup>+</sup> -3 <sup>+</sup>	0 <sup>+</sup> -3 <sup>+</sup>	3 <sup>+</sup> (2 <sup>+</sup> 1 <sup>+</sup> )	1 <sup>+</sup>	1 <sup>+</sup>	1 <sup>+</sup>	0	0.01±0.02	+1.1 ±0.3	+1.1 ±0.3	2 <sup>+</sup>	2 <sup>+</sup>
11	1910.1	6010	1	1	0 <sup>+</sup> -3 <sup>+</sup>	0 <sup>+</sup> -3 <sup>+</sup>	1 <sup>+</sup> (2 <sup>+</sup> 3 <sup>+</sup> )	1 <sup>+</sup>	1 <sup>+</sup>	1 <sup>+</sup>	0	0 ±0.02	+0.4 ±0.2	+0.4 ±0.2	(1 <sup>+</sup> )2 <sup>+</sup>	(1 <sup>+</sup> )2 <sup>+</sup>
12	2498	5418	2	2	0 <sup>-</sup> -4 <sup>-</sup>	0 <sup>-</sup> -4 <sup>-</sup>	2 <sup>-</sup> 3 <sup>-</sup> 4 <sup>-</sup>	2 <sup>-</sup> 3 <sup>-</sup> 4 <sup>-</sup>	2 <sup>-</sup> 3 <sup>-</sup> 4 <sup>-</sup>	2 <sup>-</sup> 3 <sup>-</sup> 4 <sup>-</sup>	0	0 ±0.02	-0.14±0.16	-0.14±0.16		
<sup>66</sup> Cu b)																
1	385.7	6680	1	1	1 <sup>+</sup> -3 <sup>+</sup>	1 <sup>+</sup> -3 <sup>+</sup>	1 <sup>+</sup>	1 <sup>+</sup>	1 <sup>+</sup>	1 <sup>+</sup>				+0.44±0.09	1 <sup>+</sup> 2 <sup>+</sup>	1 <sup>+</sup> 2 <sup>+</sup>
2	465.1	6600	1	1	1 <sup>+</sup> -3 <sup>+</sup>	1 <sup>+</sup> -3 <sup>+</sup>	1 <sup>+</sup>	1 <sup>+</sup>	1 <sup>+</sup>	1 <sup>+</sup>				+0.59±0.17	1 <sup>+</sup> 2 <sup>+</sup>	1 <sup>+</sup> 2 <sup>+</sup>
3	1746	5320	1+3	1+3	1 <sup>+</sup>	1 <sup>+</sup>	1 <sup>+</sup>	1 <sup>+</sup>	1 <sup>+</sup>	1 <sup>+</sup>				+0.8 ±0.3	1 <sup>+</sup> 2 <sup>+</sup>	1 <sup>+</sup> 2 <sup>+</sup>
4	2026	5042	(1+3)	(1+3)	1 <sup>+</sup>	1 <sup>+</sup>	1 <sup>+</sup>	1 <sup>+</sup>	1 <sup>+</sup>	1 <sup>+</sup>				-0.1±0.2		

- a) Ref. 6) e) Ref. 10) i) Ref. 13) m) Proposed value of  $J^\pi$  based upon the combination of our results with the work e) - i).
- b) Ref. 7) f) Ref. 8) j) Calculated from ref. 14)
- c) Ref. 8) g) Ref. 11) k) Calculated from ref. 15)
- d) Ref. 9) h) Ref. 12) l) Based upon R,  $\lambda_n$  and  $\alpha$

#### 1.4. Experimental situation Zn isotopes

(J. de Boer)

Circular polarizations of the three Zn isotopes 64, 66, 68 have been measured and  $\pm 20$  spin assignments can be expected of which 30% are already known. The remaining 70% are new or confirmations.

The single spectrum measurements are difficult to analyse in the low energy region because of the Cd contaminations (300 ppm) in the samples. At this moment the isotopically enriched samples are purified chemically. A part of the single spectra will be remeasured.

A preliminary analysis of the  $^{64}\text{Zn}(n,\gamma)^{65}\text{Zn}$  reaction shows the following results:  $E_x = 0.115 \text{ J}^\pi = 3/2^-$ ,  $E_x = 0.867 \text{ J}^\pi = 1/2^-$ ,  $E_x = 2.20 \text{ J}^\pi = 1/2^-$ ,  $E_x = 2.42 \text{ J}^\pi = 3/2^-$ ,  $E_x = 2.49 \text{ J}^\pi = 1/2^-$ . In fig. 1 the decay scheme is given.

The last three levels are believed to belong to the reaction but the final proof must come from single spectrum measurements.

#### 1.5. The reaction $^{35}\text{Cl}(n,\gamma)$ with polarized thermal neutrons

(A.M.J. Spits)

A preliminary analysis of the spectra of the circularly polarized  $\gamma$ -radiation following polarized neutron capture in  $^{35}\text{Cl}$ , revealed a discrepancy between the values of the polarization parameter R of some  $\gamma$ -transitions and those found in older, less accurate work performed in Risø on the same reaction [17].

For the level with  $E_x = 1164 \text{ keV}$  the angular correlation coefficients found by Van Middelkoop and Spilling [18] in their angular correlation measurement on the same reaction, is conflicting with the respective R-value ( $R = 0.68 \pm 0.04$ ). Besides, for the level with  $E_x = 2864 \text{ keV}$ , the R-value found ( $R = -0.16 \pm 0.04$ ) excludes the established spin-parity  $J^\pi = 3^-$  if one assumes the capture mechanism to proceed exclusively by way of the well-known negative energy resonance with  $J^\pi = 2^+$ . In order to clarify the situation and further to improve the accuracy of the R-values, the measurement has been restarted, results are not yet available.



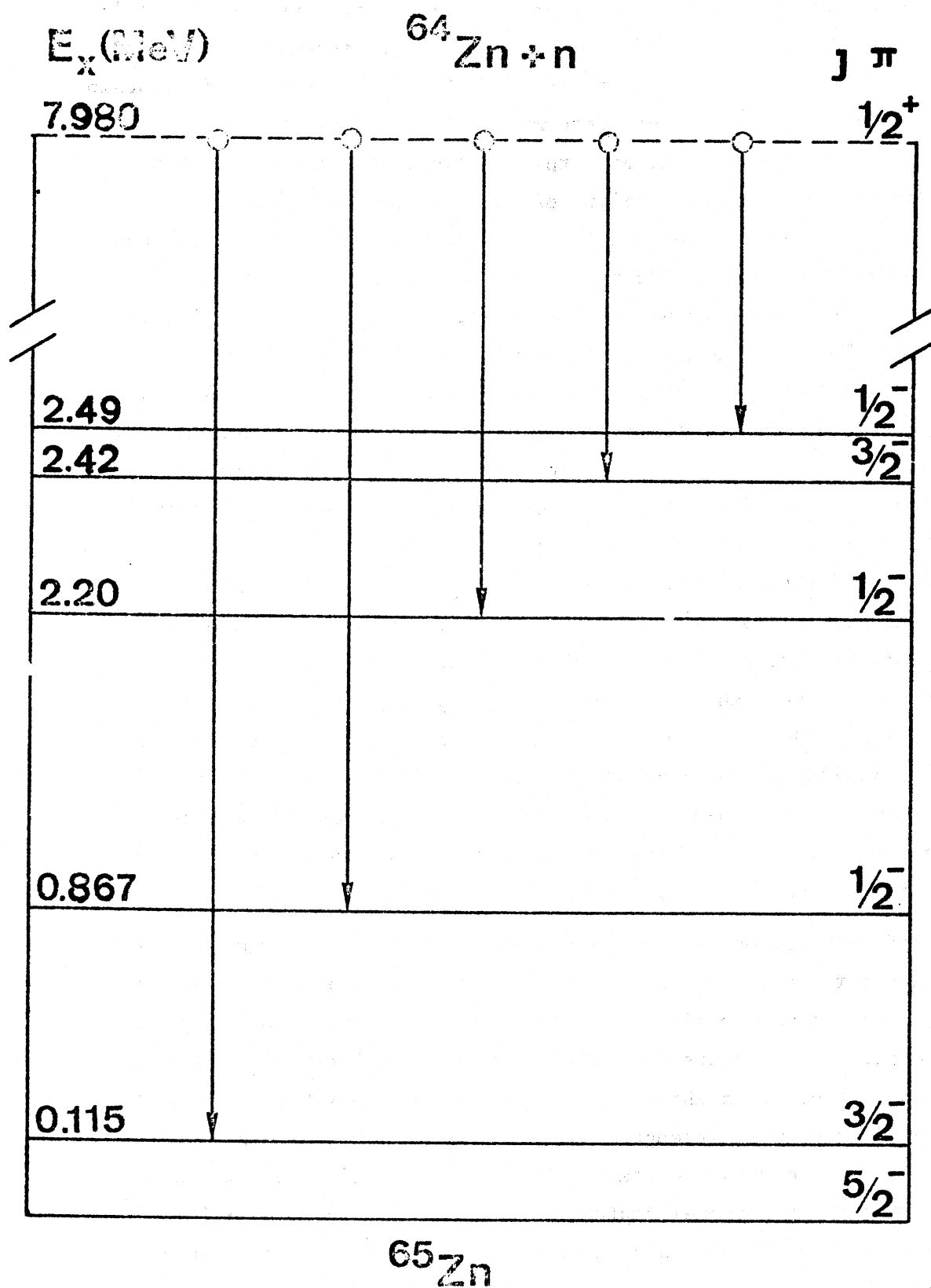


Fig. 1.

## 1.6. The $^{29}\text{Si}(n,\gamma)$ reaction

(A.M.J. Spits)

By analysing single spectra of  $\gamma$ -radiation, resulting from thermal-neutron capture in a silicon-dioxide sample enriched to 95% in  $^{29}\text{Si}$ , the accurate excitation energies (0.14 - 1.5 keV errors) and branchings of 18 levels of  $^{30}\text{Si}$ , were determined. Two new p-states at 9620 keV and 9792 keV were found. From this analysis also the ratio of the thermal capture cross sections of the  $^{28}\text{Si}$  and the  $^{29}\text{Si}$  isotopes could be deduced by normalizing the  $^{30}\text{Si}$   $\gamma$ -ray intensities in such a way that the sum of the primary  $\gamma$ -ray intensities equalled 100. An error of 4% was assumed to be associated with the normalization factor. The ratio  $\sigma_{\text{cap}}(^{28}\text{Si})/\sigma_{\text{cap}}(^{29}\text{Si})$  as following from the  $^{29}\text{Si}(n,\gamma)$  spectrum ( $^{28}\text{Si}$  contaminated) was found to be  $1.70 \pm 0.13$ , whereas the value following from the natural  $\text{Si}(n,\gamma)$  spectrum was  $1.41 \pm 0.17$ . A weighted average of  $1.59 \pm 0.14$  has been adopted. The cross sections were put on an absolute scale by using as targets a mixture of Al and Si and a  $\text{Na}_2\text{SiO}_3$  target.

From the first measurement followed  $\sigma_{\text{cap}}(^{28}\text{Si}) = 156 \pm 23$  mb, the second yielded  $163 \pm 57$  mb, a value of  $157 \pm 21$  mb has been adopted as a final result. A value for  $\sigma_{\text{cap}}(^{29}\text{Si})$  of  $99 \pm 16$  mb follows.

Cross sections used as standards were  $\sigma_{\text{cap}}(\text{Na}) = 536 \pm 8$  mb and  $\sigma_{\text{cap}}(\text{Al}) = 239 \pm 3$  mb from ref. [19]. The capture cross sections of  $^{28}\text{Si}$  and  $^{29}\text{Si}$  given above contradict the values given in the literature [19],  $80 \pm 30$  mb and  $280 \pm 90$  mb, respectively, but are consistent with the literature values of the thermal capture cross section for natural silicon,  $160 \pm 20$  mb [19].

A good correlation between (d,p) strengths and (n, $\gamma$ ) primary reduced widths for the set of nine  $\ell_n(d,p) = 1$  states excited both in the (d,p) and (n, $\gamma$ ) reactions was found, if as reduction factor for the intensities,  $E_\gamma^{-1.3}$  was used instead of the usual one,  $E_\gamma^{-3}$ . This is shown in fig. 2, in which the (d,p) strengths (black lines) compared to the (n, $\gamma$ ) strengths (open lines) for the two cases mentioned. The (d,p) strengths are taken from ref. [20]. This confirms an earlier observation for channel capture in the mass region  $A = 25 - 50$ .

An explanation of this behaviour might be found in an article by Lane and Lynn [21] according to which the partial radiation widths for capture to  $\ell_n(d,p) = 1$  states are proportional to  $E_\gamma$  for potential capture and to  $E_\gamma^2$  for resonance channel capture. (See also par. 1.7. of this report).

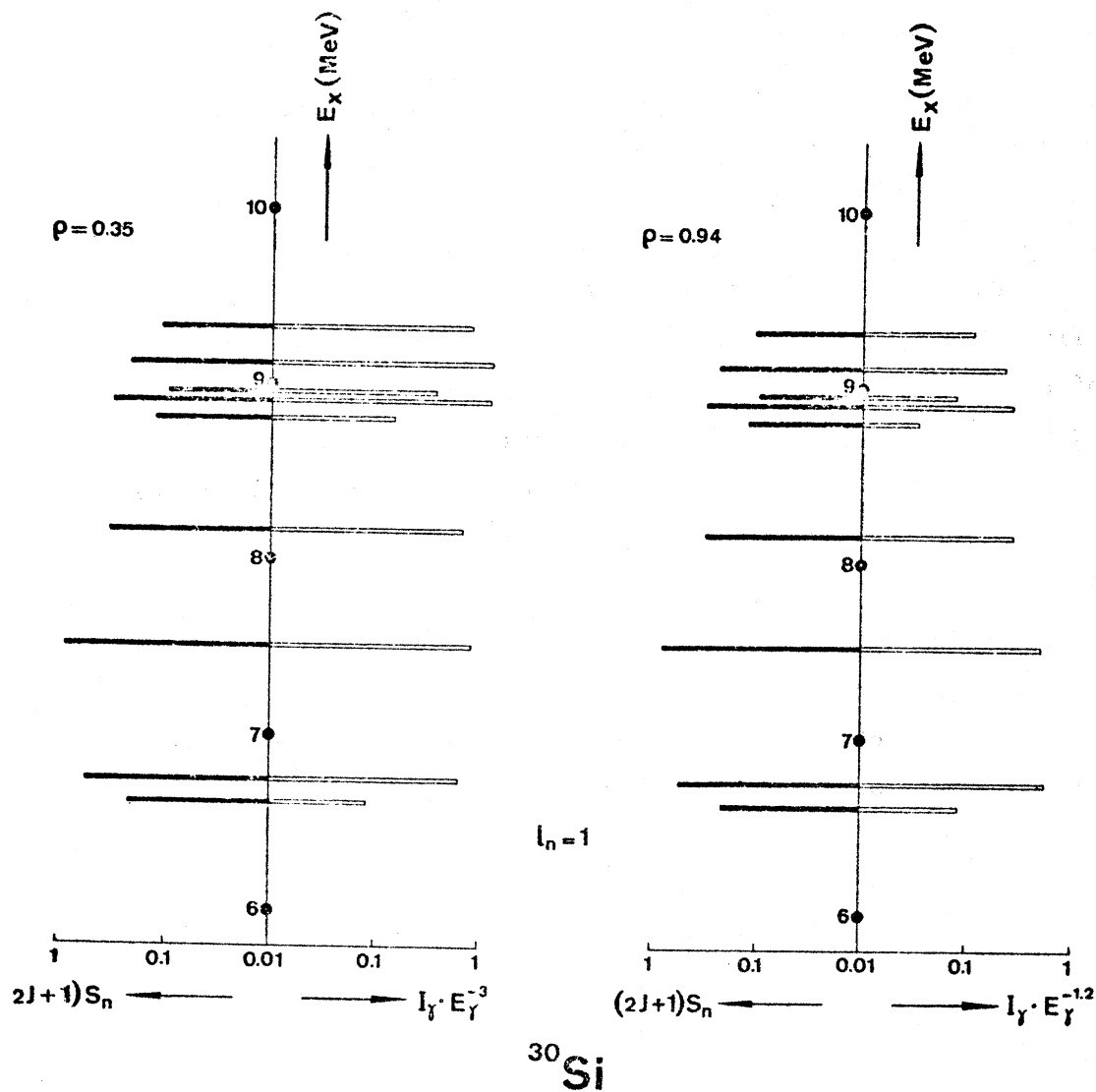


Fig. 2. Comparison of the stripping strengths  $(2J+1)S_n$  of the  $(d,p)$  reaction (black lines) and reduced transition probabilities after thermal-neutron capture (open lines) with respect to  $l_n(d,p) = 1$  levels of  $^{30}\text{Si}$  only.

A circular polarization measurement has given the R-values for three levels of  $^{30}\text{Si}$ . The results are shown in table III.

Because of the high correlation coefficient for the sets of reduced  $(n,\gamma)$  and  $(d,p)$  strengths for p-states ( $\rho = 0.94$ ; see fig. 2), the measured polarization R yields for the above levels the relative  $2p_{3/2}$  strengths  $\beta$  as defined by  $\beta = S_{3/2}/(S_{1/2} + S_{3/2})$ , where  $S_{1/2}$  and  $S_{3/2}$  denote the  $2p_{1/2}$  and  $2p_{3/2}$  reduced widths, respectively (see par. 1.8. of this report).

These results can be compared to the predictions offered by a simple shell-model calculation. Two active neutrons outside an inert  $^{28}\text{Si}$  core were considered, one in the  $2s_{1/2}$  or  $1d_{3/2}$ , the other in the  $1f_{7/2}$ ,  $2p_{3/2}$ ,  $2p_{1/2}$  or  $1f_{5/2}$  subshells. In this calculation only the states with odd J have mixed configuration, i.e. the five  $J^\pi = 1^-$  and the five  $J^\pi = 3^-$  states (there is only one  $J^\pi = 5^-$  state).

A part of the results is presented in table IV. It is seen that most of the  $2p_{3/2}$   $J = 1$  strength is concentrated in the level situated at  $E_x = 6.46$  MeV (experimentally this is the  $E_x = 6.74$  MeV level) whereas the  $2p_{1/2}$  strength is distributed over three or more levels.

The same is predicted by the "sum rule" as derived by Abrahams [22] and applied to the results of table III, as well as by the fact that the weighted spectroscopic factors for the  $^{29}\text{Si}(n,\gamma)$  reaction summed over the candidates for the  $(2s_{1/2}2p_{1/2})$  doublet ( $J^\pi = 1^-$  and  $0^-$ ) do not yield the  $(d,p)$  spectroscopic factor for the "parent" state in  $^{29}\text{Si}$ , i.e. the  $E_x = 6.38$  MeV level.

Table III. Circular-polarization results for  $^{30}\text{Si}$  bound levels

$E_x^a)$ (MeV)	$I_Y^a)$ (%)	$l_n^b)$	$R^c)$	$nlj^{\text{circ.pol. d)}$	$J^\pi$
6.74	$30 \pm 3$	1	$-0.41 \pm 0.08$	$2p_{3/2} [\beta > (0.94 \pm 0.06)]$	$1^-$ e)
7.51	$23 \pm 2$	1	$-0.36 \pm 0.08$	$2p_{3/2} [\beta > (0.91 \pm 0.06)]$	$(1,2)^-$ f)
8.16	$7.3 \pm 0.6$	1	$+0.57 \pm 0.35$	$2p_{1/2} [\beta < (0.3 \pm 0.2)]$	$1^-$ g)

- a) The excitation energy of the level is denoted by  $E_x$  and the intensity of the primary transition to this level by  $I_Y$ .
- b) Ref. [20].
- c) The possibility of a systematic error resulting from depolarization of the beam through scattering from hydrogen is not accounted for.
- d) Here  $\beta$  stands for the relative  $2p_{3/2}$  strength defined by  $S_{3/2}(S_{1/2} + S_{3/2})$  and is calculated from the formula  $\beta = (2-2R)/3$ .
- e) Ref. [23].
- f) Based upon  $l_n$  and  $R$ .
- g) Based upon  $l_n$ ,  $R$  and the existence of a ground-state transition.

Table IV. Comparison of experimental and theoretical parameters for  $J^\pi = 1^-$  states of  $^{30}\text{Si}$ .

Experiment		Theory			
$J^\pi$	$E_x$ (MeV)	Main configuration	$E_x$ (MeV)	$S_{3/2}^a)$	$S_{1/2}^a)$
$(1^-, 2^-)$	10.20	$(1d_{3/2} \ 2p_{1/2})_{J=1}$	10.39	0.005	0.010
$(1^-, 2^-)$	9.79	$(1d_{3/2} \ 1f_{7/2})_{J=1}$	9.62	0.04	0.22
$(1^-, 2^-)$	9.62				
$(1^-, 2^-)$	8.95	$(1d_{3/2} \ 2p_{3/2})_{J=1}$	8.91	0.01	0.37
$(1, 2)^-$	8.90				
$1^-$	8.16	$(2s_{1/2} \ 2p_{1/2})_{J=1}$	8.50	0.22	0.33
$1^-$	6.74	$(2s_{1/2} \ 2p_{3/2})_{J=1}$	6.46	0.73	0.07

a) Relative strengths of the  $2s_{1/2} \ 2p_{3/2}$  and  $2s_{1/2} \ 2p_{1/2}$  components, respectively.

b) The two possibilities are listed.

1.7. The (d,p)-(n, $\gamma$ ) correlations in the mass range  $A = 24 - 80$

(J. Kopecký, K. Abrahams, F. Stecher-Rasmussen and A.M.J. Spits)

For potential and channel capture of thermal neutrons the partial cross section  $\sigma_f^p$  to the p-states is proportional to the (d,p) single particle width  $\theta_f^2$  and  $\gamma$ -transition energy  $E_\gamma$ :

$$\sigma_f^p = C \theta_f^2 \left[ E_\gamma + A E_\gamma^2 + B E_\gamma^{1.5} \right]. \quad (3)$$

According to Lane and Lynn [21], the first term originates from the potential capture, while the other two terms represent the channel capture and its interference with potential capture, respectively.

Consequently in a correlation analysis the partial cross section should be generally reduced with the energy dependent factor of formula (3), instead of  $E_\gamma^3$  as hitherto has been used. A good approximation for this factor is  $E_\gamma^{-k}$ , where for  $k$  holds  $1 \leq k \leq 2$ . In fact Spits [24] observed, that  $k \sim 1.2$  is a good choice for the light nuclei and suggested a general dependence of the reduced matrix element in the Weisskopf estimate.

The properly reduced correlation coefficient  $\rho$  is plotted versus  $A$  in fig. 3. The thick and thin bars represent pure statistical errors, and combined statistically with sample size errors, respectively. For  $k$  a compromise value 1.5 has been chosen, which especially for  $A < 50$  gives a significant improvement over  $k = 3$ .

Except for  $^{51}\text{Ti}$ ,  $^{57,59}\text{Fe}$  and  $^{63}\text{Ni}$  the correlation is significant below  $A \sim 69$  for all odd -A prpduct nuclei. For heavier nuclei the correlation disappears.

Generally the even -A product nuclei are much less correlated, which is in accordance with the theory. In fig. 4 the correlation coefficient  $\sigma$  ( $k = 1.5$ ) is plotted versus the fraction of  $\sigma_{n,\gamma}^p$  to the p-states  $\sigma_{n\gamma}^{2p} = \sum_f \sigma_f^{2p}$ . The correlation is high only for low A-values and low cross sections, where the potential capture seems to be probable.

Four nuclei ( $^{44}\text{Ca}$ ,  $^{50}\text{Ti}$ ,  $^{56}\text{Mn}$  and  $^{58}\text{Fe}$ ) are exceptions to this rule and they are likely candidates for channel capture. The drawn line in fig. 4 shows the  $(\rho, \sigma_{n\gamma}^{2p})$  dependence under the assumption, that the function of  $\sigma_{n\gamma}^{2p}$  below 0.56 is always connected to pure potential capture.

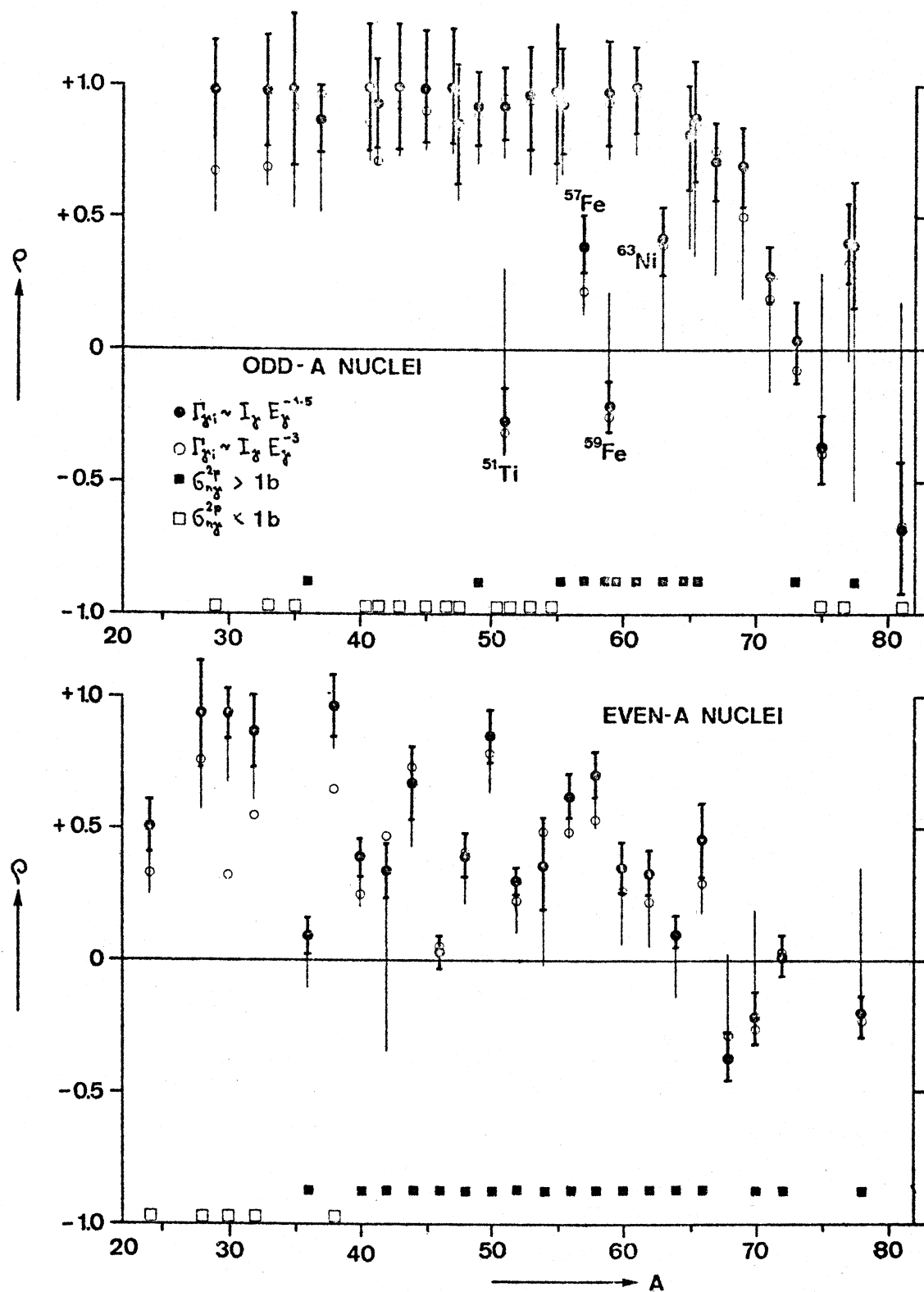


Fig. 3. The correlation coefficient  $\rho$  plotted versus  $A$ .  
The thick and thin bars represent pure statistical errors, and combined statistical with sample size errors, respectively.



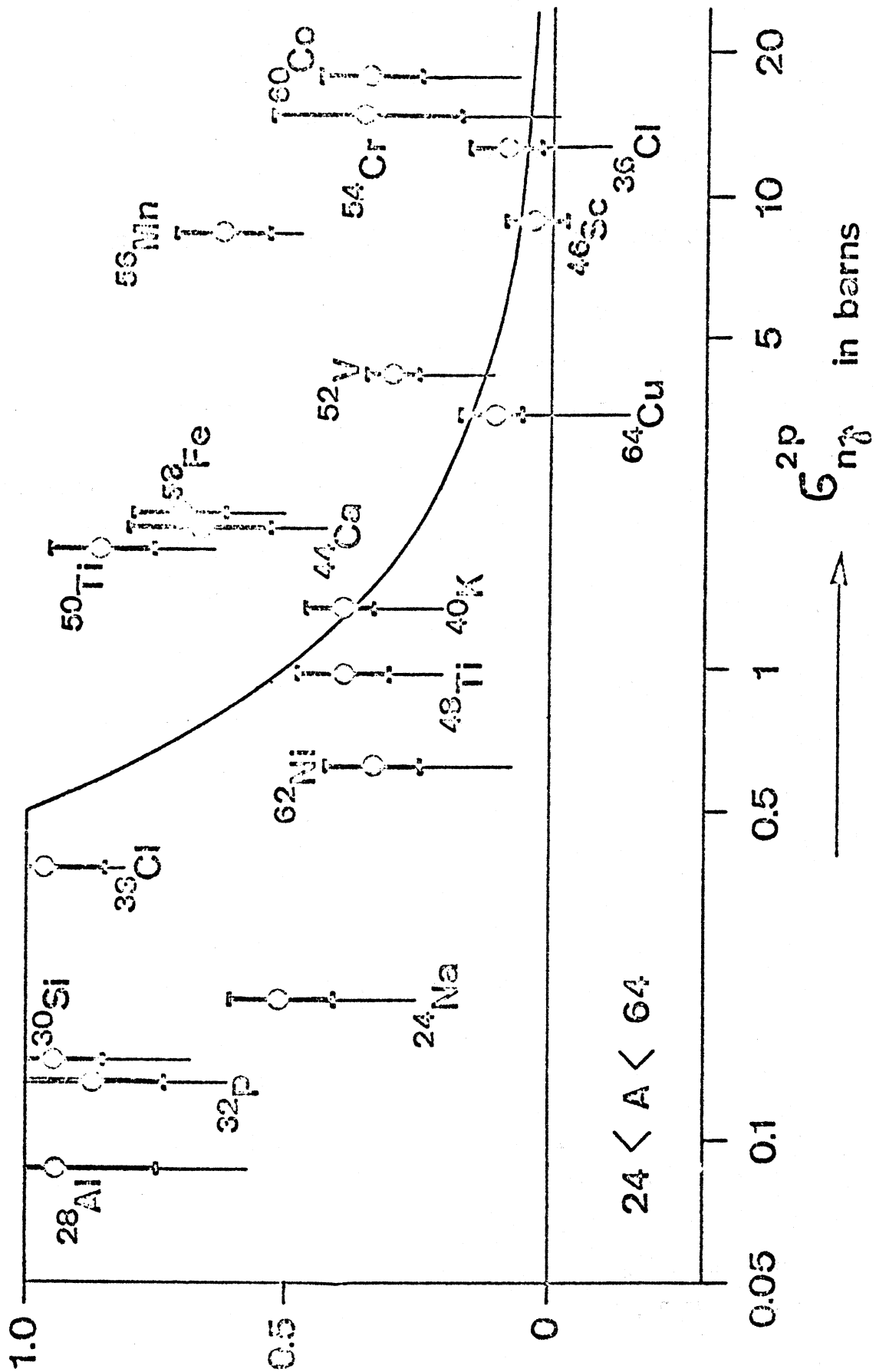


Fig. 4. The correlation coefficient  $\rho$  ( $k=1.5$ ) plotted versus the fraction of  $\sigma_{n,y}$  to the p-states  $\sigma_{n,y}^{2p} = \sigma_f^{2p}$ . The drawn line shows the  $(\sigma \sigma_{n,y}^{2p})$  dependence under the assumption, that the function of  $\sigma_{n,y}^{2p}$  below 0.56 is always connected to pure  $n_{\gamma}$  potential capture.

Seven significantly correlated nuclei ( $^{28}\text{Al}$ ,  $^{30}\text{Si}$ ,  $^{32}\text{P}$ ,  $^{38}\text{Cl}$ ,  $^{50}\text{Ti}$ ,  $^{56}\text{Mn}$  and  $^{58}\text{Fe}$ ) have been studied in more detail (see e.g. fig. 2 of par. 1.6.). It has been shown for all nuclei studied, that the transitions to the higher energy levels are responsible for the effect. A letter publication is being considered.

#### 1.8. The (n, $\gamma$ ) channel spin interference and the structure of p-states in even A nuclei

(K. Abrahams, J. Kopecký and F. Stecher-Rasmussen)

Interference of channels with spin  $J_c = J_t \pm \frac{1}{2}$  has been found for capture of slow neutrons (K. Abrahams, contribution A21, Budapest Conf. 1972). For example in case of polarized neutron capture the extreme value R of the circular polarization of the emitted dipole radiation is defined by:  $4R-1 = 3\cos(2r+f)$ . Here  $\alpha = \cos^2 r$  is the relative rate of the transition, which proceeds via channel spin  $J_c = J_t \pm \frac{1}{2}$ , and the phase factor f is determined by the spins  $J_t$  and  $J_f$  of target and final state. The function  $R(\alpha)$  is an ellipsis ranging from -0.5 to +1.0.

If the reduced (n, $\gamma$ ) strength is highly correlated with the (d,p) spectroscopic factor for p levels, it can be shown that:  $\cos(2r+f) = (S_{1/2} - S_{3/2}) / (S_{1/2} + S_{3/2})$ . Here  $S_{1/2}$  and  $S_{3/2}$  are the  $p_{1/2}$  and  $p_{3/2}$  spectroscopic factor. In this case R does no longer depend on the spins  $J_t$ ,  $J_c$  and  $J_f$ . For all nuclei, with a good (d,p)-(n, $\gamma$ ) correlation,  $S_{1/2}$  and  $S_{3/2}$  can be derived for final p-states from the measured R values. Such a measurement can be used to estimate the spin orbit splitting for even A nuclei. This is demonstrated in figures 5 and 6 for some nuclei, which have been measured by the FOM-RCN Nuclear Structure Group.

For the odd-odd nucleus  $^{56}\text{Mn}$  the first  $p_{1/2}$  level appears rather close to the ground state, just as for the odd A nuclei in this mass region. Another group of  $p_{1/2}$  levels is found at higher excitation energy, just as for the odd A nuclei. For all measured odd N nuclei in the mass region  $48 < A < 62$  such a  $p_{1/2} - p_{3/2}$  doublet has been found.

An even more convincing example is the even-even nucleus  $^{58}\text{Fe}$ , for which the relative  $p_{1/2}$ - and  $p_{3/2}$ -strengths have been determined for 15 levels. The figures show that the  $p_{1/2}$  levels appear 1-2 MeV above the strongest  $p_{3/2}$  level.



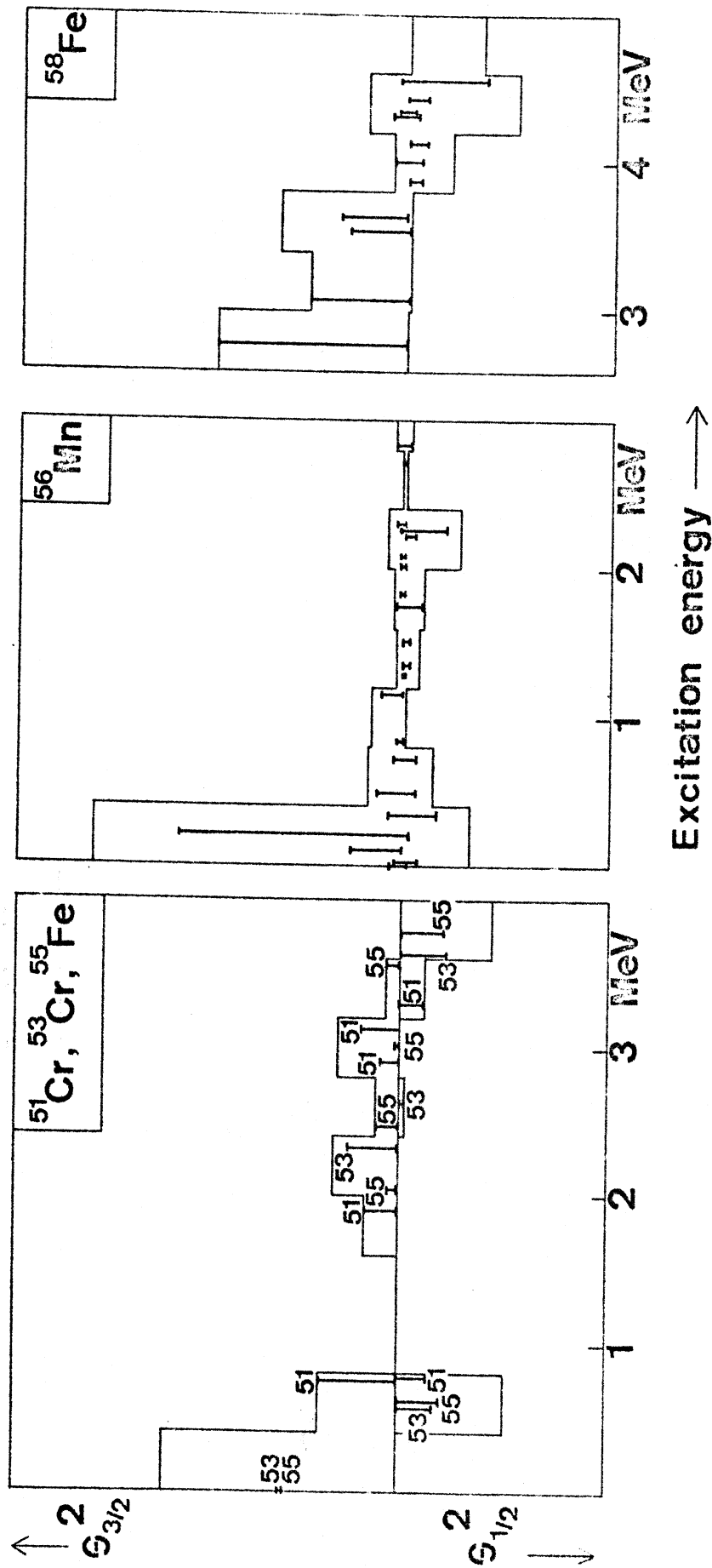


Fig. 6.

1.9. An improved system of neutron mirrors for producing an intense beam of polarised thermal neutrons.

(F. Stecher-Rasmussen)

A study is being made of the possibility to increase the flux of polarised thermal neutrons emerging from a focussing system of magnetized neutron mirrors. At present such a system is placed in front of a beam tube of the High Flux Reactor at Petten giving a flux of  $3 \times 10^7$  n/cm<sup>2</sup> s on the sample.

It is being investigated now to install such a mirror system in the thermal column of the HFR. According calculations based on the present experiences a flux of  $3 \times 10^8$  n/cm<sup>2</sup> s, so an increase with respect to the present system with a factor of 10, is expected.

A design is being made and mirror materials are being tested now. It is expected that the new system will be in operation before the end of 1975.

## References

- [1] R.I. Schermer et al., Phys. Rev. 167 (1968) 1121.
- [2] F. Poortmans et al., Proc. 2nd Int. Conf. on Nuclear Data for Reactors, Helsinki (1970) 449.
- [3] F.B. Simpson et al., Nucl. Phys. 164 (1971) 34.
- [4] W. Kane, Phys. Rev. Lett. 25 (1970) 953.
- [5] F. Corvi et al., Nucl. Phys. 203 (1973) 145.
- [6] P. Holmberg, P. Passi and R. Rieppo, Comment. Phys. Math. 41 (1971) 311.
- [7] E.B. Sherra and H.H. Bolotin, Phys. Rev. 169 (1968) 940.
- [8] Y.S. Park and W.W. Dachnick, Phys. Rev. 180 (1969) 1082.
- [9] G.A. Bartholomew and J. Vervier, Nucl. Phys. 50 (1964) 209.
- [10] S.A. Hjorth and L.H. Allen, Arkiv för Fysik 33 (1966) 207.
- [11] C.C. Wellborn, R.P. Williams and S.G. Buccino, Phys. Rev. C3 (1971) 167.
- [12] W.F. Davidson, P.J. Dallimore and J. Hellström, Nucl. Phys. A142 (1970) 167.
- [13] W.T. Bass and P.H. Stelson, Phys. Rev. C2 (1970) 2154.
- [14] G.F. Achampaugh, Univ. of California report, UCRL-50504, 1968.
- [15] W.E. Stein, B.W. Thomas and E.R. Rae, Phys. Rev. C1 (1970) 1468.
- [16] J. Kopecký, F. Stecher-Rasmussen, K. Abrahams, Nucl. Phys. A215 (1973) 54.
- [17] J. Kopecký and E. Warming, Nucl. Phys. A127 (1969) 385.
- [18] G. van Middelkoop and P. Spilling, Nucl. Phys. 77 (1966) 267.
- [19] J.D. Stehn et al., Brookhaven National Lab. Report, BNL-325, 2nd suppl. (1964).
- [20] H. Mackh et al., Nucl. Phys. A202 (1973) 497.
- [21] A.M. Lane and J.E. Lynn, Nucl. Phys. 17 (1960) 586.
- [22] K. Abrahams, Proc. Conf. on nuclear structure studies with neutrons, Budapest, 1972, p. 42.

- [23] R.D. Symes et al., Nucl. Phys. A167 (1971) 625.
- [24] A.M.J. Spits, Proc. Conf. on nuclear structure studies with neutrons, Contribution D-13, Budapest, 1972.

Publications in 1973

1. J. Kopecký, F. Stecher-Rasmussen and K. Abrahams, Nucl. Phys. A215 (1973) 54. The  $\text{Cu}(n,\gamma)$  reaction.
2. J. Kopecký, K. Abrahams and F. Stecher-Rasmussen, Nucl. Phys. A215 (1973) 45. The  $^{57}\text{Fe}(n,\gamma)$  reaction.
3. K. Abrahams, J. Kopecký and F. Stecher-Rasmussen. The  $(n,\gamma)$  channel spin interference and the structure of p-states in even A nuclei. Proceedings of the Intern. Conference on Nuclear Physics, Munich 1973, p. 636.
4. J. Kopecký, K. Abrahams and F. Stecher-Rasmussen, The  $(d,p)-(n,\gamma)$  correlations in the mass range  $A = 24 - 80$ . Proceedings of the Int. Conf. on Nuclear Physics, Munich 1973, p. 523.
5. A.M.F. Op den Kamp, Nucl. Phys. A209 (1973) 170. Circular polarization and gamma-gamma angular correlation measurements in the  $^{39}\text{K}(n,\gamma)^{40}\text{K}$  reaction.
6. A.M.J. Spits and J.A. Akkermans, Nucl. Phys. A215 (1973). Investigation of the reaction  $^{37}\text{Cl}(n,\gamma)^{38}\text{Cl}$ .
7. E.R. Reddingius, J.J. Bosman and H. Postma, A study of the  $^{59}\text{Co}(n,\gamma)$  reaction with polarized neutrons and polarized nuclei. Nucl. Phys. A206 (1973).
8. A.M.F. Op den Kamp, Investigation of thermal-neutron capture in  $^{39}\text{K}$ . Thesis Utrecht (1973).

## 2. RCN Reactor Physics Group

### 2.1. Integral measurements of fission product cross sections (J.B. Dragt et al.)

#### 2.1.1. Experiments

The project is aimed at integral measurements and analysis of fission product cross sections in the STEK critical facility at Petten (ref. [1] and [2]). During the first half of 1973 some previous cores were rebuilt for some supplementary experiments. From the end of August to early October measurements have been made in the core with the hardest neutron spectrum obtained in STEK, the STEK-500 core. In spite of the very limited time available, due to the fact that the reactor had to be closed down for financial reasons at October 3rd, reactivity worth measurements with a large fraction of the available samples and the most important central neutron spectrum measurements could be completed. The result of the STEK experiments are measured central reactivity worths for about 60 different fission product isotopes and a few mixtures in five different fast neutron spectra, which were also measured by several techniques.

A cooperation with CEA, France, on fission product capture in fast reactor spectra, which started in mid 1972, was formalized by an "Accord de Collaboration" in spring 1973.

#### 2.1.2. Pseudo fission product group cross sections

As agreed upon in the Debenelux cooperation, cross sections of mixtures of fission products have been produced by mid 1973 as an intermediate result. For the SNR-300 calculations group cross sections for the mixtures of fission products - "pseudo fission products" - of the isotopes  $^{235}\text{U}$ ,  $^{238}\text{U}$ ,  $^{239}\text{Pu}$  and  $^{241}\text{Pu}$  after a burnup of 50.000 MWd/ton metal are needed. The compositions of these pseudo fission products were obtained by a burn-up calculation. Cross sections were calculated on the basis of the 26 group (ABBEN scheme) RCN-1 set for 75 fission product isotopes (ref. [3]). Also error calculations have been performed for this set



(ref. [4]), by taking into account the uncertainties in the underlying nuclear parameters. Also errors due to uncertainties in the number of levels per energy group, Porter-Thomas fluctuations and errors in the model - both systematic and statistical - were estimated for the cross sections in the statistical region (above about 1 keV). The error calculations resulted in covariance matrices for each fission product mixture, including the correlations between different mixtures (see par. 2.1.5.). The group cross sections have been compared with several other sets. An example is given in fig. 1, where the deviations of four different sets with respect to RCN-1 are compared with one standard deviation of the RCN-1 set. Agreement is reasonably satisfactory, although this appeared to be due to a certain extent to cancellation of errors: the agreement for isotopic cross sections is far less, and the RCN-1 set seems inadequate for several of the separate isotopes, which necessitates an improved evaluation (RCN-2, see par. 2.1.6.).

### 2.1.3. Neutron spectrometry

Since an accurate knowledge of the central neutron spectrum is indispensable for the interpretation of the reactivity worth measurements, several neutron spectrometry techniques have been applied, which have been and are being intercompared with others at Mol (ref. [5]). Final analyses are not yet completed, but fig. 2 gives an impression of present results for four STEK cores (STEK-500 is not yet available).

### 2.1.4. Integral sample reactivity worths

The pseudo fission product cross sections have been checked by comparing calculated reactivity worths on the basis of the RCN-1 set with experimental results obtained in four STEK cores for three different mixtures, resembling the actual mixtures of a reactor, two of them obtained from burned fuel (HFR-1 and -2) and one from simulation (KFK). The quantity of interest is the normalized (with  $^{252}\text{Cf}$  source and  $^{235}\text{U}$  fission rate) reactivity worth, corrected for finite sample size and inelastic scattering contribution, viz. (in common notation)

$$-\left(\frac{\rho}{\rho_0}\right)_{\text{capture}} = \frac{\int \sigma_c(E) \phi(E) \phi^+(E) dE}{\int \sigma_{f,U_0}(E) \phi(E) dE \cdot \int \chi_{\text{Cf}}(E) \phi^+(E) dE},$$

where  $\sigma_c(E)$  is the fission product capture cross section of the mixture per fissioned atom. A summary of results (more details give ref. [6], [7] and [8]) is presented in table 1. A statistical test, which takes correlations between various errors properly into account, indicates a good consistency between calculation and experiment.

#### 2.1.5. Adjusted group cross sections

The fair agreement resulted in pretty small adjustments in the group cross sections of both integral samples and pseudo fission product mixtures, when the statistical adjustment technique is applied. For this adjustment the existing correlations between all group constants of all mixtures concerned (measured samples and pseudo fission products) were calculated, using the error calculation scheme mentioned in par. 2.1.2. Integral quantities, calculated from the adjusted set, appear to be slightly more accurate than from unadjusted data.

#### 2.1.6. Isotopic reactivity worths and cross sections

Final interpretations of reactivity worths of isotopes have not yet been completed. Only a few tentative conclusions could be given (see [7]). The problem of correcting for finite sample size has not yet been solved completely for these measurements.

Much work has been done and is still being done on the RCN-2 evaluation of fission product cross sections. It is based on very recent resonance parameters at low energy and on Hauser-Feshbach theory with optical model transmission coefficients in the statistical energy region.

There exist close contacts with other groups working on the same problems (e.g. Italy, U.S.A., Japan) and an intercomparison of codes for a sample problem is underway. The evaluation is primarily aimed at capture and inelastic point cross sections, with some other cross sections as a by-product.

#### 2.1.7. Completion of the programme

It is expected that the first half of 1974 will be needed for the final evaluation of all spectrum measurements and solving some discrepancies, which have been found, for calculating the effect on reactivity worths of finite sample sizes and for setting up the RCN-2 cross section codes.

After that, in the second half of 1974 and early 1975, all isotopes (nearly 60) will be analyzed one-by-one, in a certain order of practical interest, which was agreed with Interatom. In the meantime some indications of the trends with respect to the results of mid 1973 on pseudo fission products will be given.

#### References

- [1] Bustraan, M. et al., STEK, the fast-thermal coupled facility of RCN at Petten, RCN-122 (1970).
- [2] Klippel, H.Th. and J. Smit, The coupled fast-thermal critical facility STEK, RCN-206 (1974).
- [3] Lautenbach, G., Calculated neutron absorption cross sections of 75 fission products, RCN-191 (1973).
- [4] Dragt, J.B. and H. Gruppelaar, Error analysis of neutron capture group cross sections for fast reactors applied to fission products, RCN-192 (1973).
- [5] Bluhm, H. et al., Intercomparison of differential neutron spectrometry techniques in the Mol-EE fast assembly, KFK-1658 = RCN-172 = BLG-471 (1972).
- [6] Bustraan, M. et al., Experiences with STEK: Derivation of fission product cross sections and their improvement by statistical adjustment using sample reactivity worths, Paper at the International Symposium on Physics of Fast Reactors, Tokyo, October 1973.
- [7] Bustraan, M., Integral determination of neutron absorption by fission products, Paper at the IAEA panel on fission product nuclear data, Bologna, November 1973.
- [8] Gruppelaar, H. et al., RCN-1 pseudo fission-product capture group cross sections, RCN-205 (1974).

Publications in 1973

1. E.K. Hoekstra (comp.), Fast Reactor Programme. First Quarter 1973, Progress Report. RCN-187 (1973).
2. E.K. Hoekstra (comp.), Fast Reactor Programme. Second Quarter 1973, Progress Report. RCN-190 (1973).
3. E.K. Hoekstra (comp.), Fast Reactor Programme, Third Quarter 1973, Progress Report. RCN-199 (1973).
4. E.K. Hoekstra (comp.), Fast Reactor Programme, Fourth Quarter 1973, Progress Report. RCN-... report to be published.
5. M. Bustraan et al., Experiences with STEK: Derivation of fission product cross sections and their improvement by statistical adjustment using sample reactivity worths. Int. Symp. on Physics of Fast Reactors, Tokyo, 1973, Paper B26.
6. M. Bustraan, Integral determination of neutron absorption by fission products. IAEA Panel on Fission Product Nuclear Data, Bologna, 1973, Review Paper no. 14.
7. G. Lautenbach, Calculated neutron absorption cross sections of 75 fission products, RCN-191 (1973).
8. J.B. Dragt and H. Gruppelaar, Error analysis of neutron capture group cross sections for fast reactors, applied to fission products, RCN-192 (1973).
9. H. Gruppelaar, Need of Nuclear Level Schemes for Calculated Cross Sections of Fission Product Nuclei. Nuclear data in science and technology, Vol. I, IAEA, Vienna, 1973, 553.
10. H. Gruppelaar (comp.), RCN-1 Pseudo Fission-Product Capture Group Cross Sections. To be published as RCN-205.
11. H.Th. Klippel and J. Smit, The Coupled Fast-Thermal Critical Facility STEK. To be published as RCN-206.

**PROGRESS REPORT TO NEANDC  
FROM SWITZERLAND**

**June 1974**

**T. Hürlimann**

**Swiss Federal Institute for Reactor Research  
Würenlingen**

**NOT FOR PUBLICATION**

PREFACE

This document contains information of a preliminary or private nature and should be used with discretion. Its contents may not be quoted, abstracted, or transmitted to libraries without the explicit permission of the originator.

CONTENTS

	page
I. Institut de Physique, Université de Neuchâtel	3
II. Institut de Physique, Université de Fribourg	7
III. Eidgenössisches Institut für Reaktorforschung, Würenlingen	15
IV. Physikalisches Institut der Universität Zürich	22
V. Physikalisches Institut der Universität Basel	23
VI. Laboratorium für Kernphysik, Eidg. Technische Hochschule, Zürich	32
VII. Institut de Physique Nucléaire, Université de Lausanne	43

I. Institut de Physique, Université de Neuchâtel

(Dir.: Prof. Jean Rossel)

1. Phase shift and Mixing Parameters for the  
 $D(\vec{n}, n)D$  Scattering at Low Energy

D. Bovet, S. Jaccard, R. Viennet and J. Weber

It has been found that fits of equal quality may be obtained by a splitting of the quartet phase shifts or by J-degenerate phase shifts and mixing parameters [1].

Computations are in progress to obtain prediction of angular repartition of the Wolfenstein's parameters  $R$ ,  $R'$ ,  $A$  and  $A'$ . It is hoped that one of these will be more sensitive than the others to the type of model used for the analysis.

References

- {1} Proceedings of the International Conference on Nuclear Physics, München 1973, Vol. 1, p. 331  
D. Bovet, S. Jaccard and J. Weber

2. Neutron-Neutron Quasifree Scattering at 14.1 MeV\*

E. Bovet, F. Foroughi and J. Rossel

We have performed two breakup measurements from the  $D(n, 2n)p$  reaction at 14.1 MeV in the region of  $n$ - $n$  QFS ( $E_p \approx 0$ ). The neutron beam produced by the  $T(d, n)^4\text{He}$  reaction, using the associated  $\alpha$ -particle method [1], is incident on a spherical  $C_6D_6$  target. The breakup neutrons are detected in two NE 213 liquid scintillators ( $15 \times 15 \times 4 \text{ cm}^3$ ) placed at 120 cm from

the target and at symmetric angles,  $\theta_{N1} = \theta_{N2}$ ,  $\phi_{12} = 180^\circ$ , around the beam axis. Since in our kinematical situation the energy of the proton passes through zero, it was not possible to detect the breakup proton in the target (used as a scintillator). Therefore particular attention was paid to other means of background reduction. In particular, n- $\gamma$  discrimination [2] was applied to the outputs of both neutron detectors and events due to moderated background neutrons were suppressed by electronic biases. Moreover we have taken advantage of the fact that at angles  $30^\circ \leq \theta_{N1,N2} \leq 50^\circ$ , a  $^{12}\text{C}$ -based deuterated compound used as a target does not produce any detectable contamination in the kinematical region of interest. Separate measurements with a graphite target have confirmed the absence of unwanted correlations from competing reactions. Moreover they have shown that the background outside the region of interest is the same as with the deuterated target (see fig. 1a).

The preliminary results are as follows (see fig. 1b):

- 1) the differential cross section at  $\theta_{N1} = \theta_{N2} = 30^\circ$  is compatible with that obtained by Slaus et al. [3], within the limits of experimental uncertainties which are still rather large in both experiments;
- 2) the differential cross section at  $\theta_{N1} = \theta_{N2} = 40^\circ$  (exact pole location  $E_p = 0$ ) is approximatively 3 times smaller than that at  $30^\circ$  ( $E_p = 180$  keV). This drop is similar to though more marked than that found in the  $\text{D}(p,2p)n$  reaction [4].

More definitive measurements are in progress with a  $\text{C}_6\text{D}_{12}$  target.

#### References

- [1] C. Lunke, J. P. Egger and J. Rossel, Nucl. Phys. A158, 278 (1970)
- [2] E. Bovet, P. Boschung and J. Rossel, Nucl. Instr. and Meth. 101, 315 (1972)



- {3} I. Slaus, J. W. Sunier, G. Thompson, J. C. Young,  
J. W. Verba, D. J. Margaziotis, P. Doherty and R. T. Cahill,  
Phys. Rev. Lett. 26, 789 (1971)
- {4} E. Andrad, V. Valkovic, D. Rendic and G. C. Phillips,  
Nucl. Phys. A183, 145 (1972)

\* A more detailed paper has been submitted for publication  
in Phys. Rev. Lett.

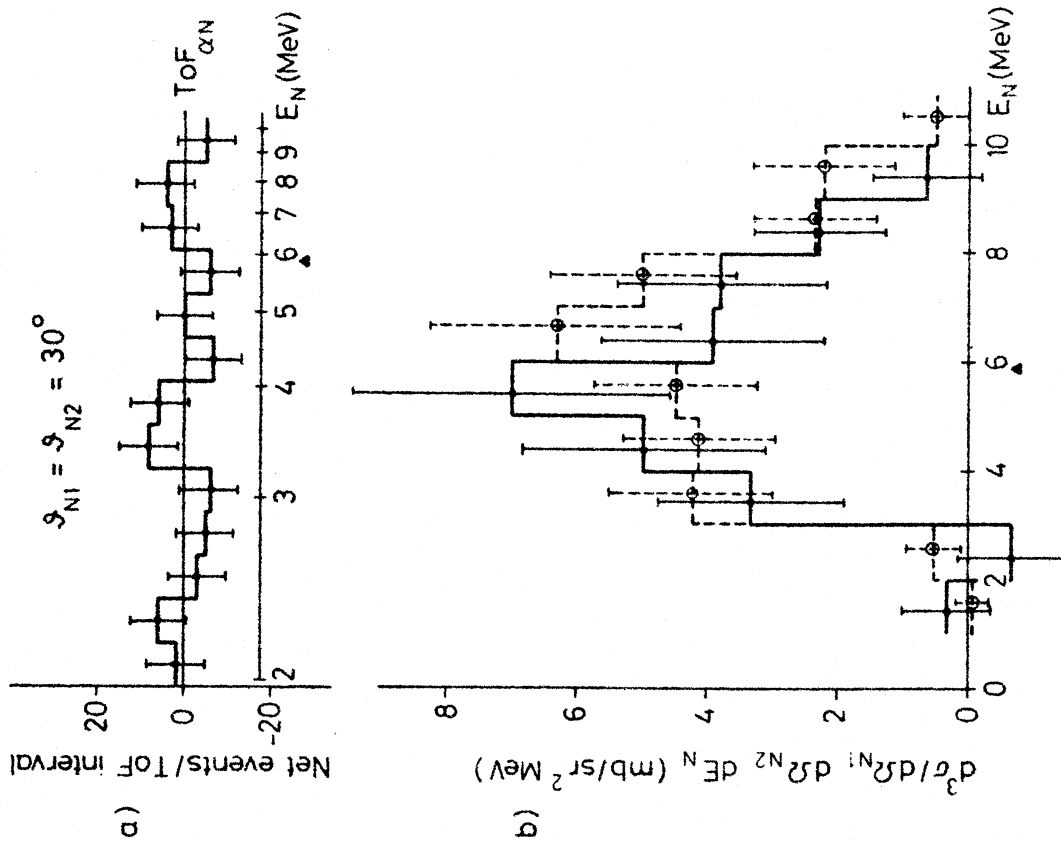


Fig. 1a :

Projections on the  $\text{ToF}_{\alpha N}$  axis of the difference between the background obtained both with the  $\text{C}_6\text{D}_6$  target (interpolated under the QFS kinematical region) and with the graphite target. The difference is seen to be zero to within experimental uncertainty. The triangles indicate the points corresponding to  $E_p \approx 180$  keV (30°), resp.  $E_p \approx 0$  (40°).

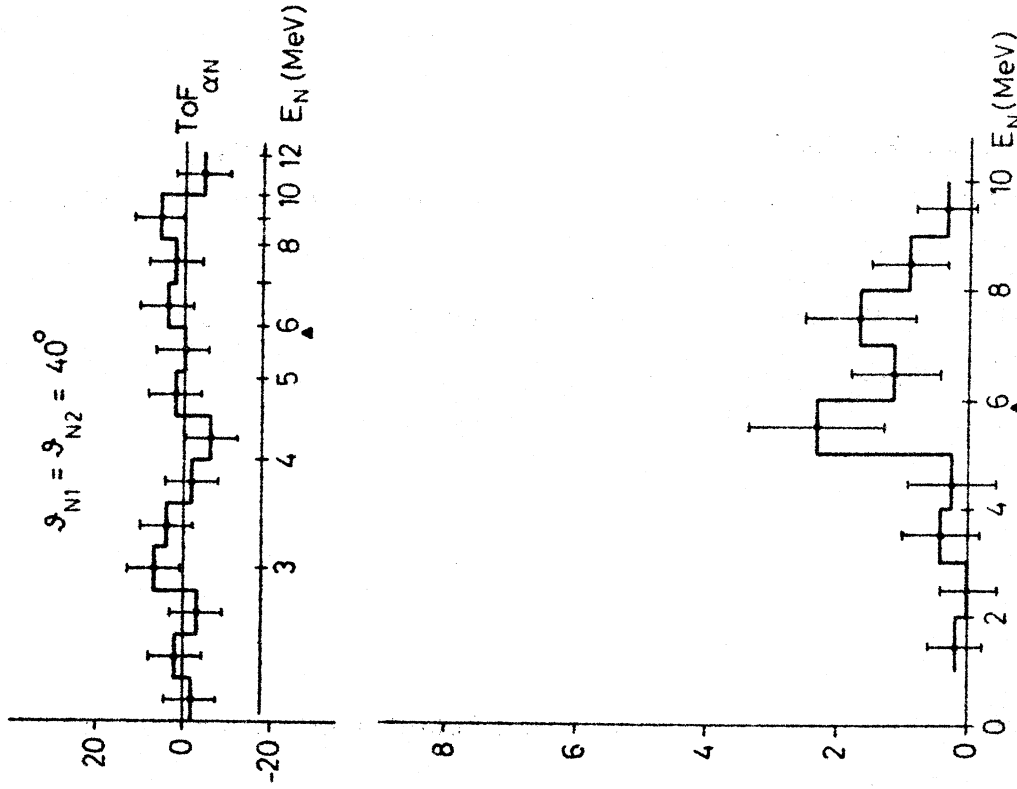


Fig. 1b :

Projections of the breakup events on the neutron energy axis. The solid line histograms represent our measurements. Besides statistical uncertainties, the error bars comprise uncertainties in the angular resolution and the detector efficiency. The broken line histogram is that of Slaus et al. (3).

## II. Institut de Physique, Université de Fribourg

(Dir.: Prof. Dr. O. Huber)

1. Study of the levels in  $^{233}\text{Th}$  using the  $^{232}\text{Th}(n,\gamma)$  reaction\*

Jean Kern and D. Duc

A total of 112 gamma rays of the reaction  $^{232}\text{Th}(n,\gamma)^{233}\text{Th}$  have been observed with the Fribourg pair spectrometer in the energy range  $2.48 < E_\gamma < 4.8$  MeV. This apparatus has been described previously [1].

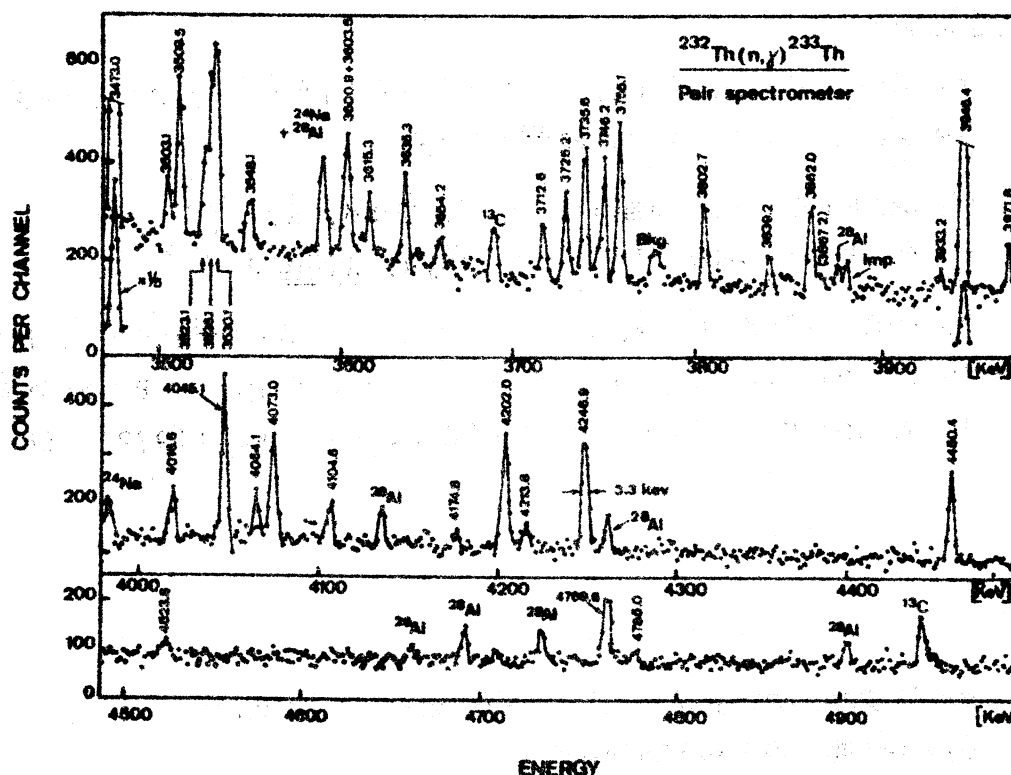


Fig. 1: Portion of the high energy  $^{232}\text{Th}(n,\gamma)$  spectrum taken in pair mode with the 20 cm<sup>3</sup> Ge(Li) detector. The solid line serves only as a guide to the eye. Identified impurities are noted. The label "Bkg" is given to an unidentified peak observed in a background run, the label "Imp" to a peak not present in the other measurements.

Two sets of experiments have been performed, one with a planar  $3 \text{ cm}^3 \text{ Ge(Li)}$  detector, the second, with a coaxial  $20 \text{ cm}^3 \text{ Ge(Li)}$  diode. As shown in fig. 1, the energy resolution was 3.3 keV FWHM for 4.2 MeV transitions in the second set.

The experiments were performed at the throughtube facility of the reactor SAPHIR in Würenlingen (EIR). At the external target position, the thermal neutron flux was about  $3 \times 10^7 \text{ n / cm}^2 \text{ s}$ .

The level scheme proposed in previous works {2}{3} has been extended. A value of  $4786.35 \pm 0.25 \text{ keV}$  has been determined for the neutron binding energy in  $^{233}\text{Th}$ .

#### References

- {1} B. Michaud, J. Kern, L. Ribordy and L. A. Schaller, *Helv. Phys. Acta* 45 (1972) 93
- {2} T. Grottdal, J. Limstrand, K. Nybø, K. Skår and T. F. Thorsteinsen, *Nucl. Phys.* A189 (1972) 592
- {3} T. von Egidy, O. W. B. Schult, D. Rabenstein, J. R. Erskine, O. A. Wasson, R. E. Chrien, D. Breitig, R. P. Sharma, H. A. Baader, H. R. Koch, *Phys. Rev.* C6 (1972) 266

\* Work supported by the Fonds National Suisse de la Recherche Scientifique

## 2. Neutron Capture $\gamma$ -rays in $^{238}\text{Np}^*$

V. A. Ionescu and J. Kern

The neutron capture gamma rays following the reaction  $^{237}\text{Np}(n,\gamma)^{238}\text{Np}$  have been investigated. The measurements were performed in an external target geometry at the tangential beam channel of the reactor SAPHIR of the Swiss Federal Institute for Reactor Research ( $\phi \approx 2 \times 10^7$  n/cm<sup>2</sup> s at target position).

The high energy spectrum has been investigated in the range 2600-5500 keV. The measurements were performed with a Ge(Li)-NaI(Tl) pair spectrometer [1]. The existence of 71 transitions has been established with an energy accuracy ranging between  $0.15 \div 0.18$  keV. Figure 1 presents a portion of high energy spectrum.

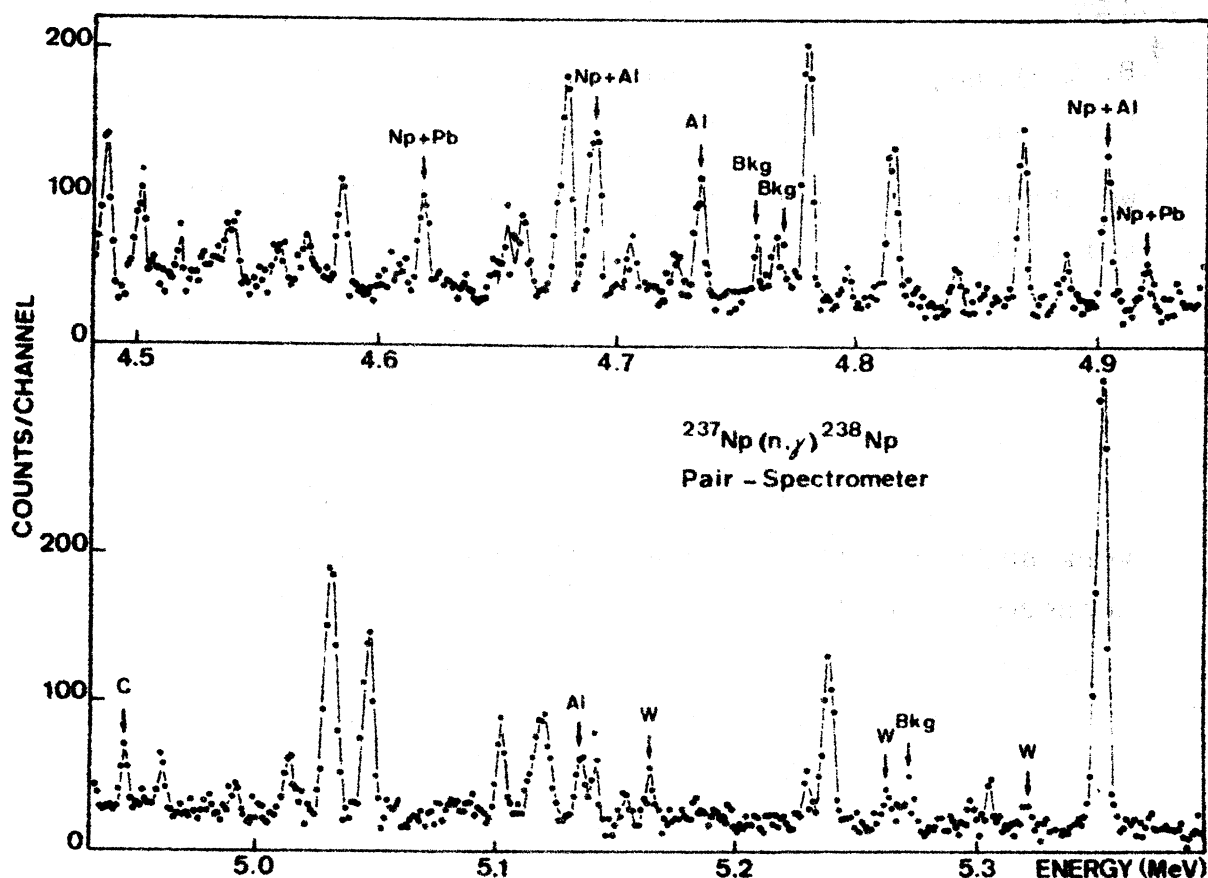


Fig. 1: High energy portion of the  $^{237}\text{Np}(n,\gamma)^{238}\text{Np}$  spectrum

The low energy spectra have been measured with the same detectors operated as an anticompton spectrometer up to 1500 keV and with a 2.4 cm<sup>3</sup> high resolution Ge(Li) detector {2} in the range 0 ÷ 700 keV. Special care was taken to separate the low energy neutron capture gamma rays from the accompanying radioactivity of <sup>237</sup>Np, <sup>238</sup>Np and <sup>233</sup>Pa. The existence of about 60 low energy transitions was established with an accuracy ranging between .030 ÷ 0.15 keV.

The neutron separation energy has been determined.

#### References

- {1} B. Michaud, J. Kern, L. Ribordy, L. A. Schaller,  
Helv. Phys. Acta 45 (1972) 93
- {2} We thank Prof. H. J. Leisi (ETH Zürich) for lending us  
this detector

\* Work supported by the Fonds National Suisse de la  
Recherche Scientifique

3. Study of the  $^{241}\text{Am} (n, \gamma) ^{242}\text{Am}$  reaction using a pair spectrometer\*

M. Gasser and J. Kern

The  $\gamma$ -rays following the thermal neutron capture in  $^{241}\text{Am}$  have been measured with the Fribourg pair spectrometer [1], but using a coaxial 20 cm<sup>3</sup> Ge(Li) diode as the central detector. The use of this larger diode and of an improved electronic setup resulted both in a better detection efficiency and better energy resolution [2].

The target consisted of 1.1g  $\text{Am}_2\text{O}_3$  powder, i. e. 3.4 Ci  $^{241}\text{Am}$ . The measurements have been performed on the reactor SAPHIR in Würenlingen. The target was exposed to a thermal neutron flux of about  $2 \cdot 10^7$  n/cm<sup>2</sup> s for about 90 hours. A portion of the  $\gamma$ -spectrum is shown in fig. 1.

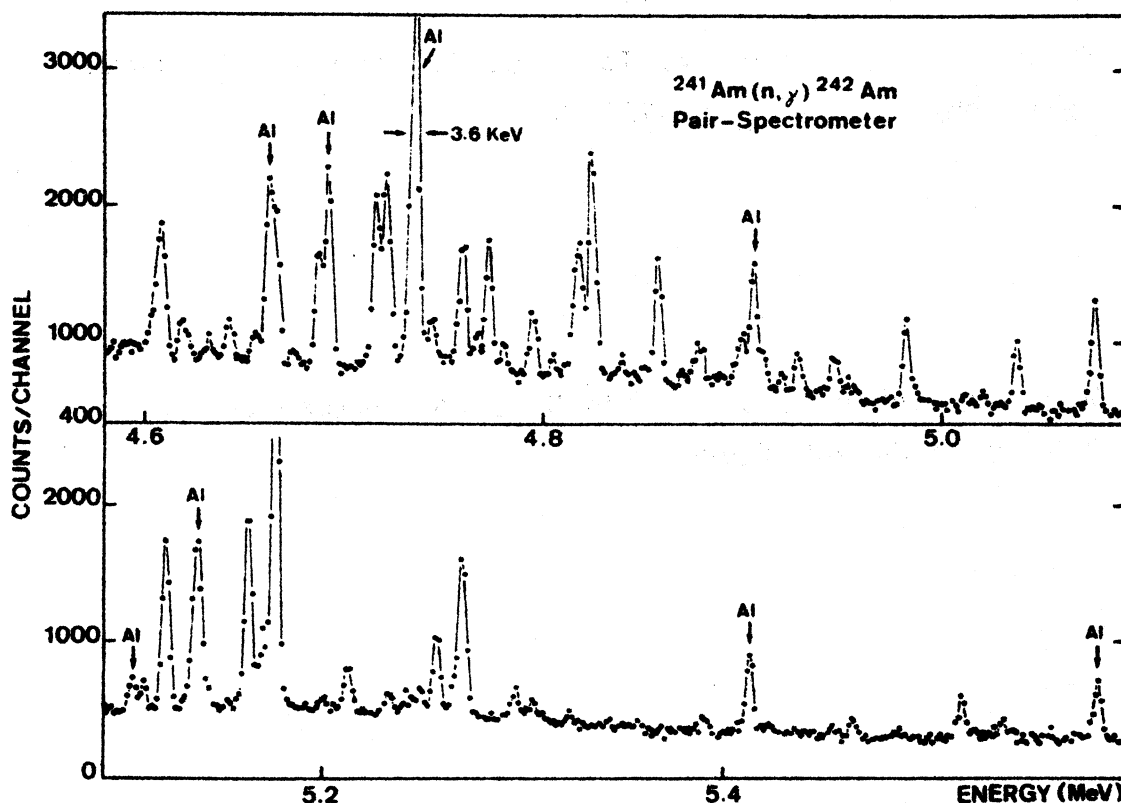


Fig. 1: Portion of the  $^{241}\text{Am} (n, \gamma) ^{242}\text{Am}$  spectrum taken with a pair spectrometer. The time of measurement was about 90 hours

Intense lines from the  $^{27}\text{Al}$  (n, $\gamma$ ) reaction originate from the thin walled aluminium box containing the  $\text{Am}_2\text{O}_3$  powder. These Al-lines were employed for energy calibration purposes. The complex spectrum has been analyzed in the region of 4.5 to 5.5 MeV (Q-value: 5.475 MeV). About 60  $\gamma$ -lines could be attributed to the  $^{241}\text{Am}$  (n, $\gamma$ )  $^{242}\text{Am}$  reaction. Energies and intensities of these lines have been determined. In order to establish a reliable level scheme data from experiments like (d,p), (n,e<sup>-</sup>), low energy (n, $\gamma$ ) etc are needed.

#### References

- {1} B. Michaud, J. Kern, L. Ribordy and L. A. Schaller,  
Helv. Phys. Acta 45 (1972) 93
- {2} M. Gasser, O. Huber, V. Ionescu, J. Kern and A. Raemy,  
Helv. Phys. Acta 45 (1972) 925

\* Work supported by the Fonds National Suisse de la  
Recherche Scientifique



#### 4. Nuclear Levels in $^{160}\text{Tb}^*$

Jean Kern, G. Mauron, B. Michaud

The high energy  $\gamma$ -ray spectrum from thermal neutron capture in natural terbium has been observed over the range of 5200 to 6400 keV with the Fribourg pair spectrometer. This apparatus, whose main component is a  $3\text{ cm}^3\text{ Ge(Li)}$  diode surrounded by a 20 cm diameter  $\text{NaI(Tl)}$  scintillator has been described previously [1]. The resolution obtained in the two main experiments are 4.0 keV and 5.2 keV FWHM for the 6218 keV transition (see fig. 1).

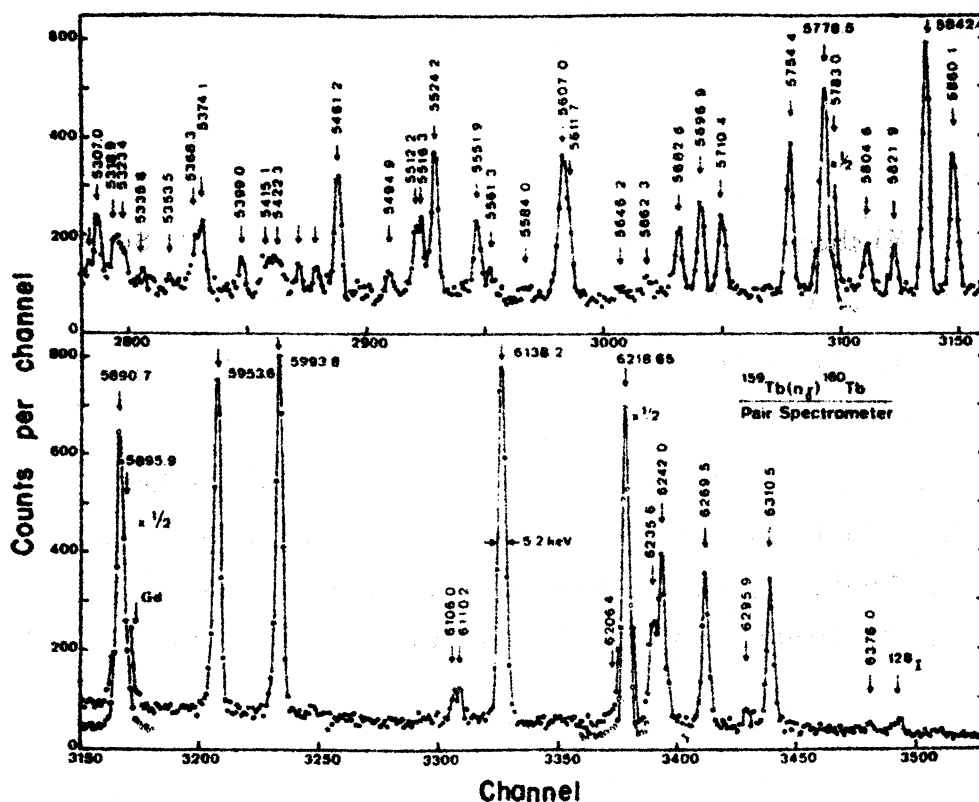


Fig. 1: A portion of the high energy  $^{159}\text{Tb}(n,\gamma)$  spectrum observed with the Fribourg pair spectrometer

The same reaction has been studied over the range 22 to 1230 keV with an anti-Compton spectrometer, which uses the same components as the pair spectrometer, but different logic circuitry. The reactor SAPHIR in Würenlingen was used as the neutron source in the two experiments.

The data have been combined with a previous  $^{159}\text{Tb}(d,p)$  investigation [2] and with the results obtained in the study of the  $(n,\gamma)$ ,  $(n,e^-)$  and  $(n,\gamma-\gamma)$  reactions in other laboratories. A level scheme has been constructed. Nine rotational bands built on two quasi-particle configurations have been disclosed.

A full account of the results has been published recently [3].

#### References

- [1] B. Michaud, J. Kern, L. Ribordy and L. A. Schaller, *Helv. Phys. Acta* 45 (1972) 93
- [2] G. L. Struble and R. K. Sheline, *Sov. J. Nucl. Phys.* 5 (1967) 862
- [3] J. Kern, G. Mauron, B. Michaud, K. Schreckenbach, T. von Egidy, W. Mampe, H. R. Koch, H. A. Baader, D. Breitig, U. Gruber, B. P. K. Maier, O. W. B. Schult, J. T. Larsen and R. G. Lanier, *Nucl. Phys.* A221 (1974) 333

\* Work supported by the Fonds National Suisse de la Recherche Scientifique

III. Eidg. Institut für Reaktorforschung, Würenlingen

1. Mass Distribution in Neutron Induced Fission

M. Rajagopalan, H. S. Pruys, A. Grütter,  
H. R. von Gunten, E. A. Hermes, E. Roessler and  
A. Schmid

A. Fission of  $^{235}\text{U}$  and  $^{239}\text{Pu}$  induced by fast neutrons from  
the reactor PROTEUS:

The yields of the fission products in the fission of  $^{235}\text{U}$  and  $^{239}\text{Pu}$  induced by fast neutrons in the core of the reactor PROTEUS are reported here. The yields were determined by a comparison method using gamma spectroscopy. The intensities of fission product gamma rays were determined in both the fast neutron and thermal neutron induced fission of  $^{235}\text{U}$  and from the known yields in the thermal neutron induced fission of  $^{235}\text{U}$ , the relative yields in the fast fission were calculated. The same procedure was adopted for  $^{239}\text{Pu}$  fission also. Two methods were adopted for gamma spectroscopy. In method A, the gamma ray intensities were measured directly after irradiation of the targets. In method B, the target material (U or Pu) was chemically separated before taking the gamma spectra of fission products so that the gamma rays from the target material did not interfere with the determination of fission product gamma ray intensities. The yields from both methods were normalized relative to the chain yield of mass number 140. The yields for  $^{235}\text{U}$  and  $^{239}\text{Pu}$  are given in Table I. For  $^{235}\text{U}$  the relative yields were converted to absolute yields by normalizing the total yield of all fission products to 200 %. The errors quoted include both statistical and systematic errors. For  $^{239}\text{Pu}$  the yields quoted are relative yields and were obtained by normalizing the yields with respect to  $^{140}\text{Ba}$ . The yield of  $^{140}\text{Ba}$  was

assumed to be 5.50 %. The errors quoted are only statistical errors. The yields quoted for  $^{239}\text{Pu}$  are only preliminary values. Further work on  $^{239}\text{Pu}$  is in progress.

B. Fission of  $^{238}\text{U}$  induced by 14 MeV neutrons:

Mass distribution in the fission of  $^{238}\text{U}$  induced by 14 MeV neutrons was determined using gamma spectroscopy. The relative fission yields in the 14 MeV neutron induced fission are given in Table II. For fission products designated with a \*, the yields were determined from the known efficiency of the detector and the known intensity ratios of gamma lines of specific fission products. For other fission products, the yields were determined by comparing the intensities with those in thermal neutron fission. All the yields were normalized to the yields of  $^{140}\text{Ba}$  which was assumed to be 4.56 %. These are only preliminary results obtained by taking gamma spectra after chemical separation of target material. For some fission products more accurate yields can be obtained by direct measurement of gamma ray intensities and such measurements are in progress.

Table I

Yields in fast neutron induced fission (PROTEUS-Reactor)

Mass No.	Element	<sup>235</sup> U Fission		<sup>239</sup> Pu Fission	
		Yield in %	Method	Yield in %	Method
87	Kr	2.66 ± 0.11	B	---	
88	Kr,Rb	4.45 ± 0.26	B	---	
91	Sr,Y	5.63 ± 0.21	A+B	2.57 ± 0.09	A+B
92	Sr,Y	5.77 ± 0.21	A+B	3.01 ± 0.08	A+B
93	Y	6.23 ± 0.21	A+B	3.49 ± 0.13	A
94	Y	6.13 ± 0.26	A	---	
95	Zr	6.49 ± 0.25	B	5.96 ± 0.24	B
97	Zr,Nb	5.97 ± 0.19	B	5.67 ± 0.47	B
99	Mo,Tc	6.23 ± 0.22	A	6.08 ± 0.20	A+B
101	Tc	5.31 ± 0.18	A	7.20 ± 0.60	B
103	Ru	3.20 ± 0.12	A	6.85 ± 0.23	A+B
104	Tc	1.87 ± 0.08	A	---	
105	Ru	1.10 ± 0.04	A	5.25 ± 0.08	A+B
129	Sb	1.08 ± 0.07	C	---	
131	I	3.06 ± 0.10	B	---	
132	I	4.59 ± 0.15	B	5.46 ± 0.25	B
133	I	7.08 ± 0.22	B	7.66 ± 0.78	B
134	I	7.77 ± 0.26	B	6.42 ± 0.36	B
135	I	7.02 ± 0.22	B	7.43 ± 0.26	B
139	Ba	6.52 ± 0.21	A	5.64 ± 0.40	B
140	Ba,La	6.27 ± 0.23	A	5.50(Ref)	A+B
141	Ba,Ce	5.52 ± 0.34	A	5.81 ± 0.04	A
142	La	5.74 ± 0.32	A+B	5.16 ± 0.19	A+B
143	Ce	5.70 ± 0.21	A+B	4.46 ± 0.31	A+B
146	Pr	2.75 ± 0.14	A	---	
147	Nd	2.26 ± 0.74	A	1.95 ± 0.05	A
149	Nd	1.05 ± 0.04	A	1.24 ± 0.26	A+B
151	Pm	0.43 ± 0.02	A	0.82 ± 0.15	A

- A: Gamma counting after chemical separation of target material  
 B: Direct gamma counting after irradiation  
 C: Radiochemical separation

Table II

Yields in the 14 MeV neutron induced fission of  $^{238}\text{U}$

Mass No.	Element	Cumulative yield
91	Sr,Y	$3.63 \pm 0.08$
92	Sr,Y	$3.81 \pm 0.08$
93	Y	$4.36 \pm 0.08$
99	Mo	$5.42 \pm 0.08$
101	Tc	$4.81 \pm 0.10$
103	Ru	$4.57 \pm 0.14$
105	Ru	$3.14 \pm 0.12$
112	Ag	$0.56^{*} \pm 0.09$
113	Ag	$0.91^{*} \pm 0.14$
115	Cd	$0.79^{*} \pm 0.12$
117	Cd	$0.70^{*} \pm 0.11$
139	Ba	$5.00 \pm 0.18$
140	Ba	$4.56(\text{Ref})$
141	Ce	$4.03 \pm 0.08$
142	La	$3.85 \pm 0.08$
143	Ce	$3.69 \pm 0.10$
147	Nd	$1.98 \pm 0.26$
149	Nd	$1.34 \pm 0.08$
151	Pm	$0.78 \pm 0.02$
156	Sm	$0.14^{*} \pm 0.02$

\* Direct Determinations

## 2. The Decay of $^{152m1}\text{Eu}$ and $^{152m2}\text{Eu}$

H. S. Pruys, E. A. Hermes, H. R. von Gunten

Energies and intensities of the  $\gamma$ -rays in the decay of  $^{152m1}\text{Eu}$  and  $^{152m2}\text{Eu}$  have been determined.  $\gamma$ -spectra above 200 keV and below 200 keV were measured with a 40 cm<sup>3</sup> Ge(Li) detector and a 5 cm<sup>3</sup> planar pure Ge detector respectively. An example of a  $\gamma$ -ray spectrum obtained with the Ge detector is shown in fig. 1.

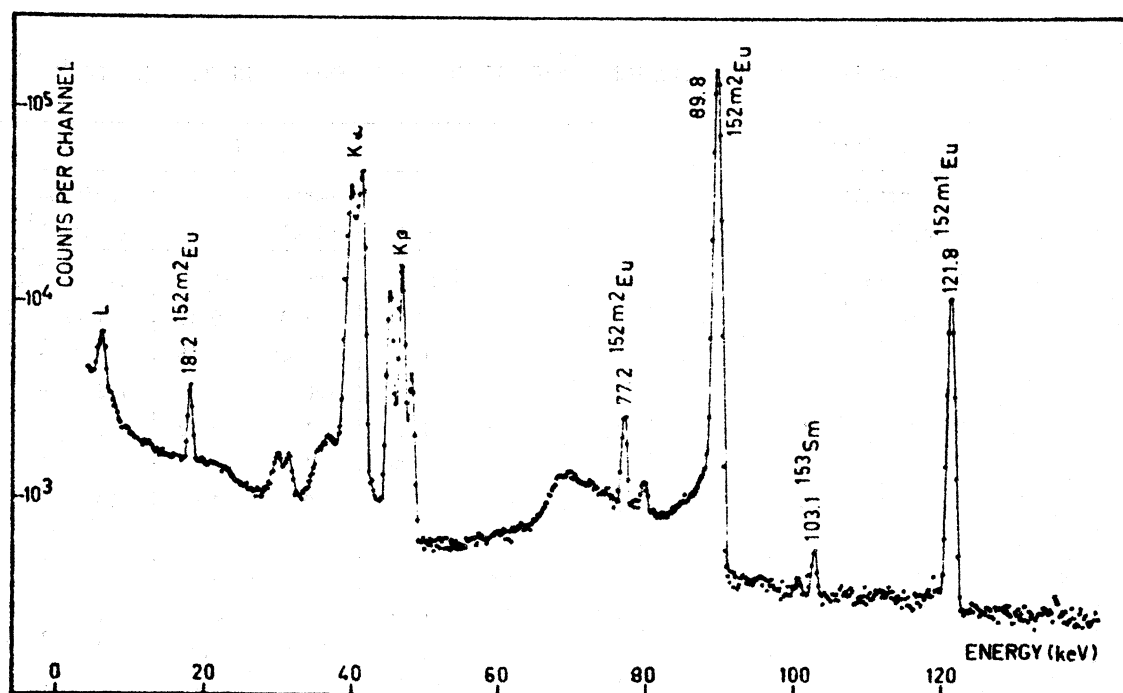


Fig. 1:  $\gamma$ -ray spectrum of 14 MeV neutron produced  $^{152m2}\text{Eu}$

Enriched  $^{151}\text{Eu}$ - and  $^{153}\text{Eu}$ -oxyde samples were irradiated with thermal neutrons and 14 MeV neutrons in order to obtain sources of  $^{152m1}\text{Eu}$  and  $^{152m2}\text{Eu}$ . The ratio of the activities of  $^{152m2}\text{Eu}/^{152m1}\text{Eu}$  was much higher in the 14 MeV neutron irradiation.

The  $\gamma$ -ray energies and intensities measured in the decay of  $^{152m1}\text{Eu}$  are presented in table 1. The results are in very good agreement with those of Barrette et al. [1]. In their work five

more  $\gamma$ -lines were detected, but only two of them could be placed in the decay scheme. The intensities reported by Ardisson et al. {2} are in considerable disagreement with the work of Barrette et al. {1} and the present work. Nine new  $\gamma$ -lines were observed by Ardisson et al. {2}, but according to our work six of them are sum peaks. The existence of the 1756.2 keV level in  $^{152}\text{Gd}$  {1} has been confirmed by our coincidence measurements since the 1411.88 keV  $\gamma$ -line was detected in coincidence with the 344.25 keV transition.

Table 1 : ENERGIES AND RELATIVE INTENSITIES OF THE  $\gamma$ -RAYS EMITTED IN THE DECAY OF  $^{152\text{m}}\text{Eu}$

$E_{\gamma}$ (keV)			$I_{\gamma}$		
this work	Barrette et al. 1)	Ardisson et al. 2)	this work	Barrette et al. 1)	Ardisson et al. 2)
121.75 $\pm$ 0.04	121.78 $\pm$ 0.03		311 $\pm$ 10	295 $\pm$ 15	410 $\pm$ 41
244.65 $\pm$ 0.06	244.66 $\pm$ 0.03	244.7 $\pm$ 0.5	0.94 $\pm$ 0.06	1.00 $\pm$ 0.15	1.42 $\pm$ 0.18
271.16 $\pm$ 0.06	271.2 $\pm$ 0.2	270.0 $\pm$ 0.5	3.39 $\pm$ 0.12	3.40 $\pm$ 0.25	4.4 $\pm$ 0.5
344.25 $\pm$ 0.04	344.31 $\pm$ 0.3		100	100	143 $\pm$ 7
443.94 $\pm$ 0.06	443.98 $\pm$ 0.05	444.5 $\pm$ 1.0	0.99 $\pm$ 0.12	1.07 $\pm$ 0.12	1.53 $\pm$ 0.24
547.4 $\pm$ 0.3	547.5 $\pm$ 0.5		0.35 $\pm$ 0.06	0.4 $\pm$ 0.2	
563.00 $\pm$ 0.04	562.99 $\pm$ 0.07	563.0 $\pm$ 0.5	9.0 $\pm$ 0.3	9.2 $\pm$ 0.5	10.5 $\pm$ 1.2
586.3 $\pm$ 0.2	586.5 $\pm$ 0.2		0.47 $\pm$ 0.05	0.4 $\pm$ 0.2	
688.70 $\pm$ 0.06	688.68 $\pm$ 0.08	688.6 $\pm$ 0.5	2.63 $\pm$ 0.12	2.7 $\pm$ 0.4	2.3 $\pm$ 0.24
699.33 $\pm$ 0.06	699.28 $\pm$ 0.15	698.8 $\pm$ 0.5	2.98 $\pm$ 0.18	2.7 $\pm$ 0.5	3.4 $\pm$ 0.4
703.55 $\pm$ 0.06	703.6 $\pm$ 0.2	703.4 $\pm$ 0.5	2.51 $\pm$ 0.18	2.6 $\pm$ 0.4	3.1 $\pm$ 0.3
810.47 $\pm$ 0.08	810.7 $\pm$ 0.3	810.1 $\pm$ 0.8	1.05 $\pm$ 0.06	0.97 $\pm$ 0.20	1.18 $\pm$ 0.24
826.01 $\pm$ 0.07	826.0 $\pm$ 0.2	825.9 $\pm$ 0.6	1.23 $\pm$ 0.12	1.20 $\pm$ 0.15	1.12 $\pm$ 0.24
841.62 $\pm$ 0.05	841.68 $\pm$ 0.08	841.4 $\pm$ 0.3	585 $\pm$ 18	595 $\pm$ 20	590
870.14 $\pm$ 0.06	870.15 $\pm$ 0.12	869.8 $\pm$ 0.5	3.63 $\pm$ 0.18	3.9 $\pm$ 0.4	3.6 $\pm$ 0.4
963.39 $\pm$ 0.05	963.36 $\pm$ 0.08	963.4 $\pm$ 0.3	487 $\pm$ 16	492 $\pm$ 15	490 $\pm$ 30
970.36 $\pm$ 0.07	970.34 $\pm$ 0.10	970.1 $\pm$ 0.3	25.2 $\pm$ 1.3	25.3 $\pm$ 0.8	43 $\pm$ 5
995.85 $\pm$ 0.08	995.77 $\pm$ 0.12	995.6 $\pm$ 0.5	2.69 $\pm$ 0.12	2.7 $\pm$ 0.3	2.8 $\pm$ 0.3
1314.65 $\pm$ 0.07	1314.58 $\pm$ 0.06	1314.5 $\pm$ 0.4	40.4 $\pm$ 1.3	39.4 $\pm$ 1.2	48 $\pm$ 4
1389.11 $\pm$ 0.07	1389.02 $\pm$ 0.06	1388.9 $\pm$ 0.3	35.0 $\pm$ 1.1	33.0 $\pm$ 1.0	34 $\pm$ 4
1411.88 $\pm$ 0.10	1411.77 $\pm$ 0.10	1411.5 $\pm$ 0.4	1.87 $\pm$ 0.06	1.82 $\pm$ 0.12	2.4 $\pm$ 0.3
1510.80 $\pm$ 0.10	1510.75 $\pm$ 0.20	1510.6 $\pm$ 0.5	0.27 $\pm$ 0.03	0.35 $\pm$ 0.10	1.36 $\pm$ 0.18
1558.90 $\pm$ 0.15	1558.78 $\pm$ 0.20	1558.7 $\pm$ 1.0	0.35 $\pm$ 0.02	0.36 $\pm$ 0.07	0.31 $\pm$ 0.06
1680.8 $\pm$ 0.2	1680.6 $\pm$ 0.3	1681.0 $\pm$ 1.0	0.27 $\pm$ 0.02	0.22 $\pm$ 0.05	0.25 $\pm$ 0.06
1756.2 $\pm$ 0.2	1755.6 $\pm$ 0.5	1755.8 $\pm$ 1.5	0.12 $\pm$ 0.03	0.09 $\pm$ 0.03	0.20 $\pm$ 0.06



The results of the measurements of the  $^{152m2}\text{Eu}$  decay are presented in table 2. The  $\gamma$ -ray energies are in agreement with the values reported in the electron conversion work of Takahashi et al. {3}. The K-shell internal conversion coefficient for the 89.82 keV transition was deduced from the measured K X-ray intensity. The value for  $\alpha_K$ ,  $0.28 \pm 0.03$ , is in agreement with previously reported values of  $0.27 \pm 0.04$  {4} and  $0.30 \pm 0.05$  {3}. The 77.23 keV  $\gamma$ -line found in our work was assigned to  $^{152m2}\text{Eu}$  on basis of its half life.

The half-lives of  $^{152m1}\text{Eu}$  and  $^{152m2}\text{Eu}$  have been measured to be  $9.30 \pm 0.05$  h and  $96 \pm 1$  min respectively in agreement with the values given in the Chart of the Nuclides {5}.

Table 2:  $\gamma$ -rays from the decay of  $^{152m2}\text{Eu}$

$E_\gamma$ (keV)		relative intensity
this work	Takahashi et al. {3}	
$18.21 \pm 0.04$	$18.25 \pm 0.10$	$1.63 \pm 0.11$
$77.23 \pm 0.04$		$0.95 \pm 0.07$
$89.82 \pm 0.04$	$89.83 \pm 0.15$	100

### References

- {1} J. Barrette, M. Barette, A. Boutard, G. Lamoureux, S. Monaro, S. Markiza, Can. J. Phys. 49 (1971) 2462
- {2} G. Ardisson, F. Armanet, A. Al Foudi, Compt. Rend. Ser B 274 (1972) 1436
- {3} K. Takahashi, M. McKeown, G. Scharff-Goldhaber, Phys. Rev. 137B (1965) 763
- {4} P. Kirkby, T. M. Kavanagh, Nucl. Phys. 49 (1963) 300
- {5} W. Seelmann-Eggebert, G. Pfennig, H. Münzel, Nuklidkarte, 3. Auflage, Bundesminister für wissenschaftliche Forschung, Bonn (1968)

IV.      Physikalisches Institut der Universität Zürich

---

(Prof. Dr. Verena Meyer)

Current experiments on Van de Graaff Accelerators:

1.      Precision measurements of p-p scattering phases at energies below 10 MeV

Measurements of the differential scattering cross-section in the energy range 320-450 keV are being made with an accuracy of approx. 12 %.

2.      Nuclear spectroscopy with high energy resolution

With the aid of high resolution ( $\Delta E \leq 500$  eV) elastic scattering an investigation is being made of nuclear states with regard to the statistics of level densities and analogue resonances. Protons are scattered elastically by  $^{32}\text{S}$  ( $T=3/2$  state),  $^{50}\text{Cr}$  and  $^{54}\text{Fe}$  (analogue states and level densities) and  $^{92}\text{Mo}$  (analogue states at  $E_p = 4.36$  and  $5.3$  MeV). Energy range  $E_p = 3.0$ - $5.4$  MeV.

3.      Measurement of short lifetimes ( $< 1$  ns)

The lifetimes of states in  $^{13}\text{C}$ ,  $^{16}\text{O}$  and  $^{39}\text{K}$  were measured with the aid of a high resolution pulsed particle beam ( $\Delta t \leq 100$  ps).

V. Physikalisches Institut der Universität Basel

1. Analyzing Power of  $\vec{n}$ -p-Scattering at 14.2 MeV

B. Leemann, R. Casparis, M. Freiswerk, H. Rudin,  
R. Wagner, P. Zupranski\*

The analyzing power  $A_y$  which is observed in the scattering of neutrons (10 - 30 MeV) from protons can be described by the expression

$$\sigma_0(\theta)A_y(\theta) = \frac{3\sin\theta}{k^2} \sin^2\delta_0 \{ \Delta_{LS}^P + 5\Delta_{LS}^D \cos\theta \}$$

A measurement of the analyzing power at an angle of  $\theta_{CM} = 90^\circ$  gives the possibility to determine the spin-orbit coupling term  $\Delta_{PS}^L$  for p-waves. An atomic beam source produced polarized deuterons ( $\sim 0.5 \mu A$ ) and the  $T(\vec{d}, \vec{n})^4He$ -reaction was used at a deuteron energy of 140 keV as a source of highly polarized 14.2-MeV-neutrons.

The neutron polarization ( $P_n = 0.53 \pm 0.02$ ) was measured with a high pressure scintillation chamber. The proton analyzing power was determined using an associated particle time of flight system.

The measurements of the asymmetry of the neutrons scattered at an angle  $\theta_{CM} = 90^\circ$  were made with cylindrical scatterers of different diameters. The measurements using the bigger scatterers ( $\emptyset = 3.81$  cm) gave an average value of the analyzing power of  $A = (2.12 \pm 0.22)\%$  which is in good agreement with earlier data [1] in this energy region. On the other hand the measurements with the smaller scatterer ( $\emptyset = 2$  cm) gave an average value of the analyzing power of  $A = (0.22 \pm 0.36)\%$ . We suppose that the measurements with the bigger scatterers are strongly influenced and masqued

by multiple scattering effects from the carbon of the scattering scintillators.

### References

- {1} G. S. Mutchler, J. E. Simmons, Phys. Rev. C4 (1971) 67,  
R. Garret et al., University of Auckland, New Zealand  
(Private Communication)

\* On leave from Instytut Badań Jądrowych, Warschau

### 2. Analyzing Power of $\vec{n}$ -d-Scattering at 14.2 MeV

M. Preiswerk, R. Casparis, B. Leemann, H. Rudin  
R. Wagner, P. Zupranski\*

We have measured the angular distribution of the analyzing power of deuterium for polarized 14.2-MeV-neutrons. There is a considerable lack of data in this energy range. Accurate data would be very helpful for a theoretical approach to the three nucleon system. Polarized deuterons ( $\sim 0.5 \mu A$ ) were produced with an atomic beam source and the  $T(\vec{d}, \vec{n})^4He$ -reaction was used as a source of highly polarized neutrons. The results of our asymmetry measurements are in good agreement with the experimental  $\vec{p}$ -d-data at 14.5 MeV of Faivre et al. {1} and also with the theoretical  $\vec{n}$ -d-predictions of Pieper {2}. (Fig. 1/2)

### References

- {1} J. C. Faivre et al., Nucl. Phys. A127 (1969) 169  
{2} S. C. Pieper, Nucl. Phys. A193 (1972) 529  
{3} P. Doleschall, Nucl. Phys. A201 (1972) 264

\* On leave from Instytut Badań Jądrowych, Warschau

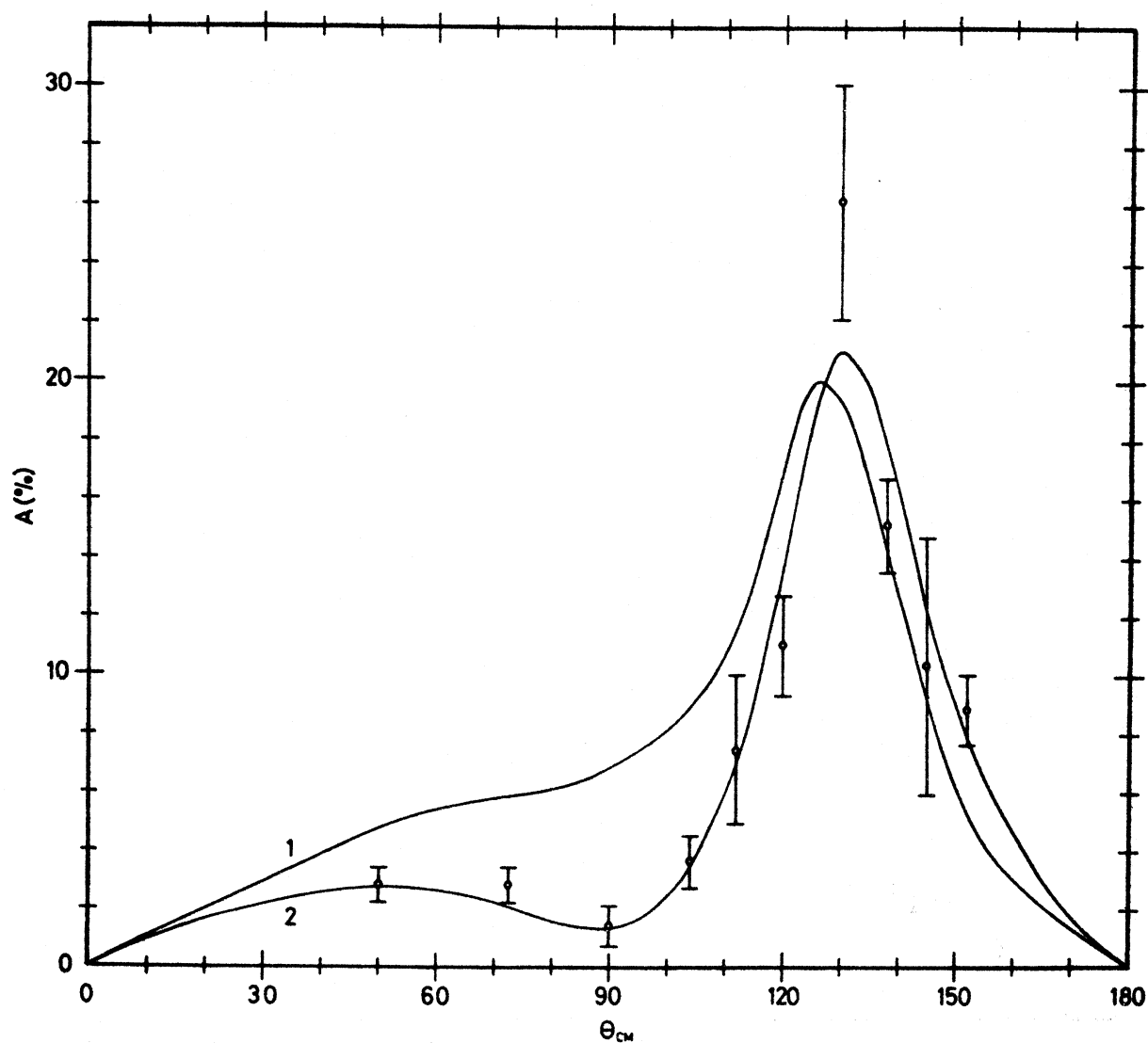


Fig. 1: Comparison of our measurements of the analyzing power of deuterium for polarized 14.2-MeV-neutrons with the theoretical curves of Doleschall {1} and Pieper {2}. The perturbation method of Pieper gives better agreement with the measurements than the calculations of Doleschall {3} which use the solution of the Faddeev-equations. The experimental points are shown with their statistical errors.

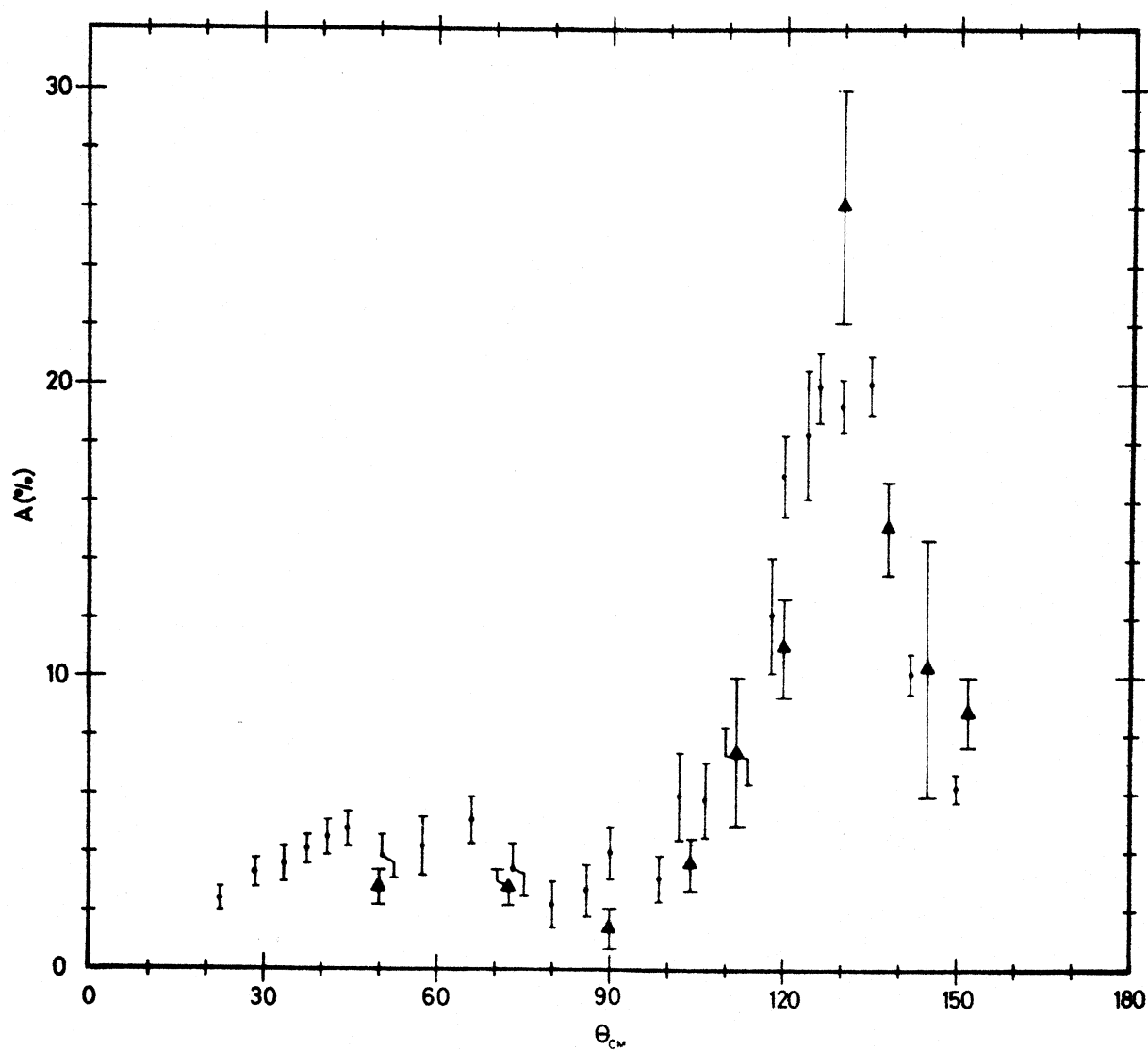


Fig. 2: Comparison of our  $\vec{n}$ -d-results (triangles) with the experimental  $\vec{p}$ -d-data (points) at 14.5 MeV of Faivre.

3. Scattering of 14-MeV Polarized Neutrons by  $^{12}\text{C}$

R. Casparis, M. Preiswerk, H. Eudin, R. Wagner,  
P. Zupranski\*

At  $E_n = 14.2$  MeV measurements of the angular distribution of the asymmetry  $A(\theta)$  for the  $^{12}\text{C}(n,n')^{12}\text{C}^*$ -inelastic-scattering ( $Q = -4.43$  MeV) and the neutron polarization  $P(\theta)$  for elastic scattering are in progress. The polarized neutrons are produced with the  $T(\vec{d},\vec{n})^4\text{He}$ -reaction using polarized deuterons. A time of flight technique allows separation of elastically and inelastically scattered neutrons. Up to  $90^\circ$  (Lab) a graphite cylinder serves as scatterer, above  $90^\circ$  carbon recoils in a plastic scintillator give an additional information. The experimental results for the neutron polarization in the elastic scattering are in good agreement with data of Mack et al. [1] and also with comparable  $^{12}\text{C}(p,p)^{12}\text{C}$ -data [2]. The measured asymmetry  $A(\theta)$  of the inelastic scattering shows a similarity with  $^{12}\text{C}(p,p')^{12}\text{C}^*$ -scattering results [2] up to  $90^\circ$  but deviates from this behaviour for larger angles.

References

- [1] Mack et al., Proc. 3rd Symp. Polarization Phenomena, Madison (1970), p. 615
- [2] Darriulat et al., Proc. 2nd Symp. Polarization Phenomena, Basel (1966) p. 342

\* On leave from Instytut Badań Jądrowych, Warschau

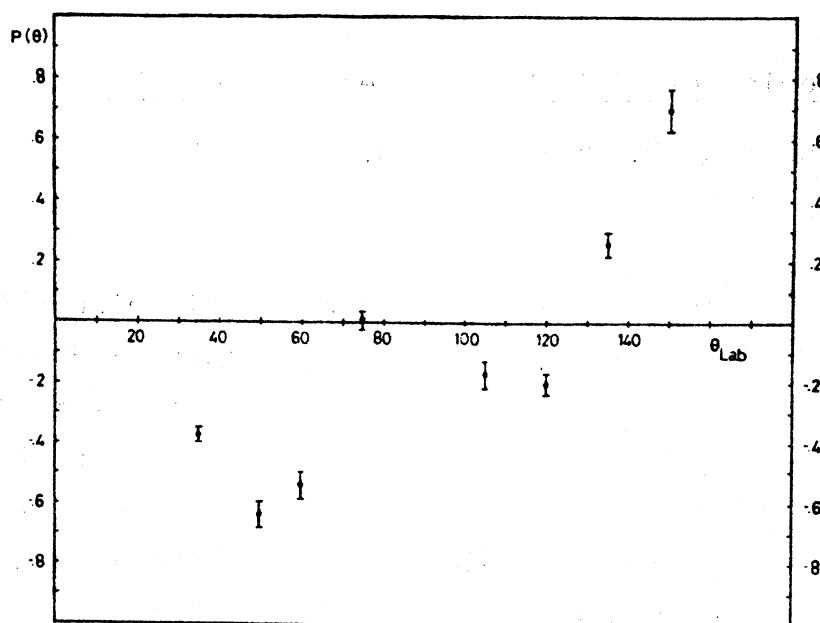


Fig. 1: Polarization  $P(\theta)$  of the  $^{12}\text{C}(n,n)^{12}\text{C}$ -scattering,  
 $E_n = 14.2$  MeV

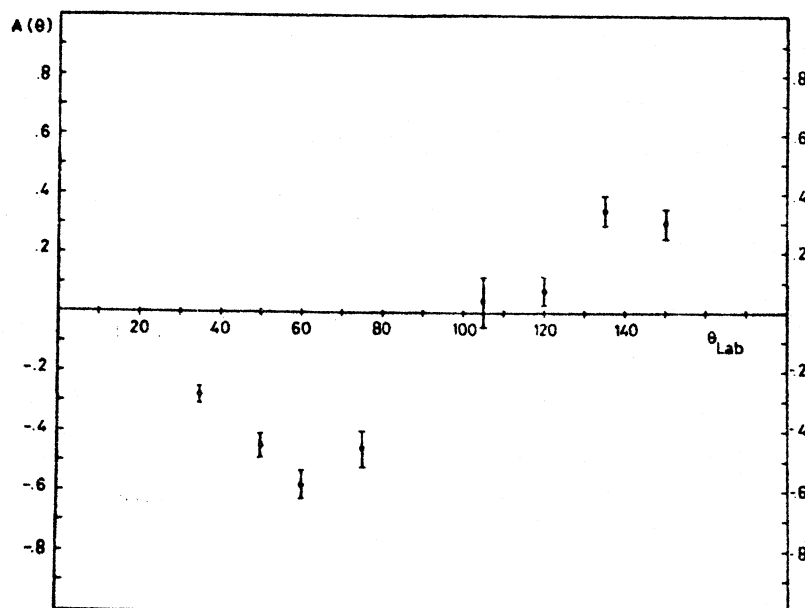


Fig. 2: Asymmetry  $A(\theta)$  of the  $^{12}\text{C}(n,n')^{12}\text{C}^*$ -scattering  
 $(Q = -4.43 \text{ MeV})$  at  $E_n = 14.2$  MeV



4. Fragment Anisotropy at the  $^{238}\text{U}(n,2nf)$ -Threshold

R. Abegg and R. Wagner

Angular distributions of fragments from neutron induced fission of  $^{238}\text{U}$  have been measured in the energy region  $13.5 \leq E_n (\text{MeV}) \leq 17.5$ . The experimental results show a strong rise in the anisotropy  $A = W(0^\circ)/W(90^\circ) - 1$  (fig. 1) at the thrid-chance fission threshold.

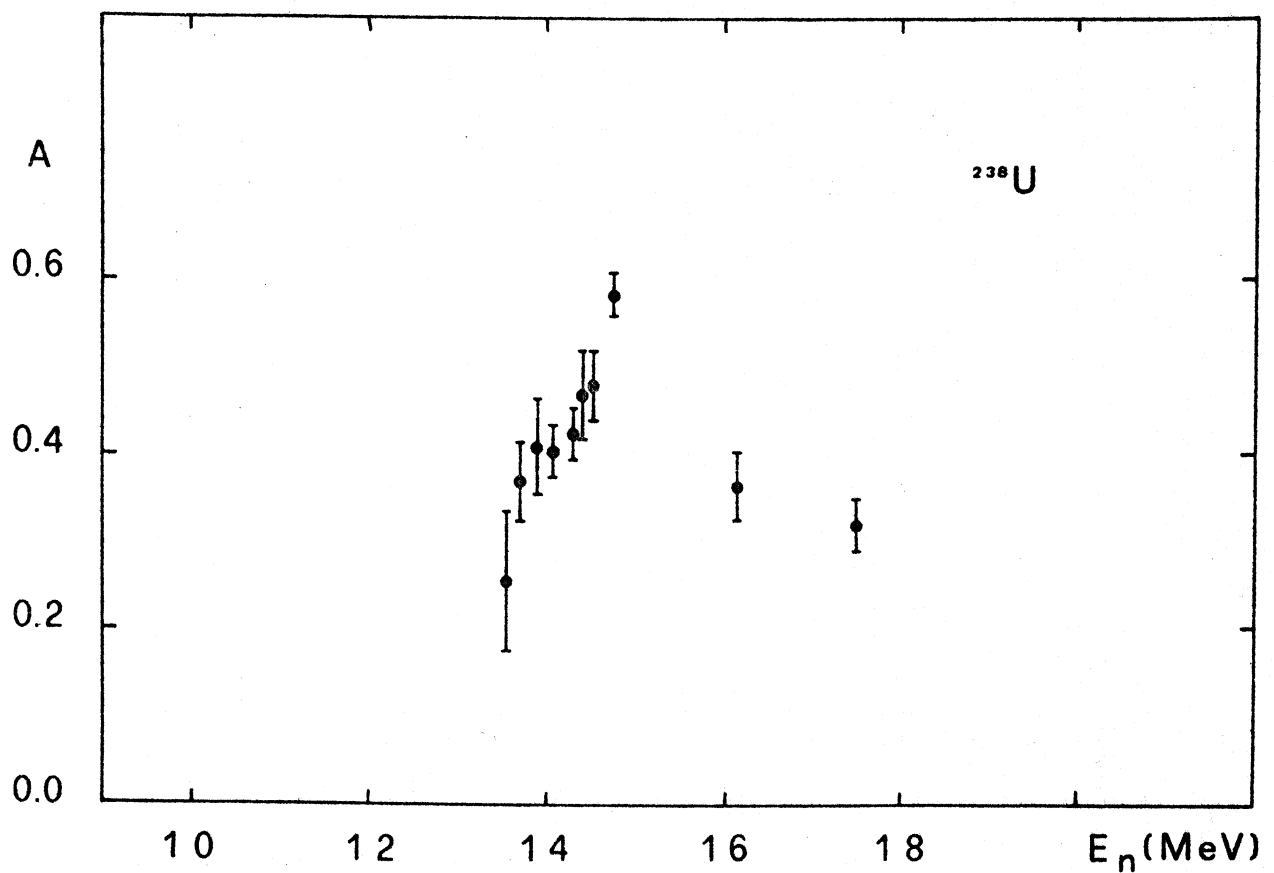
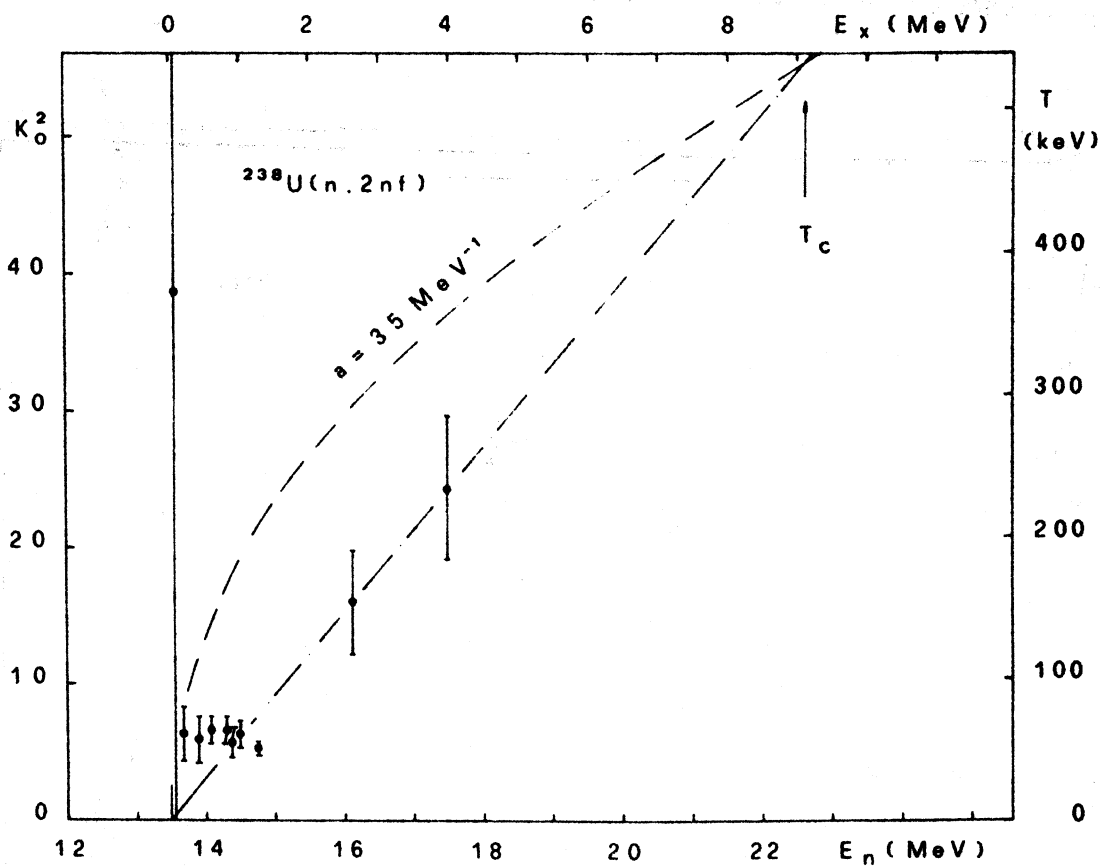


Fig. 1: Anisotropy  $A$  versus neutron energy  $E_n$  (MeV)

The behaviour of the anisotropy in this energy region has been analyzed in the framework of the statistical model. The excitation function of the quantity  $K_O^2$ , which determines the angular momentum distribution along the symmetry axis of the compound nucleus  $^{237}\text{U}$ , as well as the energy dependence of the nuclear temperature  $T$  have been calculated (fig. 2).



**Fig. 2:** Energy dependence of  $K_O^2$  and of the nuclear temperature  $T$ .  $E_x$  represents the excitation energy above the  $(n,2nf)$ -threshold. ---  $E_x = aT^2 - T$  with a level density parameter of  $35 \text{ MeV}^{-1}$ . -.- linear dependence of  $T$  on  $E_x$  as predicted by the BCS-Model.  $T_c$  : transition energy of the  $^{237}\text{U}$ -nucleus corresponding to an "energy gap" of  $\Delta = 1.8 \pm 0.3 \text{ MeV}$ .

5. (d,p) - stripping reactions on nickel isotopes

P. Staub, H. Schär and E. Baumgartner

The differential cross sections for (d,p)-reactions on  $^{58}\text{Ni}$ ,  $^{60}\text{Ni}$ ,  $^{62}\text{Ni}$  and  $^{64}\text{Ni}$  were measured at 2.8 MeV.

The proton energy spectra were fitted by a special "Gauss-fit" program. Parameters of the optical model derived from elastic scattering data were used for calculating the (d,p) cross sections by means of DWBA (DWUCK). Spectroscopic factors were obtained for approx. 20 excited states in the nickel isotopes.

6. Proton-Proton Scattering in the Energy Range  
500-2000 keV

H. Wassmer, H. Mühry

Precise differential cross sections for proton-proton scattering have been measured at the energies 1.881 MeV, 0.992 MeV and 0.499 MeV simultaneously at angles  $24^\circ$ ,  $50^\circ$  and  $90^\circ$  in the centre-of-mass system. The total uncertainties vary from about 0.1 % at 1.881 MeV and 0.992 MeV to 0.8 % at 0.499 MeV and  $90^\circ$ . A satisfactory agreement between a phase shift analysis and the data can only be obtained by introducing a 'strength factor'  $\Lambda$  for the vacuum-polarization contribution.

A detailed paper has been published in *Helv. Phys. Acta* 46 (1973), 626

VI.      Laboratorium für Kernphysik, Eidg. Technische  
Hochschule, Zürich

---

1.      Deuteron break-up and proton scattering on  $^{58}\text{Ni}$

A. Buta\*, J. Lang, S. Micek\*\*, E. Müller,  
J. Unternährer and E. Viatte

The break-up of deuterons on  $^{58}\text{Ni}$  has been measured. Contrary to gold the energy-angle correlation of this process shows pronounced structure due to excitation of levels in the intermediate configuration  $^{59}\text{Cu}$ . The proton spectra are confronted with the excitation curves of the proton scattering on the same target.

A detailed paper has been submitted for publication in Physics Letters B.

\*      On leave from Institute for Atomic Physics, Bucarest, Romania

\*\*     On leave from Jagellonian University, Cracow, Poland

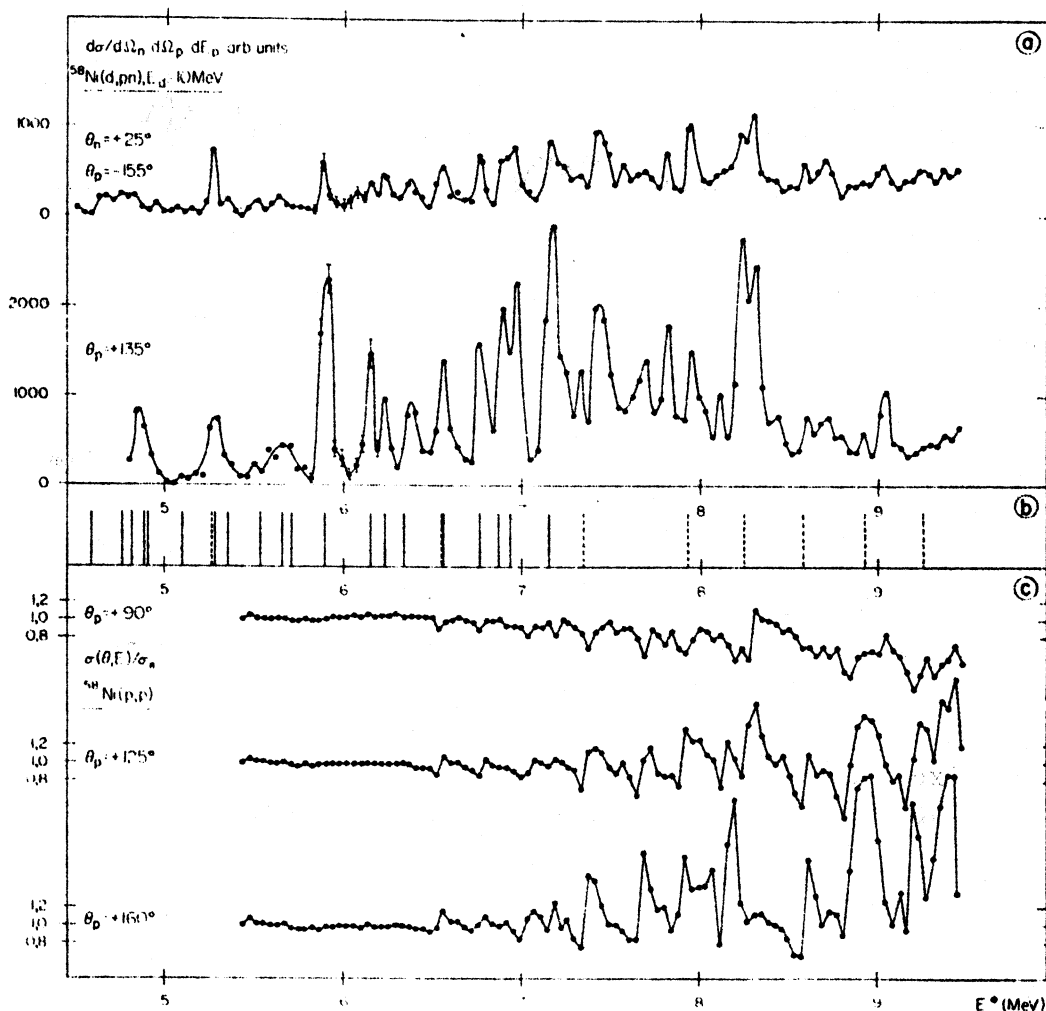


**Fig. 1:** a. Proton spectra  $d\sigma/d\Omega_n d\Omega_p dE_p$  for the reaction  $^{58}\text{Ni}(d,pn)^{58}\text{Ni}$  with  $E_d = 10$  MeV, at the neutron emission angle  $\theta_n = 25^\circ$  and for the proton angles  $\theta_p = +135^\circ$  (proton counter placed on the same side of the beam as the neutron counter) and  $\theta_p = -155^\circ$  (opposite side). As in all other figures in the x-axis the excitation energy of  $^{59}\text{Cu}$  is plotted.

b. Levels in  $^{59}\text{Cu}$

————— ref.5, - - -  $E^* < 7$  MeV: ref.7,  $E^* > 7$  MeV: ref. 6.

c. Excitation curves (cross section divided by Rutherford cross section) for proton elastic scattering on  $^{58}\text{Ni}$  at the angles  $90^\circ$ ,  $125^\circ$ ,  $160^\circ$ , for proton energies from 2 to 6 MeV.

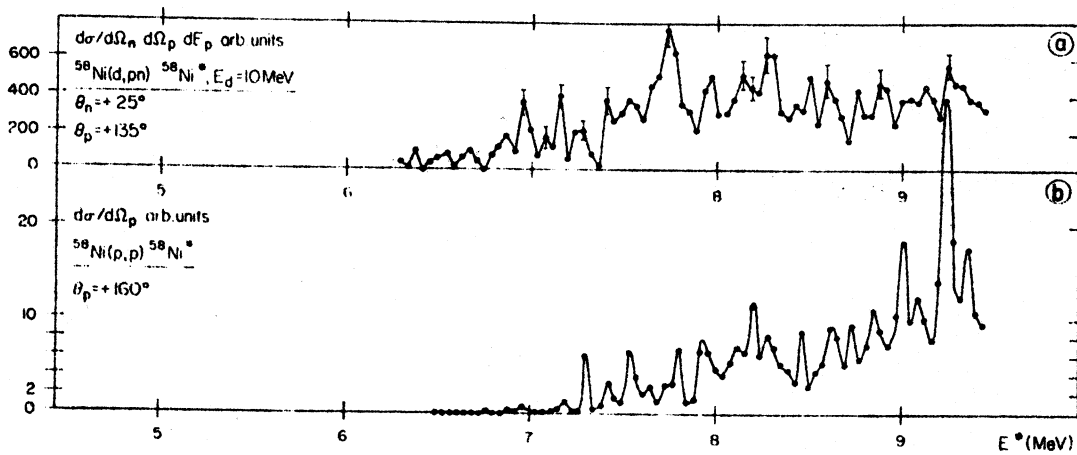


**Fig. 2:** a. Differential cross section  $d\sigma/d\Omega_n d\Omega_p dE_p$  for break-up on  $^{58}\text{Ni}$  leading to the first excited state of the target nucleus with  $E_d = 10$  MeV, neutron angle  $\theta_n = 25^\circ$ , and proton angle  $\theta_p = +135^\circ$ .  
b. Excitation function of the inelastic scattering  $^{58}\text{Ni}(p,p')^{58}\text{Ni}^*$  at  $160^\circ$  with excitation of the first  $2^+$  level.

## 2. Calibration of a Neutron Detector

J. Unternährer, J. Lang, R. Müller, P. Viatte

The sensitivity of a neutron detector, consisting of a NE 213 liquid scintillator and a XP 1040 photo multiplier was measured and calculated for neutrons in the energy range 0.4 MeV to 5 MeV. Pulse height was discriminated at 60 keV equivalent electron energy (Am-bias). To determine source strength the  $^2\text{H}(d,n)^3\text{He}$  and  $^3\text{H}(p,n)^3\text{He}$  reactions were counted by the method of associated particles. For the calculations a Monte-Carlo-program was used. Five different processes of energy loss of neutrons within the scintillator were taken into account. Most important are elastic collisions with hydrogen and carbon atoms.

3. Investigation of the  ${}^6\text{Li}(d,\alpha){}^4\text{He}$  Reaction by  
Polarized Deuterons

R. Risler, W. Grüebler, A. A. Debenham, V. König,  
D. Boerma and P. A. Schmelzbach

The nucleus  ${}^8\text{Be}$  is of great theoretical interest since it is considered to have a simple alpha-particle like structure. This clustering is expected for at least the states with low excitation energy but also states at higher energy are likely to have a quartet configuration. Below an excitation energy of 16 MeV the level structure seems to be well understood. Above this energy the level structure becomes more complex as other configuration like  $p + {}^7\text{Li}$ ,  $n + {}^6\text{Li}$  are also important.

In the last few years much experimental evidence for highly excited states in  ${}^8\text{Be}$  has been found. Phase shift analysis of  $\alpha$ - $\alpha$  scattering seems to give the best information on levels with alpha-particle configuration [1]. However levels having other configurations are mostly detected by the absorption part of the phase shifts and are shown only very weak if the transition to this configuration is small. Also high spin levels, particularly the broad ones, would be difficult to observe experimentally by  $\alpha$ - $\alpha$  scattering. In these cases a resonance will escape observation since the change in the corresponding phase shift would be very weak.

The  ${}^7\text{Li}(p,\alpha){}^4\text{He}$  and the  ${}^6\text{Li}(d,\alpha){}^4\text{He}$  reactions have been the favorites in order to study the even spin and parity levels, because their spin structure is relatively simple, due to the two identical spinless particles in the exit channel. Most of these experimental results consist of differential cross section data and measurements with vector polarized proton and deuteron beams. Over a very limited deuteron energy range (0.40 to 0.96 MeV)

corresponding to an excitation energy in  ${}^8\text{Be}$  from 22.6 to 23.0 MeV, tensor analysing power measurements of the  ${}^6\text{Li}(d,\alpha){}^4\text{He}$  reaction were reported.

In spite of the large amount of experimental data ambiguous assignments have come from the different analyses. All R-matrix and S-matrix analyses of the above mentioned reactions require at least three levels in  ${}^8\text{Be}$  between 22 and 26 MeV excitation energy in order to explain the experimental data. Several level sequences with  $0^+$ ,  $2^+$  and  $4^+$  states are proposed [2] all fitting the differential cross section equally well. On the other hand the polarization data are too scarce in order to differentiate between these different assignments.

The  $\alpha$ - $\alpha$  phase shift analysis shows clear evidence for a  $2^+$  doublet near 17 MeV and three states with  $4^+$ ,  $2^+$  and  $0^+$  around 20 MeV excitation energy, however the higher states show up less convincing. At excitation energies higher than 26 MeV no indications for further resonances exist.

This unsatisfactory situation suggests that more experimental information is needed for a final assignment of the level structure at energies higher than 20 MeV. The particles in the entrance channel of the  ${}^6\text{Li}(d,\alpha){}^4\text{He}$  reaction have a binding energy of 22.28 MeV above the ground state of  ${}^8\text{Be}$ . The necessary information for an improved R-matrix analyses could be provided by measurements of vector and tensor analysing powers over an extended energy range. Recently it has been shown that these quantities can reveal essential information on the level structure in the corresponding compound nucleus [3].

In the present work data on the cross section, the vector analysing power  $iT_{11}$  and the three tensor analysing powers  $T_{20}$ ,  $T_{21}$  and  $T_{22}$  in the energy range between 1.5 and 11.5 MeV are reported. The results are shown in figs. 1 to 5.



References

- {1} A. D. Bacher, F. G. Resmini, H. E. Conzett, R. de Swiniarski,  
H. Meiner and J. Ernst, Phys. Rev. Lett. 29 (1972) 1331
- {2} Tsan Ung Chan, J. P. Longequeue and H. Beaumevieille,  
Nucl. Phys. A 124 (1969) 449
- {3} F. Seiler, Nucl. Phys. A 187 (1972) 379

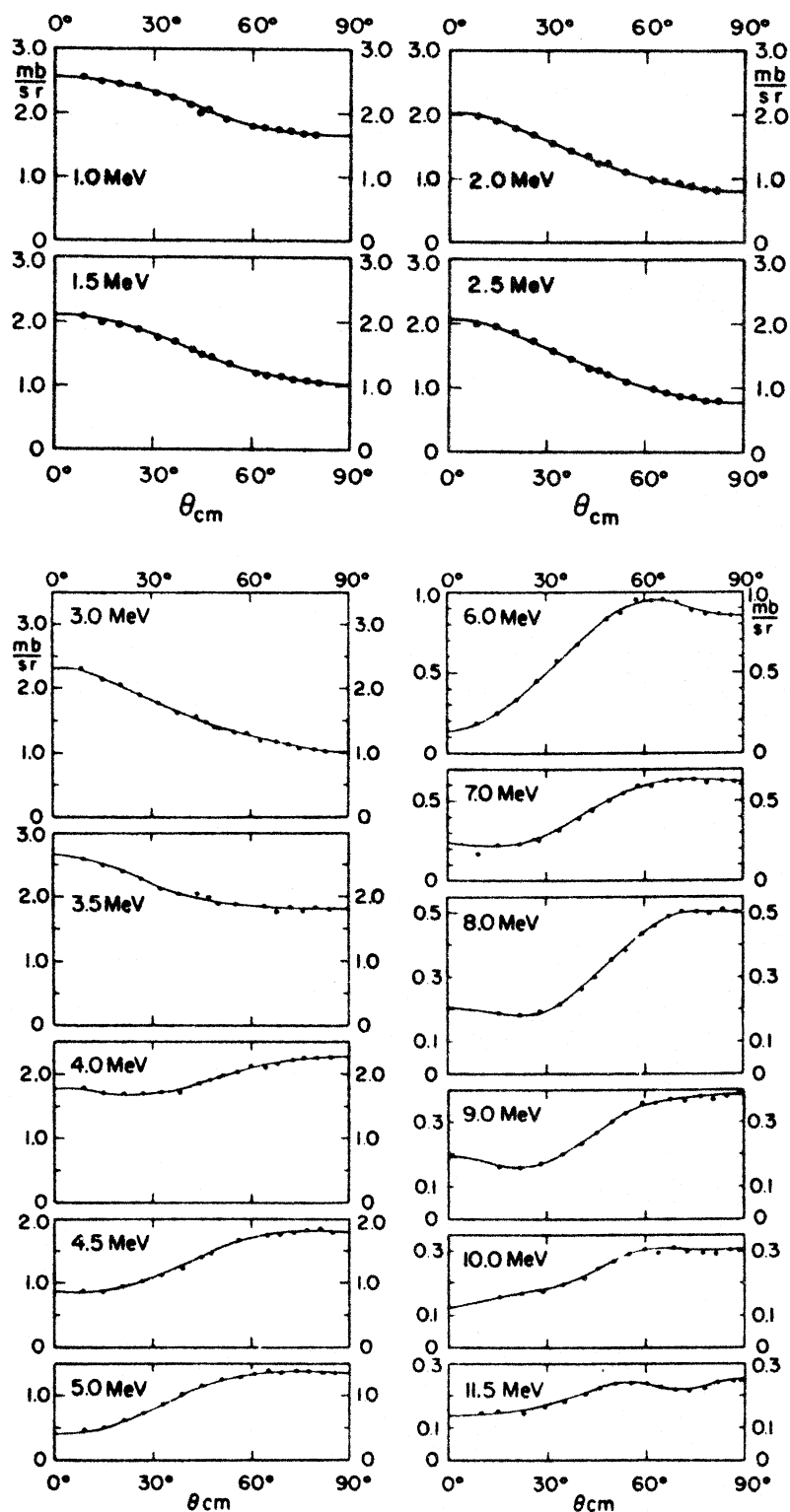


Fig. 1: Angular distributions of the cross section for the  ${}^6\text{Li}(d,\alpha){}^4\text{He}$  reaction

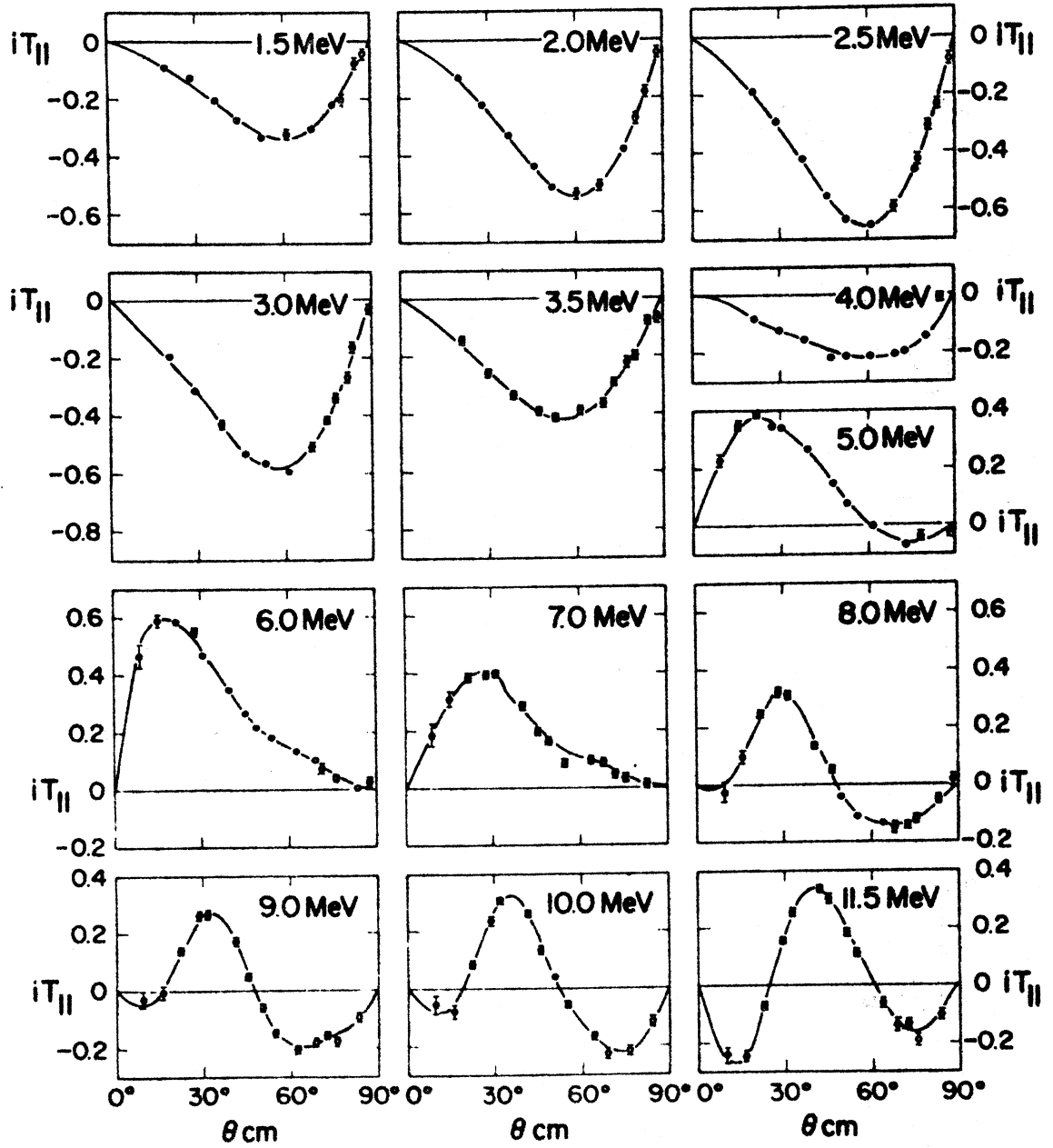


Fig. 2: The vector analysing power  $iT_{11}$

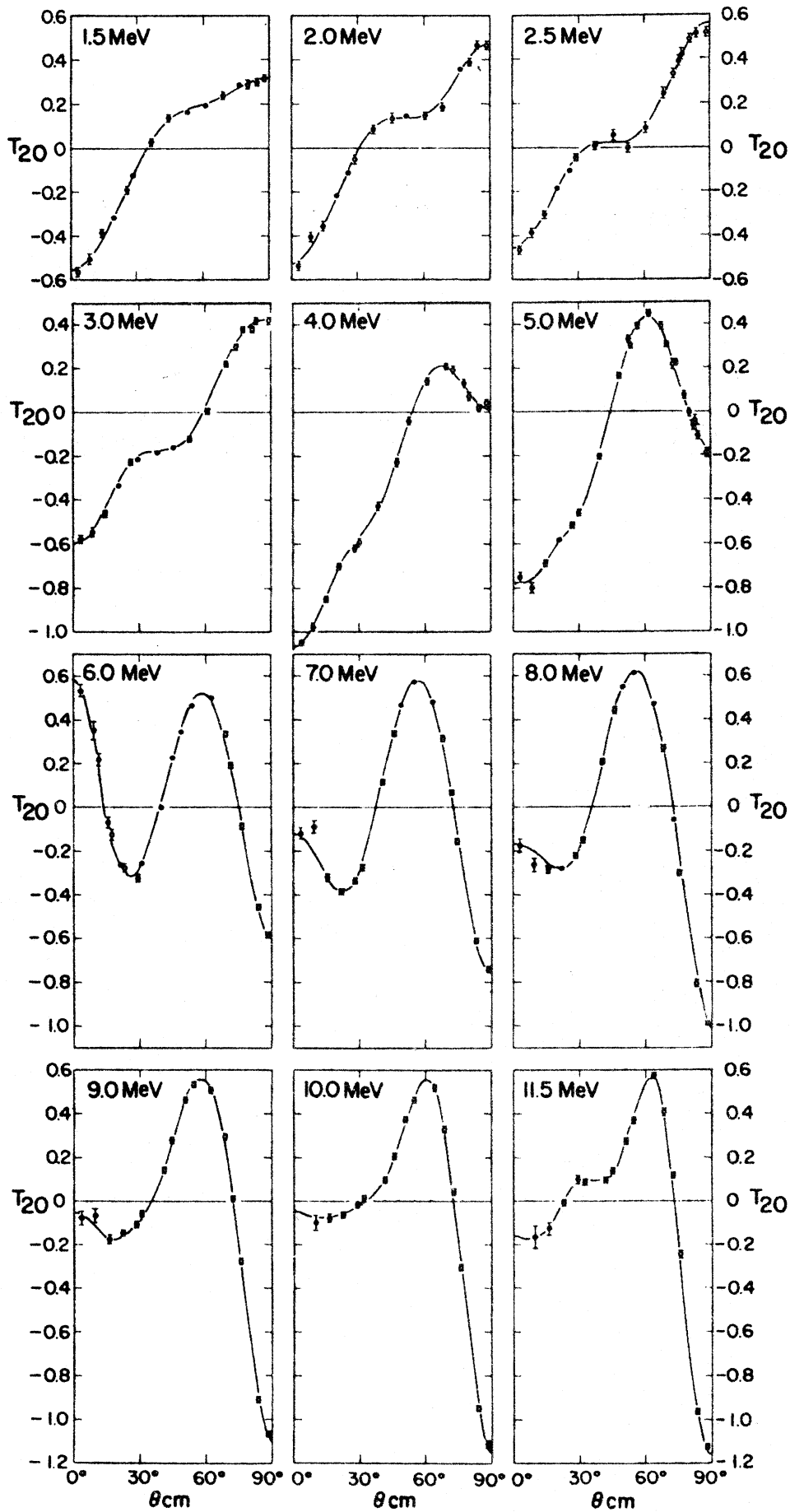


Fig. 3: The tensor analysing power  $T_{20}$

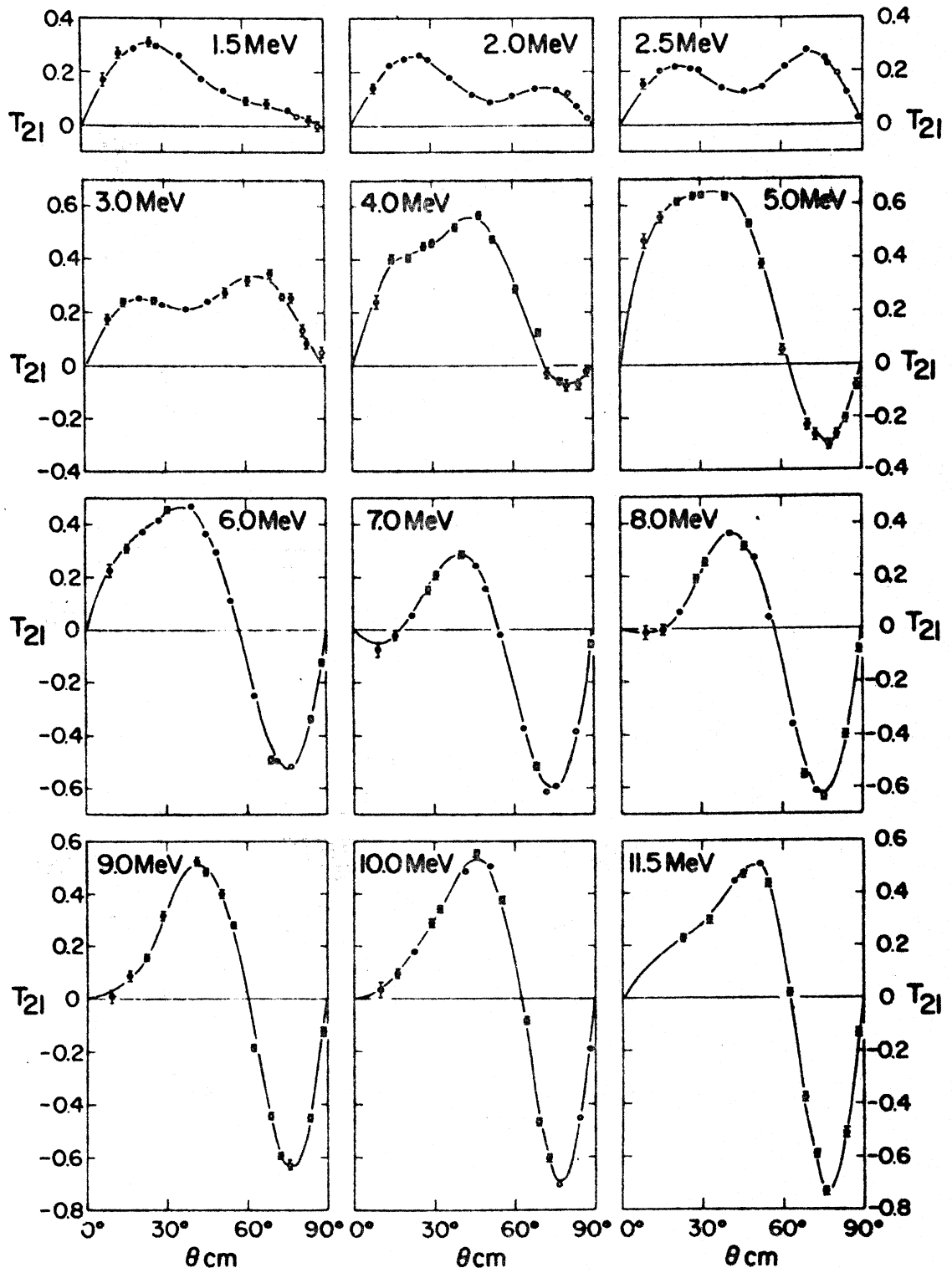


Fig. 4: The tensor analysing power  $T_{21}$

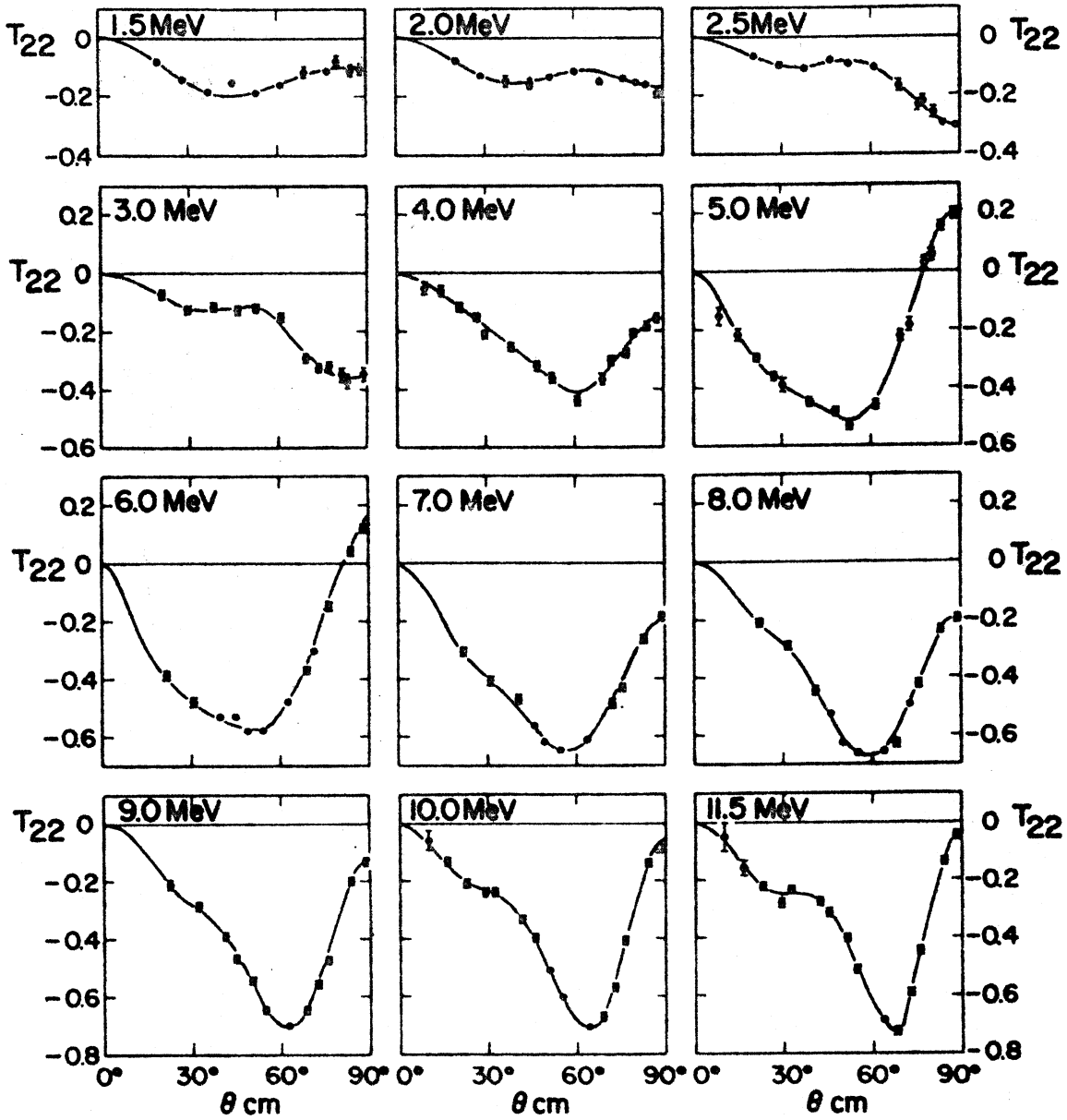


Fig. 5: The tensor analysing power  $T_{22}$

VII. Institut de Physique Nucléaire, Université de  
Lausanne

(Dir.: Prof. Dr. M. Gaillard)

1. (n,p), (n,d), (n,t) and (n, $\alpha$ ) Reactions at 14 MeV

Ch. Sellem and J. P. Perroud

The experimental results have been analyzed by means of two identification methods. The first, simple method yields the differential cross section in mb/sr.

a)  $^{10}\text{B} (n, \alpha_0 + \alpha_1) ^7\text{Li}$  and  $^{10}\text{B} (n, \alpha_2) ^7\text{Li}^*$  reactions:

$\theta_{\text{Lab}} (\text{deg})$	20	40	60	80	100	120	137
$(n, \alpha_0 + \alpha_1)$	0.83 ( $\pm 0.09$ )	0.62 ( $\pm 0.06$ )	1.1 ( $\pm 0.06$ )	1.0 ( $\pm 0.09$ )	0.8 ( $\pm 0.08$ )	1.2 ( $\pm 0.09$ )	1.8 ( $\pm 0.16$ )
$(n, \alpha_2)$	3.8 ( $\pm 0.2$ )	1.8 ( $\pm 0.1$ )	1.5 ( $\pm 0.1$ )	1.2 ( $\pm 0.08$ )	1.3 ( $\pm 0.07$ )	1.8 ( $\pm 0.1$ )	3.5 ( $\pm 0.2$ )

b)  $^{10}\text{B} (n, t_0) ^8\text{Be}$  reaction:

$(n, t_0)$	0.56 ( $\pm 0.1$ )	0.2 ( $\pm 0.04$ )	0.3 ( $\pm 0.06$ )	0.44 ( $\pm 0.06$ )			
------------	-----------------------	-----------------------	-----------------------	------------------------	--	--	--

c)  $^{10}\text{B} (n, d_0) ^9\text{Be}$  and  $^{10}\text{B} (n, d_1) ^9\text{Be}^*$  reactions:

$\theta_{\text{Lab}}$ (deg)	20	20	60	80	100	120	137
$(n, d_0)$	5.67 ( $\pm 0.3$ )	1.9 ( $\pm 0.2$ )	1.9 ( $\pm 0.1$ )				
$(n, d_1)$	3.9 ( $\pm 0.25$ )	1.1 ( $\pm 0.1$ )					

d)  $^{10}\text{B} (n, p_0) ^{10}\text{Be}$  and  $^{10}\text{B} (n, p_1) ^{10}\text{Be}^*$  reactions:

$(n, p_0)$	0.16 ( $\pm 0.02$ )	0.14 ( $\pm 0.04$ )	0.13 ( $\pm 0.05$ )	0.13 ( $\pm 0.05$ )			
$(n, p_1)$	1.1 ( $\pm 0.1$ )	1.0 ( $\pm 0.08$ )	0.75 ( $\pm 0.09$ )	0.65 ( $\pm 0.09$ )			

It is found that

- For the  $^{10}\text{B} (n, \alpha_0 + \alpha_1) ^7\text{Li}$  and  $^{10}\text{B} (n, \alpha_2)$  reactions our measured cross sections are  $\sim 30\%$  higher than the results reported by Antolkovic et al. [1], whose measurements were performed only up to  $90^\circ$  (CM).
- For the  $(n, p)$  and  $(n, d)$  reactions our results are  $30\%$  lower than those reported by Valkovic et al. [2]. Their measurements were performed over the angular range  $0^\circ$ - $130^\circ$  (CM).
- For the  $(n, t)$  reactions our results are  $20\%$  lower than those reported by Valkovic [3] which were measured up to  $130^\circ$  (CM).



A more sophisticated identification method will yield the remaining cross sections in the  $0-137^{\circ}$  (Lab) range shortly.

The full results and a discussion of the discrepancy with respect to the authors quoted will be reported. {4} and {5}.

The apparatus used and the identification methods will be described in a subsequent paper {6}.

#### References

- {1} B. Antolkovic, J. Huldomalj, B. Janko, G. Paic and M. Turk,  
Nucl. Phys. A 139 (1969) 10-16
- {2} V. Valkovic, P. Thomas, J. Slaus and M. Cerineo,  
Glasnik Matematicko-Fisicki i Astronomski. Tom 19, No. 3-4
- {3} V. Valkovic, Nucl. Phys. 54 (1964) 465-471
- {4} Ch. Sellem, Thesis (to be submitted to EPFL)
- {5} to be submitted to Helv. Phys. Acta
- {6} to be submitted to Nucl. Instr. & Methods



PROGRESS REPORT ON NUCLEAR DATA ACTIVITIES

OF THE ANKARA NUCLEAR RESEARCH CENTER

May 1974

## FAST NEUTRON ACTIVATION ANALYSIS

S.Dinçer, E.Barutçugil, H.Özyol, H.Sevimli

Fast neutrons having 14 MeV energy were used for some research work on the application of neutron activation analysis. Simple and accurate methods were used for determination of nitrogen amount in wheat grain samples (1), for oxygen determination in steel samples (2), and for the determination of trace amounts of Fe, Al and Si in rock samples (3).

- (1) H.Sevimli, H.Özyol, E.Barutçugil, S.Dinçer, Ankara Nuclear Research Center, Technical Journal, Vol.1, No.1, 15(1974)
- (2) S.Dinçer, H.Özyol, H.Sevimli, E.Barutçugil, to be published
- (3) H.Özyol, E.Barutçugil, S.Dinçer, Ankara Nuclear Research Center, Report RNF-1-74.

ENERGY AND SPACE DEPENDENCE OF D+T NEUTRONS IN SMALL SAMPLES  
OF IRON, ALUMINIUM AND LUCITE

C.Özmutlu, E.Barutçugil, H.Özyol

The induced activity variations of Cu, Al and In detectors located in r and z directions of small samples of iron, aluminium and lucite having the size of 4 cm. in diameter and 7 cm. in length were measured. On the basis of these activity measurements and the excitation functions of threshold detectors, the relative neutron flux distribution for the energy intervals of 14-12.9 MeV, 12.9-6.0 MeV, 6.0-1.65 MeV and for thermal region was obtained. The semiempirical relationships were derived in this work for the neutron flux distribution in r and z directions. Flux distribution in for all energies, but the one in z direction by the sum of two exponential functions for energies other than thermal energy and also by cosine function for thermal energy (1).

- (1) H.Özyol, E.Barutçugil, C.Özmutlu, Ankara Nuclear Research Center, Technical Journal, Vol.1, No.1, 3(1974).